

AMERICAN UNIVERSITY OF BEIRUT

MICROFOSSILS AND FACIES ANALYSIS OF THE NEOGENE
DEPOSITS OF THE WESTERN BEKAA VALLEY (LEBANON).
PALEOECOLOGY, PALEOBIOGEOGRAPHY AND
PALEOCLIMATE

by
CATHERINA MOUFID KHAIRALLAH

A thesis
submitted in partial fulfillment of the requirements
for the degree of Master of Science
to the Department of Geology
of the Faculty of Arts and Sciences
at the American University of Beirut

Beirut, Lebanon
April 2019

AMERICAN UNIVERSITY OF BEIRUT

MICROFOSSILS AND FACIES ANALYSIS OF THE NEOGENE
DEPOSITS OF THE WESTERN BEKAA VALLEY (LEBANON).
PALEOECOLOGY, PALEOBIOGEOGRAPHY AND
PALEOCLIMATE

by

CATHERINA MOUFID KHAIRALLAH

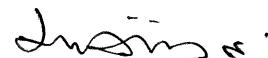
Approved by:



Dr. Josep Sanjuan Girbau,
Department of Geology,
American University of Beirut

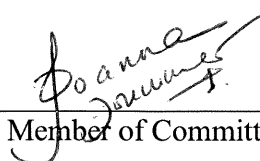
Advisor

Dr. Ali Haidar,
Department of Geology,
American University of Beirut



Member of Committee

Dr. Joanna Doummar,
Department of Geology,
American University of Beirut



Member of Committee

Dr. Dany Azar,
Department of Life and Earth Sciences,
Lebanese University



Member of Committee

Date of thesis defense: April 24, 2019

AMERICAN UNIVERSITY OF BEIRUT

THESIS, DISSERTATION, PROJECT RELEASE FORM

Student Name: Khairallah Catherina Noufid
Last First Middle

Master's Thesis
Dissertation

Master's Project

Doctoral

I authorize the American University of Beirut to: (a) reproduce hard or electronic copies of my thesis, dissertation, or project; (b) include such copies in the archives and digital repositories of the University; and (c) make freely available such copies to third parties for research or educational purposes.

I authorize the American University of Beirut, to: (a) reproduce hard or electronic copies of it; (b) include such copies in the archives and digital repositories of the University; and (c) make freely available such copies to third parties for research or educational purposes after : **One --- year from the date of submission of my thesis, dissertation, or project.**
Two --- years from the date of submission of my thesis, dissertation, or project.
Three ~~X~~ years from the date of submission of my thesis, dissertation, or project.



Signature

May 2nd, 2019

Date

ACKNOWLEDGMENTS

I would first like to express my profound gratitude to my thesis advisor Dr. Josep Sanjuan Girbau for the patient guidance, encouragement and advice he has provided throughout my time as his student. I have been extremely lucky to have a supervisor who cared so much about my work, and who responded to my questions and queries so promptly.

I also wish to thank the members of my committee: Dr. Ali Haidar, Dr. Dany Azar, and Dr. Joanna Doummar for generously offering their time, support, guidance and good will throughout the preparation and review of this document.

I am especially indebted to the experts for their help during fieldtrips and in the taxonomic classification of the aquatic mollusks, ostracods and vertebrate remains recovered from the studied sections: Dr. Thomas Neubauer, Dr. Jonathan Holmes, Dr. Raquel López-Antoñanzas, Dr. Fabien Knoll and Dr. George Kachacha. Without their passionate participation and input, the validation survey could not have been successfully conducted.

Fieldtrip expenses and materials used during this thesis were funded by the URB project of the American University of Beirut entitled: “Fossil Charophytes from Lebanon” (Project number AUB-23936).

I am very thankful to research assistants that helped me during the fieldtrips, sample treatment and microfossil picking process: Aliaa Hammoud, Beshar Al Amine, Celine Eid, George Wanna, Nabih Kazzi and Samar Ghadban. The thesis has also benefited from the help and technical support of Mr. Maroun Ijreis, Mrs. Nisrine Lababidi Hawi, Mrs. Rania Shatila (Central Research Science Laboratory of the American University of Beirut), previous graduates at the department and SEM technicians during the thin section and SEM sessions.

Finally, I must express my very profound gratitude to my parents and to my boyfriend for providing me with unfailing support and continuous encouragement throughout my years of study and through the process of researching and writing this thesis. This accomplishment would not have been possible without them. Thank you.

AN ABSTRACT OF THE THESIS OF

Catherina Moufid Khairallah for Master of Science
Major: Geology

Title: Microfossils and Facies Analysis of the Neogene Deposits of the Western Bekaa Valley (Lebanon). Paleocology, Paleobiogeography and Paleoclimate

The initiation of the Dead Sea Fault system during the Neogene and subsequent transpression in Lebanon caused maximum uplift of Mount Lebanon and Anti Lebanon ranges and maximum sedimentation within the Bekaa continental basin. Continental sedimentary rocks from the margins of the Central Bekaa Valley (Lebanon) have been studied from the sedimentological and micropaleontological viewpoints. Six closely-spaced stratigraphic sections were raised near the town of Zahle, and two other sections northwards near the villages of Niha and Cherara. Three facies assemblages has been characterized (1) a massive conglomerate unit interpreted as alluvial fan deposits, (2) a fossiliferous yellowish marls and marly limestones interpreted as perennial lacustrine deposits, and (3) an organic-rich marls rich in edaphic structures and lignites intercalated with volcanic ash horizons interpreted as a palustrine interval. These lacustrine-palustrine deposits provided a diverse microfossil assemblage composed of 5 species of stoneworts (charophytes), 14 species of terrestrial and aquatic snails (gastropods), 1 species of clamshell (bivalve), 5 species of crustaceans (ostracods) as well as other vertebrate remains such as bone fragments and teeth of fishes, amphibians, reptiles and mammals. These microfossils are here described and illustrated for the first time, and discussed in terms of their present and past ecology and geographical distribution. The paleoenvironmental characteristics and evolution of the lacustrine deposits are inferred through facies analysis and through comparison of microfossil tolerances with the ecological requirements of their nearest living relatives. Results suggest that during the late Miocene, the Bekaa Valley was occupied by a relatively shallow, stable, oligotrophic freshwater or slightly oligohaline lake that evolved to a very shallow eutrophic lake with a dense palustrine vegetation belt. The paleolake ultimately regressed to the south due to climatic changes and tectonic stresses leaving the lacustrine deposits exposed in the western margin of the basin as an erosional surface. A warm climatic phase probably prevailed in the area as indicated by the presence of hot-climate related fossils such as several groups of snails and crocodile remains. This study also provides valuable data about the paleogeographic distribution of several mollusks, ostracods and charophytes during the late Miocene representing a key geographic area to understand their dispersion routes and distribution patterns.

Keywords: Neogene, Miocene, lacustrine, microfossil, sedimentology, paleocology, paleoclimate, paleobiogeography, Bekaa basin.

CONTENTS

AKCNOWLEDGMENTS.....	v
ABSTRACT	vi
CONTENTS	vii
ILLUSTRATIONS.....	xii
TABLES	xx

Chapter

1. INTRODUCTION	1
1.1 Thesis Main Aims.....	1
1.2 Geologic Overview of Lebanon	1
1.3 Area of Study. The Bekaa Valley.....	8
1.4 Historical Geology of the Bekaa Basin	10
1.5 Previous Studies in Neogene Deposits of the Bekaa Valley	15
1.6 Lacustrine and Palustrine Sedimentology	18
1.7 Micropaleontology	22
1.7.1 Microfossils in Lacustrine Deposits	24
1.7.2 Paleoecology and Taphonomy	34
2. METHODOLOGY.....	36

2.1 Planning and Outcrops Exploration.....	36
2.1.1 Bibliography and Map Consultation	36
2.1.2 Geologic Exploration	36
2.2 Fieldwork.....	37
2.2.1 Field Tools and Equipment Used	37
2.2.2 Field Techniques and Fieldwork	37
2.3 Labwork.....	39
2.3.1 Soft Samples Treatment	39
2.4 Microfossil Treatment	41
2.5 Cabinet.....	44
3. STRATIGRAPHY	45
3.1 Section 1	47
3.1.1 Detailed Description from Base to Top.....	47
3.2 Section 2	55
3.2.1 Detailed Description from Base to Top.....	55
3.3 Section 3	59
3.3.1 Detailed Description from Base to Top.....	59
3.4 Section 4	66

3.4.1 Detailed Description from Base to Top.....	66
3.5 Section 5	68
3.5.1 Detailed Description from Base to Top.....	70
3.6 Section 6	79
3.6.1 Detailed Description from Base to Top.....	80
3.7 Section 7	84
3.7.1 Detailed Description from Base to Top.....	85
3.8 Section 8	87
3.8.1 Detailed Description from Base to Top.....	88
4. FACIES ASSEMBLAGES AND INTERPRETATION	91
4.1 Alluvial	91
4.2 Lacustrine Facies	91
4.3 Palustrine Facies	93
4.4 Fluvial.....	95
5. MICROPALAEONTOLOGY	96
5.1 Mollusca (GASTEROPODA)	98
5.1.1 Aquatic Gastropods	99
5.1.2 Terrestrial Gastropods	110

5.2 Mollusca (BIVALVIA)	113
5.3 Crustacea (OSTRACODA)	117
5.4 Charophyta (CHAROPHYCEAE)	125
5.5 Other Microfossils	133
5.5.1 MAMMALIA, RODENTIA	134
5.5.2 MAMMALIA, LAGOMORPHA	137
5.5.3 MAMMALIA, EULIPOTYPHLA	137
5.5.4 FISH REMAINS (ACTINOPTERYGII)	137
5.5.5 AMPHIBIA	139
5.5.6 REPTILIA	139
6. DISCUSSION	142
6.1 Microfossil Taphonomy and Paleoecology	142
6.2 Tectonic Implications	146
6.3 Climatic Implications	147
6.3.1 Global Late Miocene Climate Context:.....	148
6.3.2 Microfossil Paleoclimatic Inferences:	149
6.4 Paleobiogeography	153
6.4.1 Charophytes:.....	153
6.4.2 Aquatic mollusks:.....	155
6.4.3 Ostracods:	155
6.4.4 Vertebrates:	156

7. CONCLUSION.....	157
7.1 Stratigraphy and Sedimentology	157
7.2 Micropaleontology	157
7.3 Paleoecology and Paleoenvironment.....	158
7.4 Paleoclimate and Landscape.....	158
8. REFERENCES.....	160

ILLUSTRATIONS

Figure	Page
1. Figure 1: Geostructural map of Lebanon showing the major faults trends and structures (Hawie <i>et al.</i> , 2014).	2
2. Figure 2: Location map showing the topography, bathymetry and the major geostructural elements bounding the Levant basin. The major gas fields recently discovered are colored in red (Hawie <i>et al.</i> , 2013b).	3
3. Figure 3: A) Map of Lebanon showing the location map of the Bekaa Valley. The rectangle delineates the areas of study B) Geologic map of the southern Bekaa Valley. Rectangles represent the two areas of study (modified from Dubertret, 1955).	9
4. Figure 4: Synthetic geologic map showing the Quaternary, the Mesozoic and Paleogene deposits filling the basin and the surrounding areas. The studied lithological unit i.e. Zahle Formation is highlighted and labelled ZF in the map. A) Southern Bekaa, B) Middle Bekaa and C) Northern Bekaa. Note that the Miocene deposits illustrated in the Map represent the deposits encountered during field work and studied in the thesis (modified from Lateef, 2006).	10
5. Figure 5: 3D geologic sketch showing the three morphostructural divisions of Lebanon during the middle Eocene (Lateef, 2007). Note that the western and eastern Lebanese mountain ranges had already emerged. Note the location of the Bekaa Valley flooded by the ocean forming a seaway. Note that this figure does not highlight the change of thickness explained previously in text; it just shows the location of Mount Lebanon, Anti Lebanon and the Bekaa Valley.	12
6. Figure 6: 3D geological sketch showing the morphostructural context of Lebanon during the middle-late Miocene. During this stage, major uplift of Lebanese ranges and down-warping of the Bekaa basin (arrows) took place in association with the appearances of some elements of the Lebanese segment of Dead Sea Fault System (red line). Note the presence of alluvial fans in both sides of the Bekaa Valley and two large lacustrine systems i.e. A) South-middle Bekaa paleolake and B) Al Hermel paleolake at the north (Lateef, 2007).	14
7. Figure 7: A 2D cross section depicting the subaqueous zones of a lake (webpage: http://mtlakebook.org/how-lakes-function).	19
8. Figure 8: Palustrine-calcrete facies associations and their common petrographic aspect (Alosnso-Zarza and Wright, 2010).	22
9. Figure 9: Vegetative parts of a charophyte. a) Complete charophyte showing the plant structure divided in nodes and internodes (real scale), b) Detailed draw of a node showing the stipulodes, the corticated cells, the female reproductive organ (oogonium) and spine cells (23 X	

magnifications), c) Detail of the oospore (40 X magnifications). d) Detail of the antheridium being the male reproductive organ at 40 X magnifications (Feist <i>et al.</i> , 2005).	26
10. Figure 10: Female reproductive organs of a charophyte (40 X magnifications) 1) Oospore, 2a) Outer morphology of a gyrogonite (calcified oospore), 2b) Longitudinal section of a gyrogonite showing its internal structure; dotted lines represent the uncalcified parts of spiral and coronular cells that do not calcify (Feist <i>et al.</i> , 2005).....	27
11. Figure 11: Terminology of gyrogonite shapes used in this master's thesis. Percentages represent the isopolarity index i.e. LPA/LED X100. LPA, length of polar axis; LED, largest equatorial diameter; AND, distance from apical pole to LED (Feist <i>et al.</i> , 2005).....	27
12. Figure 12: Lateral views of gastropod shells showing different shape types. a) Elongate conic, b) Elongate cylindrical, c) Globose, d) Depressed and e) Discoidal (Smith, 2005).	30
13. Figure 13: Morphological features of a gastropod shell. Upper image: dorsal view showing the whorls and the apex where the protoconch or larva shell is located. Central image: lateral view showing the profile of the shell and the aperture structure Lower image: basal view showing the umbilicus in the center (from: http://www.wikiwand.com/en/Gast).	30
14. Figure 14: Sketch of a bivalve shell showing the main morphological features of the inner (left image) and outer (right image) shell (modified from Cesari and Pellizzato, 1990).....	31
15. Figure 15: Sketch showing the main morphological features of two different idealized ostracod carapaces. The image located above represents an interior shell. The image below represents an exterior shell (Horne <i>et al.</i> , 1990).....	34
16. Figure 16: A flowchart showing the different steps of a paleoecological reconstruction (Birks and Birks, 1980).....	35
17. Figure 17: Picture of Drs. Fabien Knoll and George Kachacha extracting about 500 kg of sediments from sample Z-8 at section 3. Note that they are using a driller instead of a hammer to be able to extract large amount of sediments.	39
18. Figure 18: First stage of the sample treatment. Graduate students are removing the undesirable remains and crashing the indurated rock blocks.	40
19. Figure 19: Picking process using binocular of microfossils from the scattered grains placed on a plate with a fine brush while light is directed towards the grains.	42

20. Figure 20: Graduate students describing microfossils and taking photographs during a SEM session in the CRSL.....	43
21. Figure 21: Geologic map showing the location of sections 1 till 6 at Zahle (modified from Dubertret, 1955).	46
22. Figure 22: Geologic map showing the location of sections 7 and 8 at Cherara and Niha villages (modified from Dubertret, 1955).....	46
23. Figure 23: Detailed image of the Eocene Nummulitic limestone at the basal part of section 1. Note the axial sections of <i>Nummulites</i> shells. ..	48
24. Figure 24: Field picture facing the west showing the upper part of the massive conglomerate interval (Co) and the overlying lacustrine marls (Lm) located at the base of the section 1, next to Monte Alberto hotel.	48
25. Figure 25: Detailed photograph of the basal conglomerates at section 1. A) Nummulitic limestone clasts and B) Marly matrix surrounding the clasts.....	49
26. Figure 26: Field photo showing the alternation between conglomerate (Co) and siltstone (Si) intervals at the base of section 1. Note the stratigraphic location of the sample Z-0.	50
27. Figure 27: Field image facing the northeast showing the middle part of section 1.	52
28. Figure 28: Field picture showing the alternation of marl and limestone layers at the top of section 1. Note the stratigraphic location of the hard sample ZL.	53
29. Figure 29: Detailed photograph of the thin section of sample ZL. Note the dissolved gastropod shells at the center of the figure (secondary porosity) and the precipitated calcite crystals within the dissolved shells to the upper right corner of the picture.	53
30. Figure 30: Stratigraphic log for section 1 showing a detail of a shallowing sedimentary cycle. Z-0 to Z-4 represent the stratigraphic position of samples extracted for microfossils. ZL represents the location of the extracted hard sample for microfacies analysis.....	54
31. Figure 31: Field image (facing the east) showing the basal strata of the section 2.	56
32. Figure 32: Field picture (facing the east) of the uppermost part of section 2. Lower marl strat (Ma) are overlain by marly limestone (No) pedogenic structures (caliche). Pale red marl interval (Rm) occurs at the top of these layers.	57
33. Figure 33: Stratigraphic log for section 2. Z-5 and Z-6 represent the stratigraphic position of samples extracted for microfossils.	58

34. Figure 34: Photograph of the upper part of the section 3 showing the organic-rich marl deposits.	59
35. Figure 35: Detailed picture of the lignite layers recently excavated directly below the sample Z-9 in the section 3.	60
36. Figure 36: Detailed photograph of the rhizoliths in sample Z-9.....	61
37. Figure 37: Detailed photograph (facing the east) at the upper part of section 3. Note the alternation between the marl layers and organic rich interval, separated by an erosive base (marked by the dashed line).	62
38. Figure 38: Detailed image showing the contact between a yellowish fossiliferous marl bed and an organic-matter rich interval at the top of the section 3. Note the rhizoliths located at the top of the marl interval.	63
39. Figure 39: Stratigraphic log for the section 3 showing a detail facies assemblage at its top. Z-7 to Z-11 represent the stratigraphic position of samples extracted for microfossils.....	64
40. Figure 40: Stratigraphic logs for sections 1, 2 and 3 of the lacustrine deposits of Zahle showing their correlation and their facies associations. Z-0 to Z-11 represent the stratigraphic position of samples extracted for microfossils. ZL refers to the stratigraphic position of the sample recovered for microfacies analysis.	65
41. Figure 41: Field photograph (facing the east) showing the semicovered dark grey marl layers at the base of section 4. Note the hole in the section representing the stratigraphic location of the sample Z-12.	66
42. Figure 42: Stratigraphic log for section 4 showing a detail of two intervals. Z-12, Z-13 and Z-14 represent the stratigraphic position of the studied samples.	68
43. Figure 43: General field photograph (facing the west) showing the basal part of the section 5. Note the stratigraphic location of samples Z-15 and Z-16.....	69
44. Figure 44: General field photograph (facing the northwest) showing the basal part of the section 5. Note the stratigraphic location of samples Z-15 and Z-16. Drs George Kashasha and Fabien Knoll are extracting soft rocks from the organic-rich marl interval (Z-16).....	69
45. Figure 45: Detailed photograph (facing the west) showing the marl layers of sample Z-15 in section 5. Note the presence of rhizoliths.	70
46. Figure 46: Detailed photograph (facing the west) of the sample Z-16 in section 5. Note the dark color of this fossiliferous marl interval.....	71
47. Figure 47: Detailed photograph of the caliche in section 5.	72

48. Figure 48: General field photograph (facing the west) showing the upper part of section 5. Note the thicknesses and colors of different strata and the location of samples Z-17, Z-17' and Z-18.	73
49. Figure 49: Detailed photograph (facing the west) showing a coquina interval. A) From base to top: yellowish marl layer showing rhizoliths (Rm), a coquina interval (Co) from where the sample Z-17' was recovered, and the grey marl interval showing caliche (No). B) Detailed photograph of a coquina.	74
50. Figure 50: Detailed photo showing a large shell of <i>Melanopsis buccinoidea</i> from sample Z-17'. Note the original coloration preserved.	75
51. Figure 51: Detailed photograph of reed-like leaf impressions above the sample Z-17'.....	75
52. Figure 52: Detailed photograph showing the nodular structures (caliche) located above the sample Z-17'. The dashed line outstands some caliche.	76
53. Figure 53: Stratigraphic log for the base of the section 5. Zahle 15 (Z-15) to Zahle 17 (Z-17) represent the stratigraphic location of the samples extracted for microfossils.....	78
54. Figure 54: Stratigraphic log for the top of the section 5. Z-17' and Z-18 represent the stratigraphic location of the samples extracted for microfossils.	79
55. Figure 55: Field photograph (facing the north) showing the basal part of section 6. Note the location of the samples Z-20.....	80
56. Figure 56: Field photograph of the upper part of section 6 showing the reddish clay and conglomerates.	82
57. Figure 57: Conglomerate contact showing imbrication fabrics and erosive base (marked with a dashed line).	82
58. Figure 58: Stratigraphic log for the section 6. Z-19 and Z-20 represent the stratigraphic location of the samples extracted for microfossils.....	84
59. Figure 59: General field photograph of the section 7 at Cherara.....	85
60. Figure 60: Field photograph of the upper part of section 7. Note the alternation between the marls and whitish marly limestone layers. The star represents the location of the sample Z-21.	86
61. Figure 61: Stratigraphic log for the section 7. Z-21 represents the stratigraphic location of the sample extracted for microfossils.	87
62. Figure 62: Field photograph of section 8 near the Niha ruins. The star represents the location of the sample Z-22.	88

63. Figure 63: Field photograph showing the basal portion of section 8. Note the location of the sample Z-22. 89
64. Figure 64: Stratigraphic log for the section 8 showing the stratigraphic location of sample Z-22 that was extracted for microfossil analysis..... 90
65. Figure 65: Biometric values of *Valvata saulcyi* (n = 10 shells). A) Shell height (mm) and B) Shell width (mm)..... 100
66. Figure 66: Schematic draw of a *Melanopsis* shell. Shell conchometric's abbreviations: SH, shell-height; MH, mouth-height; SD, shell-diameter; MD, mouth-diameter; f, whorl; e, last whorl. (Heller *et al.*, 2005). 102
67. Figure 67: Mollusks recovered from Miocene lacustrine deposits near Zahle. A-C) *Valvata saulcyi*, sample Z-8. D-E) *Bithynia* sp. (opercula), sample Z-8. F) *Melanopsis buccinoidea*, sample Z-6. G-H) *Semisalsa* sp., both from sample Z-5. I) *Pseudamnicola* sp., sample Z-4. J) *Islamia* sp., sample Z-5. K) *Islamia* sp., sample Z-1. L) *Radix* sp., sample Z-10. M) *Gyraulus* cf. *hebraicus*, sample Z-8. N) *Gyraulus* cf. *piscinarum*, sample Z-5. O) *Gyraulus* cf. *piscinarum*, sample Z-1. P) *Carychium* sp., sample Z-8. Q) *Vertigo* cf. *antivertigo*, sample Z-8. R) *Strobulops* sp., sample Z-11. S-U) *Pisidium* cf. *moitessierianum*, sample Z-6. 115
68. Figure 68: Mollusks recovered from Zahle. A) *Valvata saulcyi*, sample Z-13. B) *Valvata saulcyi*, sample Z-16. C) *Bithynia* sp. operculum, sample Z-13. D) *Semisalsa* sp. (broken aperture), sample Z-19. E) *Semisalsa* sp., sample Z-14. F-G) *Islamia* sp., sample Z-17. H-I) *Phenacolimax* sp. sample Z-19. J) *Gyraulus* cf. *piscinarum*, sample Z-16. K) *Pisidium* cf. *moitessierianum*, sample Z-16..... 116
69. Figure 69: SEM images of *Melanoides* cf. *tuberculata* from sample Z-17'. Shells show their last whorl broken. 117
70. Figure 70: Biometric values of *Cyprideis* sp. (n = 48 carapaces). A) Carapace's height (μm) and B) Carapace's length (μm). 120
71. Figure 71: Ostracods from lacustrine deposits of Zahle in section 1, 2 and 3. A-J) *Cyprideis* sp., sample Z-7. K) *Cyprideis* sp., sample Z-0. L) *Cyprideis* sp., sample Z-5. M) *Cyprideis* sp., sample Z-8. N) *Cyprideis* sp., sample Z-5. O) *Cypris pubera*, sample Z-6. P) *Strandesia* sp., sample Z-1. Q) *Candona* cf. *angulata*, sample Z-5. 124
72. Figure 72: Ostracod assemblage recovered from sections 4, 5, and 7 near Zahle. A) *Candona* cf. *angulata*, sample Z-12. B) *Candona* cf. *angulata*, sample Z-15. C-D) *Cyprideis* sp., sample Z-17. E) *Cyprideis* sp., sample Z-21. F) *Cyprideis* sp., sample Z-14. G) *Ilyocypris* sp., sample Z-14. H) *Ilyocypris* sp., sample Z-13. I) *Cyprideis* sp., sample Z-14. 125
73. Figure 73: Biometric values of *Nitellopsis (T.) merianii* from sample Zahle 2 (n = 100 gyrogonites). A) Gyrogonite height (μm), B) Gyrogonite width (μm), C) Number of convolutions visible in lateral view and D) Isopolarity index ($\text{ISI} = \text{h/w} \times 100$). 130

74. Figure 74: Gyrogonites from lacustrine deposits of sections 1 and 3 near Zahle. A–C) *Nitellopsis (T.) merianii*, sample Z-2 (A. apical view, B. lateral view, C. basal view). D–F) *Lychnothamnus barbatus* var. *megalicarpus*, sample Z-2 (D. apical view, E. lateral view, F. basal view). G–J) *Chara microcera*, sample Z-1 (G. apical view, H. lateral view, I. lateral view, J. basal view). K–N) *Chara* cf. *globularis*, sample Z-1 (K. apical view, L. lateral view); sample Z-8 (M. lateral view, N. basal view). O–Q) *Sphaerochara* sp., sample Z-10 (O. apical view, P. lateral view, Q. basal view). 132
75. Figure 75: Assemblage of gyrogonites extracted from section 4 near Zahle (sample Z-13). A–C) *Nitellopsis (T.) merianii* (A. lateral view, B. basal view, C. apical view). D–G) *Lychnothamnus barbatus* var. *megalicarpus* (D–E. lateral view, F. basal view, G. apical view). H–L) *Chara* cf. *globularis* (H–J. lateral view, K. basal view, L. apical view). 133
76. Figure 76: SEM image of a rodent jaw of *Apodemus* sp. showing the location of the three lower and upper molars respectively in plan view. Image provided by Dr. Raquel López-Antoñanzas. 134
77. Figure 77: Plan view of a M2 of *Progonomys* showing its major morphological features. (Dr. Raquel López-Antoñanzas personal photo). 135
78. Figure 78: Assemblage of rodent and lagomorph teeth extracted from sections 3 and 5 near Zahle. A and D) Second upper molar (M2) of a *Progonomys* sp., sample Z-16. C) Second upper molar (M2) of a *Progonomys* sp., sample Z-8. B) Incisive tooth of an undetermined Murid, sample Z-8. E) Third molar (M3) of an undetermined Murid, sample Z-16. F) Tooth of *Prolagus* sp., sample Z-16. G) Third molar (M3) of *Byzantinia* sp., sample Z-16. H) First molar (M1) of an undetermined Cricetid, sample Z-16. 136
79. Figure 79: Assemblage of fish remains extracted from Zahle. A–B) Fish teeth of the Cyprinidae family, sample Z-16. C) Small fish tooth of the Cyprinidae family, sample Z-17. D) Otolith of *Aphanius* sp., sample Z-15. 138
80. Figure 80: Assemblage of vertebrate fragments extracted from section 5 near Zahle. A) Crocodile osteoderm, sample Z-16. B–C) Micromammal phalange bone, sample Z-16. D) Reptile osteoderm fragment, sample Z-16. E) Fragment of a lower frog jaw, sample Z-16..... 140
81. Figure 81: A–B) Undetermined molar tooth of a shrew from sample Z-16 (A. plan view, B. lateral view) and C) Broken tooth of a crocodile from sample Z-2. 141
82. Figure 82: Paleoecological models showing the location of the sections 1 till 8 in Zahle paleolake system, as well as their lithologies and microfossil content. The upper model represents the deep oligotrophic

lacustrine conditions in sections 1, 2, 4, 7 and 8 while the lower model represents the extremely shallow and eutrophic palustrine conditions in the upper section 3 and complete section 5.	144
83. Figure 83: Photo of the savanna type habitat from NW Nairobi (Kenya, Africa), considered.....	152
84. Figure 84: Paleogeographic map of the Mediterranean region during the Late Miocene showing the distribution of the two main charophyte species <i>Nitellopsis (T.) merianii-obtusa</i> and <i>Lychnothamnus barbatus</i> var. <i>antiquus</i> . Be= Bekaa Valley (Lebanon), Ç= Çankiri Basin (Turkey), Ma= Maoce Basin (Montenegro), Ca= Carpatian Basin (Austria), Su= Suceava area (Romania), SFD= Southern Federal District (Russia), Pr= Provence (France), Py= Pyrenees (Spain), E= Ebro Basin (Spain), Po= Portugal, Ak= Ait Kandoula Basin (Morocco). Dotted line circle represents the present biogeographic distribution of the two considered species. Note position of the new populations in Be= Bekaa Valley (modified from Blakey, 2011).	154

TABLES

Table	Page
1. Table summarizing the facies description in sections 1 till 8 and their associated environment.....	95
2. Table showing the relative abundance of microfossils recovered from sections 1, 2 and 3 based on a semi-quantitative visual estimation. Note that samples Z-0 till Z-11 follow a stratigraphic order, Z-0 being extracted from the lowermost layers and Z-11 being taken from the uppermost layers.	97
3. Table showing the relative abundance of microfossils recovered from sections 4, 5, 6, 7 and 8 based on a semi-quantitative visual estimation. Note that samples listed in this table do not follow a stratigraphic order.	98

CHAPTER 1

INTRODUCTION

1.1 Thesis Main Aims

This master's thesis aims at performing detailed sedimentological and micropaleontological analyses of the complete Neogene rocks of the Zahle Formation at the town of Zahle and villages of Cherara and Niha (western Bekaa Valley, Lebanon). These rocks are studied in detail to perform a multidisciplinary approach in stratigraphy, sedimentology, micropaleontology and paleoecology. Results obtained from this master's thesis help in the characterization of the Bekaa Valley from the viewpoints of basin evolution and landscape reconstruction during the late Miocene.

Four aims have been covered in this research work:

- Stratigraphic study and sedimentological analysis of the Neogene deposits of the Zahle Formation.
- Taxonomic classification of the microfossil assemblage recovered in the Neogene deposits of Zahle and nearby northern villages such as Cherara and Niha.
- Reconstruction of the paleoenvironmental conditions that prevailed during the late Miocene in the area of Zahle and its surroundings.
- Discussion about the paleogeographical, paleoecological and paleoclimatological implications on the basis of the microfossil assemblage.

1.2 Geologic Overview of Lebanon

Lebanon is located at the east of the Levant basin and on the NW margin of the Arabian plate. From the tectonic point of view, this margin corresponds to the left-

lateral transform plate boundary i.e. the Dead Sea Transform Fault that is responsible to the formation of a complex fault system in the country (fig. 1).

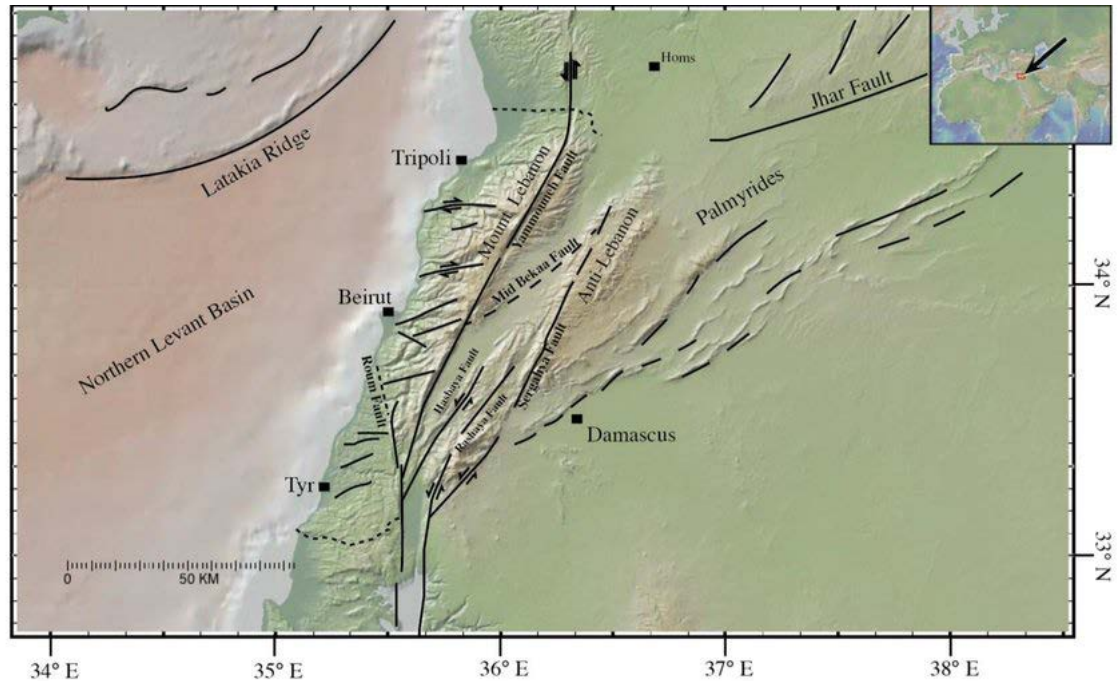


Figure 1: Geostructural map of Lebanon showing the major faults trends and structures (Hawie *et al.*, 2014).

The topography of Lebanon consists mainly of two NNE-SSW mountain chains (the Mount Lebanon at the west and the Anti-Lebanon to the east) separated by the Bekaa Valley or Bekaa basin. The left-lateral strike slip active Yammouneh fault is considered the longest and most important fault in Lebanon (Walley, 2001). This transpressional fault is linked southward to the Dead Sea rift complex and has a general NNE-SSW trend. The Yammouneh fault traverses the whole country along the western margin of the Bekaa basin and connects to the Ghab fault northwards. Other active faults in Lebanon are the Serghaya, Roubi, Chebaa-Rachaya, as well as other smaller faults that have been suggested in the area.

The Levant basin is located within the eastern Mediterranean (fig. 2). Cyprus and Larnaca Thrust zones are located to the north of the basin, whereas the Eratosthenes

Seamount occurs to the west of the Levant and the Nile Delta deep-sea cone is located to its southwest (Roberts and Peace, 2007; Homberg and Bachmann, 2010).

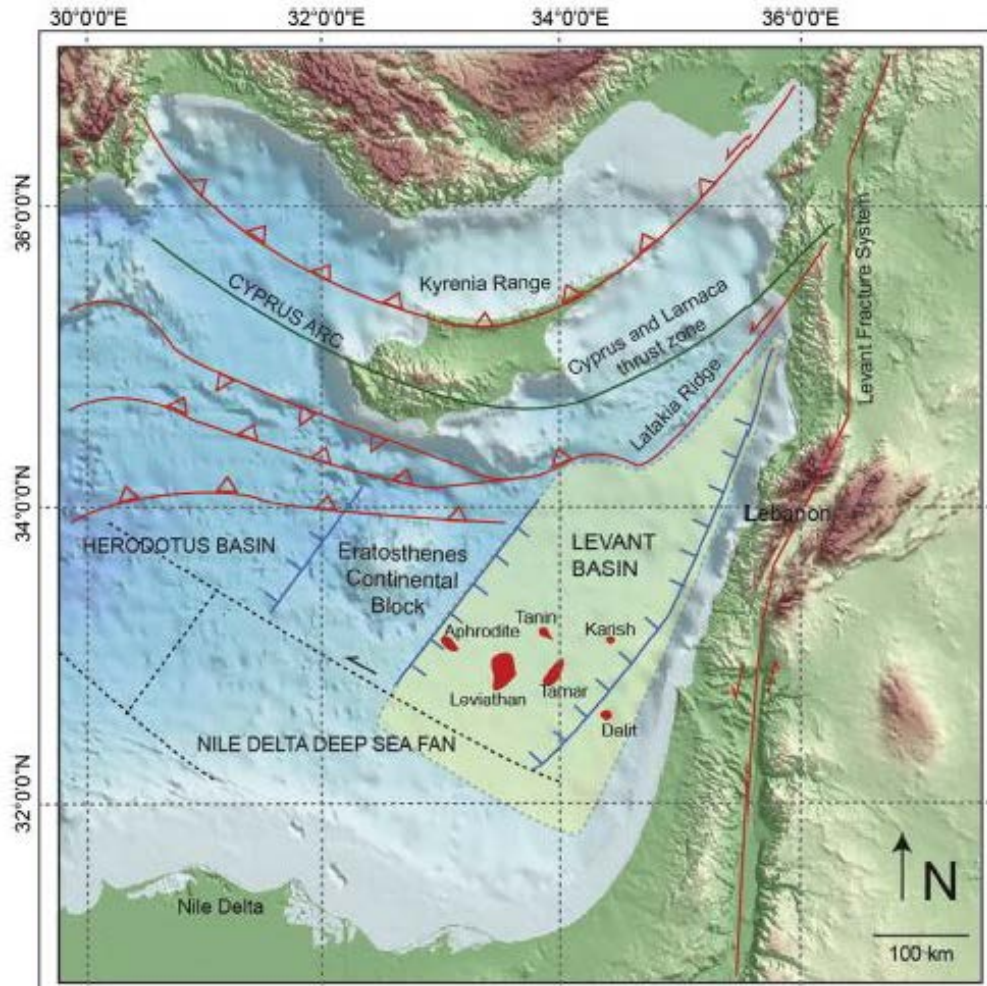


Figure 2: Location map showing the topography, bathymetry and the major geostructural elements bounding the Levant basin. The major gas fields recently discovered are colored in red (Hawie *et al.*, 2013b).

The geological history of Lebanon can be divided in two main rifting stages. The first rifting stage initiated during the late Paleozoic/early Mesozoic with some pulses during the middle Triassic (Gardoch *et al.*, 2010; Youssef *et al.*, 2010). Restricted depositional environment during the Triassic was indicated by a carbonate and evaporitic sedimentary sequence composed of limestone, dolomite, shale and gypsum (Zak, 1963, 1968; Druckman, 1974; Brew *et al.*, 2001). A second rifting pulse

during the early Jurassic resulted in the deposition of thick pyroclastics and volcanic rocks along the Levant margin (Druckman, 1977; Hirsch *et al.*, 1998). In contrast, contemporaneous Jurassic deposits are located within the eastern Mediterranean basins. These deposits consist of shallow marine marls and shales passing upwards to deep marine sediments composed of hemipelagic material interbedded by silt, shales and carbonates (Gardosh *et al.*, 2006).

The rifting period stopped during the late Jurassic and the development of a post-rift passive margin allowed the deposition of thick marine carbonates and deep-water siliclastic deposits (Gardosh, 2002; Roberts and Peace, 2007).

During the early Cretaceous, a period of emersion and erosion promoted the deposition of siliclastic materials in the basin (Walley, 1997; Brew *et al.*, 2001; Ziegler, 2001). Lower Cretaceous deposits have been traditionally related to a transgressive sequence passing from fluvial-lacustrine to swamp environments topped by a shallow marine deposits (Walley, 1997; Litak *et al.*, 1998; Brew *et al.*, 2001; Wood, 2001). This limestone formation forms an outstanding pale grey cliff along the east and west sides of the Mount Lebanon.

Shallow marine conditions prevailed in the area until the initiation of a compression phase during the Late Cretaceous, following the collision between the Afro-Arabian and the Eurasian plates. Many authors considered that the compressional strength started in the region during the Late Cretaceous and lasted until the Pleistocene (Ponikarov, 1967; Dubertret, 1975; Hancock and Atiya, 1979; Khair *et al.*, 1997). This compressional episode is known as the Syrian Arc tectonic event. This event is geologically expressed as a line of folds extending NE-SW from western Egypt, passing through Lebanon and reaching the Palmyrides belt in Syria (Krenkel 1924 a, b).

According to Walley (1998), the first Syrian Arc depositional episode of compression started during the Late Cretaceous (Coniacian-Santonian) as a result of the closure of the Tethys Ocean. The second Syrian Arc episode is associated with the collision between Arabian and Eurasian plates along the Bitlis suture zone which began during the late Eocene and ended in the late Oligocene (Walley, 1998).

During the early Paleogene, further emergence took place in the nowadays Lebanon area, and larger parts of the low-amplitude anticlines emerged forming longitudinal islands oriented NE-SW within the shallow Tethys Sea. These longitudinal islands represent the young stages of the well-known morphostructural zones of the “Mount Lebanon” and “Anti-Lebanon” in Lebanon (Lateef, 2007). Located between these two elongated islands a marine basin was formed. This marine basin represented the first geologic stage of the Bekaa Valley (proto-valley), whose deposits result from the erosion of the uplifted structures becoming thick towards the southeast (Lateef, 2007).

According to Walley (1998), the formation of the Mount Lebanon and Anti-Lebanon occurred in two main phases: the first gentle uplift took place during the Late Cretaceous and the second dominant uplift occurred during the late Eocene. These two phases took place during the first and the second Syrian Arc deformational events, respectively.

During the late Miocene, westward movements of the Anatolian Plate resulted in the opening of the Gulf of Aden and the Red Sea. This caused the development of the Dead Sea transform fault (Hempton, 1987; Beydoun, 1999), which corresponds to the first phase of tectonic activity in Lebanon. The Dead Sea transform fault extends about 800 km from the Gulf of Aqaba in the south to Syria towards the north, without major

connection to east Anatolian fault. The Dead Sea fault is divided in three main parts: the Southern Dead Sea, the Central Dead Sea (including the Lebanese restraining bend), and the Northern Dead Sea (Searle *et al.*, 2010). The 150 km long sinistral NNE-SSW trending Yammouneh fault is the main branch of the Dead Sea System in Lebanon linking the Jordan Valley fault in the south and the Al Ghab fault to the north (Daeron *et al.*, 2004). It is still debatable whether the Yammouneh fault started its activity in Lebanon during the late Miocene or during the Pleistocene. A transpressional deformational phase took place during the late Miocene due to right fault bending of the Dead Sea transform system in Lebanon (Beydoun, 1999; Gomez *et al.*, 2006). This deformation induced the general uplift of the Mount Lebanon and neighbor structures such as the Bekaa basin. This progressive uplift was responsible for the development of non-marine conditions within the entire basin where alluvial, fluvial and lacustrine depositional environments prevailed (Lateef, 2007).

The drop of the sea level at the end of the Miocene epoch related to the Messinian salinity crisis was responsible for intense erosion and valley incisions along the margins of the whole Levant basin (Cita and Ryan, 1978). The enclosure of the Mediterranean Sea resulted in deposition of an up to 2 km thick evaporitic sequence in some areas of the Mediterranean basin (Hawie *et al.*, 2013). Upper Miocene lacustrine deposits in the Bekaa Valley as well as several basins in Turkey suggest that wet climatic conditions prevailed in the eastern Mediterranean basin during the salinity crisis in a general deteriorate dry climatic trend of the whole Mediterranean area (Lateef, 2007).

By the Pliocene time, the extension of the Red Sea continued and the motion of the Arabian and African Plates became independent (Hempton, 1987). This time was an

important phase during mountain building in the Middle East and the complete Levant regions (Lateef, 2007). A second phase of active tectonism initiated in Lebanon during late Pliocene with further uplift of the Mount Lebanon. This phase was followed by a decline of the tectonic activity (Lateef, 2007). During this epoch, the sea level dropped, followed by high stand levels at coastal areas. Low lying areas in Lebanon were still covered by water due to uplift of Lebanese ranges (Mount and Anti Lebanon), resulting in deposition of up to 250 to 400 m thick basalts, marls, chalky limestones and clays in north western Lebanon. Fluvial and lacustrine environments kept being dominant in inner basins such as the Bekaa Valley (Dubertret, 1975; Druckman *et al.*, 1995; Müller *et al.*, 2010). Towards the emergent hinterland, thick alluvial conglomerates were deposited in the Bekaa Valley (Dubertret, 1955).

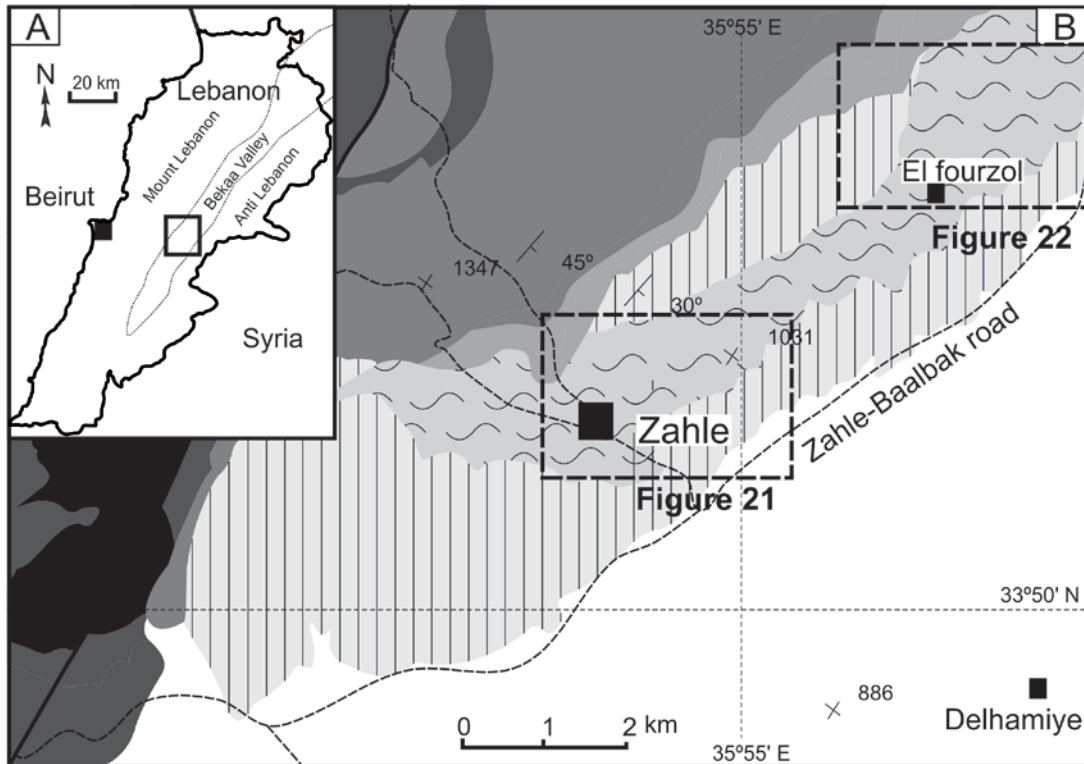
Tectonic activity in Lebanon started to decrease during the late Pleistocene time. Quaternary deposits on the coast are composed of sand or low cemented sandstone rich in quartz and carbonate grains cemented with calcite (Nader, 2014). Another type of recurrent Quaternary deposit in Lebanon is represented by red soils or “*terra rossa*” composed of red clays and quartz. This type of soil forms as a byproduct of the limestone dissolution which is very common in coastal areas at Tripoli and Beirut. Beach and dune sands are also common in many coastal areas in Lebanon. Dubertret (1955) referred to these deposits using the term “*sables littoraux*”. Quaternary alluvial and colluvial deposits are common in elevated areas within Mount and Anti Lebanon. However, calcrete soils¹ and clay surfaces occur in the Bekaa Valley (Lateef, 2007).

¹ Calcrete soil (caliche): hardened carbonate layer in the soils formed under dry conditions in arid and semi-arid regions where dissolved calcite in groundwater precipitates.

1.3 Area of Study. The Bekaa Valley

The Bekaa Valley is located at an altitude of about 900 m above sea level with a mean temperature of 19.8 °C (in Zahle). It has a width (west-east distance) of around 8-12 km with a maximum value of 25 km in Hermel (north of the Bekaa Valley) and a length (north-south distance) of 120 km (www.cas.gov.lb/ and references herein). This valley is considered one of the most important agricultural areas in Lebanon since most of it is covered with fertile soils (www.cas.gov.lb/ and references herein).

From the geological viewpoint, the Bekaa Valley is a tectonic basin representing a syncline located in the Levant area (east of Lebanon) bounded by two anticline-systems i.e. the western Lebanese anticlines forming the Mount Lebanon, and the eastern Lebanese anticline represented by the Anti-Lebanon mountain range. The Bekaa basin represents a NNE-SSW trending plain covering an area of about 900 km² (fig. 3). According to Lateef (2004), this basin is subdivided into 3 main morphostructural areas: 1) Northern area -comprising Ras el Asi and Al Hermel area, 2) Middle area which comprises the localities of Horsh and Barada and 3) Southern Bekaa which comprises Zahle and the Bar Elias plain (fig. 4).



Legend














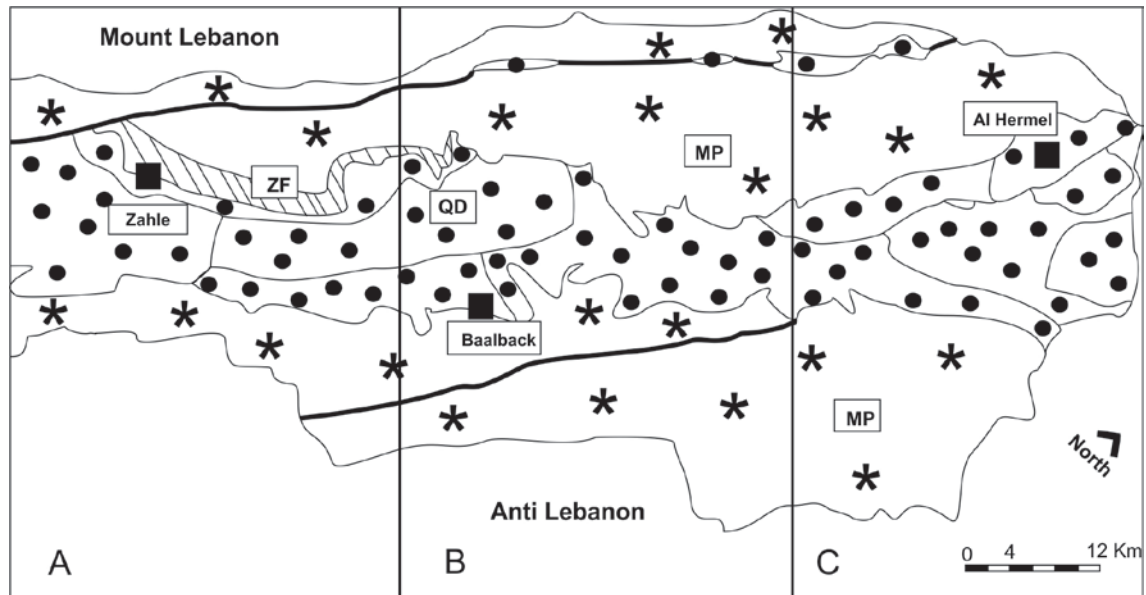
- | | | | |
|---|-----------------------------------|---|---------------------|
|  | Pliocene - Recent (Alluvial) |  | Village |
|  | Zahle Formation (Lacustrine marl) |  | Section |
|  | Miocene (Conglomerate) |  | Road |
|  | Eocene (Nummulitic limestone) |  | Faults |
|  | Upper Cretaceous (Limestone) |  | Dipping |
|  | Lower Cretaceous (Marl) |  | Elevation point (m) |
|  | Jurassic (Limestone) | | |

Figure 3: A) Map of Lebanon showing the location map of the Bekaa Valley. The rectangle delineates the areas of study B) Geologic map of the southern Bekaa Valley. Rectangles represent the two areas of study (modified from Dubertret, 1955).



Legend:

— Major faults in the area.

* Mesozoic and Paleogene rocks (MP).

● Quaternary deposits (QD).

▨ Miocene Zahle Formation (ZF) composed of conglomerates and lacustrine marls.

Figure 4: Synthetic geologic map showing the Quaternary, the Mesozoic and Paleogene deposits filling the basin and the surrounding areas. The studied lithological unit i.e. Zahle Formation is highlighted and labelled ZF in the map. A) Southern Bekaa, B) Middle Bekaa and C) Northern Bekaa. Note that the Miocene deposits illustrated in the Map represent the deposits encountered during field work and studied in the thesis (modified from Lateef, 2006).

1.4 Historical Geology of the Bekaa Basin

The Bekaa Valley is considered a mesostructural basin² composed of deposits ranging in age from Paleogene to Quaternary. This basin was created along with Mount Lebanon and Anti Lebanon ranges by the initiation of compression in Lebanon during the Late Cretaceous (Ponikarov *et al.*, 1967; Garfunkel and Ben Avraham, 1996; Brew *et al.*, 2001).

During the Late Cretaceous, the geographic area representing nowadays Lebanon was still submerged under the Tethys Ocean in shallow marine conditions. These conditions prevailed during the deposition of Cenomanian sediments represented by the Sannine Formation (Lateef, 2007). Marine conditions remained constant throughout the

² Mesostructural basin: basin of intermediate size formed mechanically by adjacent folding.

complete Turonian (Maameltein Formation). In the Senonian (Coniacian to Maastrichtian), deep marine conditions were established in the Bekaa basin and were responsible of the deposition of marl and chalks of the Chekka Formation, probably related to local subsidence of the basin. The Coniacian to Maastrichtian strata are well exposed at the south of the Bekaa Valley and decrease in thickness towards the middle part of the Bekaa; these layers are almost absent northwards. Mount Lebanon and Anti Lebanon were still under the shallow sea during this period. By the end of the Maastrichtian, Mount Lebanon and Anti Lebanon ranges emerged over the shallow ocean forming northeast (NE)-southwest (SW) elongated islands (fig. 5). The uplift of these islands proceeded until the early Paleogene. According to Lateef (2007), sediments deposited in the Bekaa basin during this period include Paleocene and early Eocene chalky limestone and middle Eocene limestone. Lower/middle Eocene facies assemblages change towards the margins of basin where characteristic fossiliferous limestone rich in *Nummulites* outstands (Walley, 1997); these fossils were classified as *N. irregularis* and *N. gizehensis* (Alqudah *et al.*, 2019). According to Lateef (2007), the thickness of this Nummulitic limestone decreases from the SW towards the NE and has a maximum thickness of 900 m in south of the Bekaa. This lateral change in thickness suggests that the sea that flooded the Bekaa Valley during the Paleogene was deeper in the southern Bekaa and shallower in the north. It also indicates that the gradient of the basin floor was directed towards the SW due to the tectonic uplift affecting the north of the Bekaa basin (Lateef, 2007). These Eocene Nummulitic limestones have a wide lateral extension; they are found in northern and southern Palestine but are absent from the coastal regions to the west where pelagic facies are abundant (Benjamini, 1995).

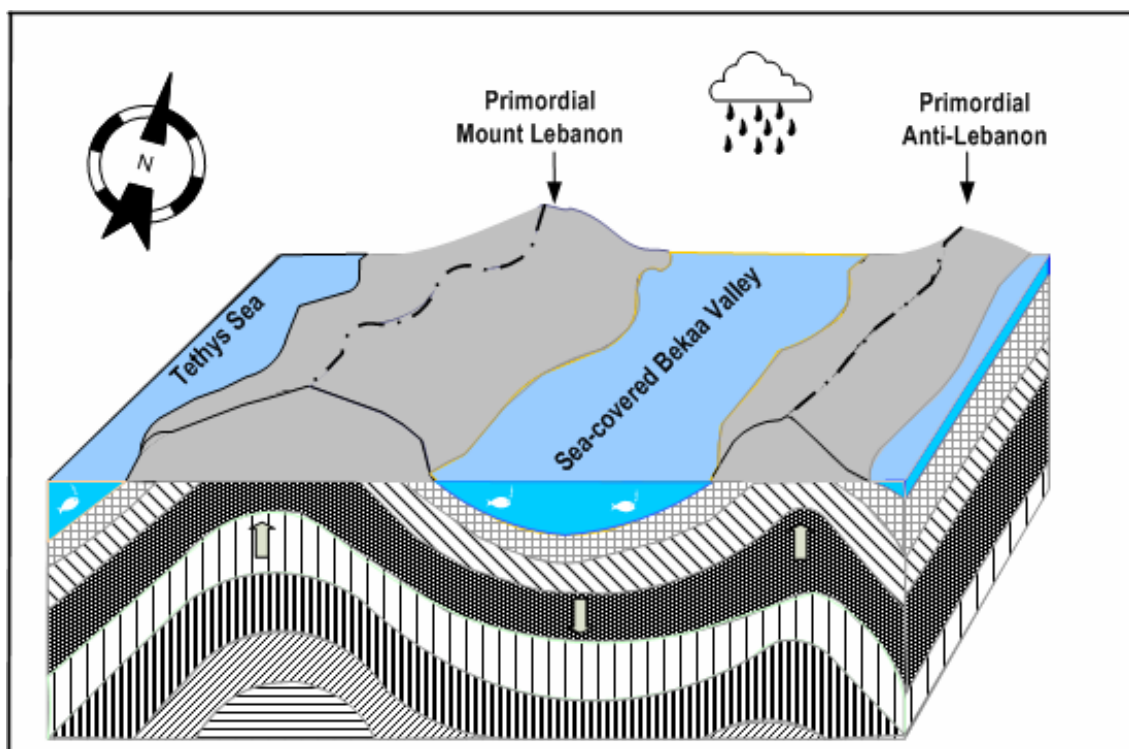


Figure 5: 3D geologic sketch showing the three morphostructural divisions of Lebanon during the middle Eocene (Lateef, 2007). Note that the western and eastern Lebanese mountain ranges had already emerged. Note the location of the Bekaa Valley flooded by the ocean forming a seaway. Note that this figure does not highlight the change of thickness explained previously in text; it just shows the location of Mount Lebanon, Anti Lebanon and the Bekaa Valley.

During the late Eocene-Oligocene, the convergence between the African/Arabian and the Eurasian plates caused further uplift of the Bekaa basin and resulted in a change from shallow marine to non-marine depositional conditions (Dubertret, 1955; Beydoun, 1999). However, late Eocene, Oligocene, and early Miocene deposits have never been identified in the Bekaa until now. The absence of these deposits within the basin have been related either to the limited budget of sediments from the fairly uplifted Lebanese mountain ranges or to the location of these deposits in deeper strata within the basin (Lateef, 2007).

With the initiation of the Dead Sea Fault System during the middle and late Miocene, the first active tectonism phase initiated in Lebanon (Quennell, 1958, 1984;

Hempton, 1987; Beydoun, 1988). Therefore, further uplift of Mount Lebanon and Anti Lebanon caused more erosion hence sediment deposition within the basin.

Simultaneously, tectonic activity during the Miocene resulted in basin sinking, increasing the accommodation space and allowing further deposition of sediments.

Alluvial fan deposits composed of poorly sorted, massive conglomerates formed in the basin margins (Walley, 1997). However, lacustrine conditions prevailed in the inner parts of the valley. At least two large lacustrine systems formed in the southern and middle areas of the Bekaa basin (fig. 6). According to Dubertert (1955), fossiliferous marls occasionally rich in organic matter were mainly deposited within these lakes. The lacustrine system at the northern Bekaa basin was shallower with higher energetic environments than the southern system. Facies include marls alternated with breccias and massive, well-lithified conglomerate strata (Lateef, 2007). According to this author, paleoenvironmental homogeneity in the Bekaa basin during the Miocene was deduced from the similarity of lacustrine depositional conditions within the different areas or subbasins (south, middle and north Bekaa). Facies assemblages of these lacustrine systems indicate that wet climatic conditions prevailed during the late Miocene in a context of Mediterranean drying salinity crisis (Lateef, 2007).

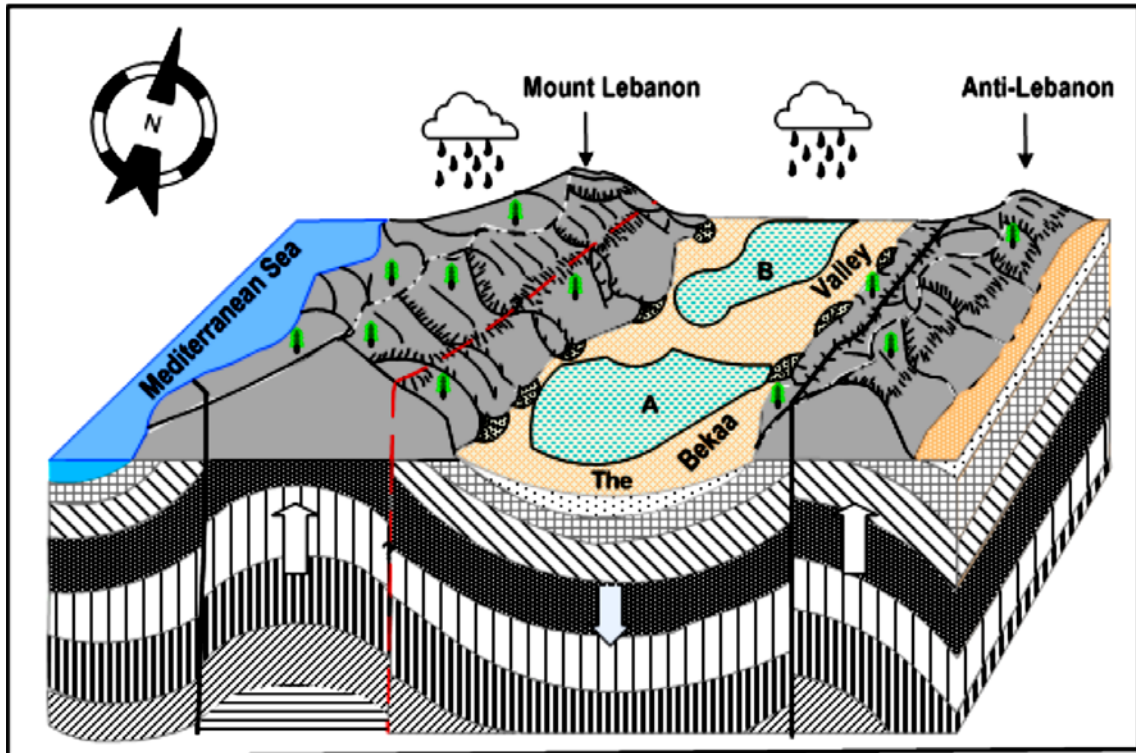


Figure 6: 3D geological sketch showing the morphostructural context of Lebanon during the middle-late Miocene. During this stage, major uplift of Lebanese ranges and down-warping of the Bekaa basin (arrows) took place in association with the appearances of some elements of the Lebanese segment of Dead Sea Fault System (red line). Note the presence of alluvial fans in both sides of the Bekaa Valley and two large lacustrine systems i.e. A) South-middle Bekaa paleolake and B) Al Hermel paleolake at the north (Lateef, 2007).

The late Pliocene marks the initiation of the second active tectonic phase in Lebanon, (Girdler and Southern, 1987). This new tectonic phase affected the Bekaa Valley and resulted in the development of two local uplifts i.e. the Tamnine and the Kneisa-Laboua structural uplifts. These two uplifts divided the Bekaa basin into three sub-basins, while the complete Bekaa basin was submerged forming one large lake (Lateef, 2007). The Tamnine uplift affected the original extension of the middle-south Bekaa lake. According to Lateef (2007), this lake progressively shrank towards the south changing the location of the depocenter. Additional folding and faulting during the late Pliocene created further small basins in the middle and north Bekaa. According to Lateef (2007), deposition of gravels prevailed on the eastern side of the middle Bekaa

basin. The western side however, was dominated by anticlines and ridges due to faulting activity. In the northern Bekaa basin, a small lake existed during early Pleistocene and early middle Pleistocene, and alluvial fans developed on its margin. Tectonic activity reached its maximum stage during the late middle Pleistocene resulting in a high elevation of the Mount Lebanon. Climatic deterioration during the late middle Pleistocene favored the development of semi-deserted conditions in the north of the Bekaa basin (Lateef, 2007). During the late Pleistocene, compressive strengths decreased resulting in a reduction of the general uplift and an erosion of the Mount and Anti- Lebanon. The southern Bekaa basin was the major depocenter for fine-grained sediments deposition. Alluvial fans of gravels dominated the eastern margin, with alteration into shallow water, wet and dry conditions. In the northern Bekaa sub-basin, channel deposits and alluvial fans were still dominant. During the early Holocene, a humid phase was dominated by abundant vegetation while during the late Holocene, deforestation and overgrazing characterized an arid phase. At about 6000-5000 B.P., climate became similar to that of present day, with coarse gravel deposition (Lateef, 2007). Wetlands in the central and south of the Bekaa persisted until historical times. Archeological studies suggest that wetlands were pretty widespread during the Roman Empire times (Sommer, 2001). Nowadays one single protected wetland i.e. Ammiq Wetland still persists in the south of the Bekaa.

1.5 Previous Studies in Neogene Deposits of the Bekaa Valley

Paleogene and Neogene rocks of the Bekaa Valley were first studied by Dubertret (1945, 1955) in the area of Zahle, who identified and described a stratigraphic set of beds termed in French “*poudingues et marnes lacustres de Zahlé*” i.e. conglomerates

and lacustrine marls. This author defined this interval as a sequence of conglomerates passing upwards to thick, finely stratified marl deposits, rich in gastropods and intercalated with thin layers of lignite. Dubertret (1945) noted that neither vertebrate fossils nor other biostratigraphically useful fossils were recovered from these deposits. However, he was able to infer a relative age of middle-upper Miocene by imprecise lithostratigraphic correlation with similar rocks exposed northwards in the basin, in the areas of Tripoli (north of Lebanon) and Homs (southwest of Syria). Walley (1997) informally referred to this sedimentary sequence as “Zahle Formation”. These deposits vary in thickness but may be as much as 1.5 km (Walley, 1997); they unconformably overlie an Eocene fossiliferous limestone bed rich in macroforaminifers i.e. *Nummulites*. Zahle Formation is composed of clastic and carbonate deposits (calcareous breccias and conglomerates, sandy silty marls, lignites, limestones and lacustrine marls), and is separated from the overlying Pleistocene fluvial conglomerates by an erosional surface (Walley, 1997).

Biostratigraphic significant fossils from Zahle Formation were first discovered by Kansou (1961) who found a horse tooth of *Hipparion* suggesting a Miocene age. Malez & Forsten (1989) described in detail and illustrated this horse tooth from Zahle and reported a new *Hipparion* fossil locality southwards near the village of Kefraya. These authors also recovered a fossil assemblage near Zahle composed of several bone and teeth remains attributed to large extinct species of herbivore mammals such as elephants, antelopes and wild pigs. An unpublished PhD thesis described in detail these deposits taking into consideration the type of facies and the fossil content (Haj-Chahine, 1973). However, these data have never been published. Haj-Chahine (1973) performed sedimentological and stratigraphic analyses of the *Pontien* (middle-late

Miocene) conglomerates and marls in Zahle region. During her work, this author described different compacted, friable and granular limestone facies. Moreover, Haj-Chahine (1973) described a microfossils assemblage composed of charophytes, gastropods (Hydrobiids and Melanopsis) as well as indeterminate ostracods. Based on the facies analysis and the microfossil remains, Haj-Chahine (1973) concluded that an aquatic quiet environment persisted in the Zahle area during the middle-late Miocene with some palustrine intervals. Recently, López-Antoñanzas *et al.* (2015) recovered several bone fragments and teeth of micromammals from one sample located at the base of the Zahle Formation nearby the Zahle town. López-Antoñanzas *et al.* (2015) described a mammal assemblage composed of rodents belonging to genus *Progonomys* and *Ctenodactylina*. According to these authors, the occurrence of this fossil assemblage is significant from the biostratigraphic viewpoint supporting the correlation with the European Mammal Neogene zones³ MN 10 or MN 11. These mammal zones i.e. MN 10 and MN 11 are late Miocene in age and they have been extensively used in many Neogene European continental basins. Sanjuan and Alqudah (2018) recently described and illustrated a complete charophyte assemblage composed of 4 species from four samples also located at the base of the lacustrine deposits of Zahle. In fact, the location of one of the lowermost charophyte samples coincides with the mammal fossil site described by López-Antoñanzas *et al.* (2015). However, the biostratigraphic distribution in Europe of the charophyte assemblage reported by Sanjuan and Alqudah (2018) does not exactly coincide with the previous biostratigraphic attribution based on mammals. These authors suggest that the lowermost part of the lacustrine Zahle Formation may be middle Miocene in age. The relative age suggested by mammals and

³ European Mammal Neogene Zones (MN): specific assemblage of mammal fossils recovered from Neogene non-marine strata in Europe.

charophytes are in agreement with the maximum age of the overlying basalts located northwards of the studied area performed by Lateef (2003). This author obtained an absolute age of 10.4 ± 0.37 Ma and 10.87 ± 0.31 Ma for the basalts pouring north of Bekaa Valley in Al Hermel region situated laterally and above the lacustrine deposits of Zahle, which corresponds to late Miocene age. In this thesis we consider that the Zahle Formation is late Miocene in age since the non-marine biostratigraphy based on mammals is more solid than the biostratigraphy based on charophytes for the Neogene.

1.6 Lacustrine and Palustrine Sedimentology

The Neogene sedimentary sequence studied in this master's thesis are mainly related to lacustrine and palustrine deposits. Hence, a brief synthesis of the main characteristics of these deposits is here provided.

Lakes are continental depressions created by a variety of mechanisms such as tectonic movements (rifting or folding), glacial processes (ice scouring and moraine damming), mass movements, volcanic activity (lava damming or crater collapse), wind deflation scour⁴ and channel abandonment forming oxbow lakes (Boggs, 2014). Lakes can be perennial or temporary. The term “perennial lake” refers to a continental depression with a continuous coverage by a water column (subaqueous conditions), whereas the term “ephemeral lake” describes a continental depression with periodic exposure of its sediments (subaqueous to subaerial conditions).

The subaqueous lake zone extends from the shoreline to the open water depocenter. The shallow water zone around the lake margin is termed the “littoral

⁴ Wind scour: erosion resulting from wind action, whereby the surface material is removed and the rock fragments carried by the wind.

zone''. Aquatic plant communities and macrophytes⁵ thrive in this well –illuminated zone (fig. 7). The littoral zone extends to depths where sunlight penetration is insufficient for photosynthesis. On the other hand, the profundal zone represents the deepest part of the lake where sunlight can hardly penetrate. The upper illuminated portion of the profundal zone is termed the pelagic (limnetic) zone and has an average depth of around 3 km with a maximum of 11 km (Gierlowski-Kordesh, 2010). The sublittoral zone marks the transition between the shallow -littoral- and the deep – profundal and pelagic- water zones. It has an average depth of 150-300 m (fig. 7). Generally, major biological processes in diluted lakes occur within this illuminated or photic zone when sufficient light penetrates promoting the growth of planktonic and benthonic algae and macrophytes (Boggs, 2014).

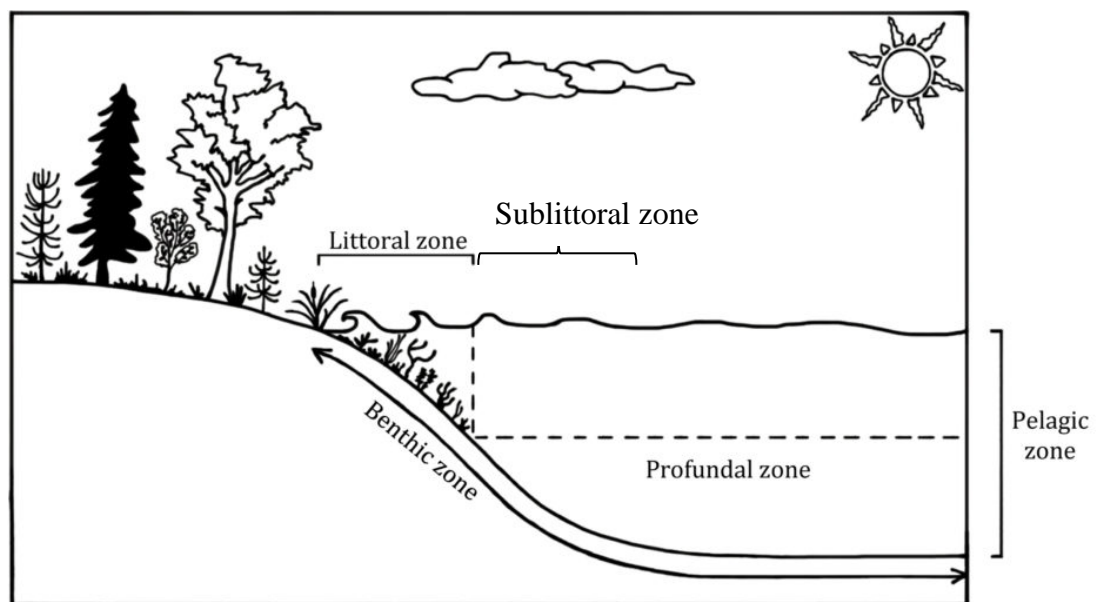


Figure 7: A 2D cross section depicting the subaqueous zones of a lake (webpage: <http://mtlakebook.org/how-lakes-function>).

From the hydrological point of view, lakes can be classified into open or closed systems. Open lake systems are common in humid climatic conditions where

⁵ Macrophyte: aquatic plant that thrives in or near the water.

continuous water inflow from rivers balance between inflow and outflow. Sediments deposited within these lakes are mainly fine-grained clastic deposits that were suspended in river waters (Einsele, 2000). On the other hand, closed lake systems are common in warm and semi-arid climates and have no surface outflow. In closed lake systems, the concentration of dissolved elements increases with time and with lowering the water table (Einsele, 2000).

According to Håkanson (2007), lacustrine sediments may have five different origins: 1) allochthonous or lithogenous particles or aggregates such as clay, silt and sand that are transported by rivers from the land to the lake, 2) autochthonous or biogenous sediments that are produced by organisms living inside the lakes such as charophytes, mollusks and ostracods, 3) hydrogenous sediments originating from material that precipitate out of solution inside the lake such as carbonates and evaporates, 4) wet and dry deposition of surface lake sediments, which generally have a very small contribution on the sedimentation process within lakes and 5) direct emission of matter from the source, which is the case of urbanism and industries.

Sedimentation within lakes is affected by physical (wind, river inflow, and atmospheric heating), chemical (precipitation of salts and carbonates) and biological (accumulation of shells and animal burrowing) processes (Boggs, 2014). Physical processes result in the input of generally fine sediments into the lake through plumes and density underflow currents. Chemical processes are more significant in closed lakes where water contains high concentration of dissolved salts. Aquatic organisms represent the main sediment producers in many lakes. They extract chemical elements from lake waters to form their shells and/or skeletons. The abundance of these organisms and their distribution is mainly dependent on the climate, water quality and type of lake substrate

(Gierlowski-Kordesh, 2010). In general, physical, chemical and biologic processes simultaneously affect sedimentation within the lacustrine system. For instance, in small lakes, plant photosynthesis increases the lake alkalinity and favors carbonate precipitation inside the system (Boggs, 2014). Carbonate deposition in lakes can also be attributed to other processes such as concentration through evaporation, biogenic mediation (including high productivity of micro- and picoplankton, microfauna shell formation, and encrustations on any substrate), water-borne clastic input, and eolian supply (Gierlowski-Kordesh, 2010 and references herein).

Palustrine sediments are shallow fresh-water deposits showing evidence of subaqueous deposition and subaerial exposure due to fluctuating water table (Alonso-Zarza, 2003). These deposits are mainly composed of carbonates, display abundant pedogenic features and are typically deposited around the margins of lakes (Alonso-Zarza, 2003). As a result of that, palustrine deposits display interbedding of lacustrine and pedogenic facies such as pedogenic carbonates, paleosols and calcretes formed by accumulation of calcium carbonates within unconsolidated carbonate-rich soils (Flügel, 2004). These carbonates form by the precipitation of calcium carbonate from groundwaters, surface or groundwater-fed rivers and lakes (Alonso-Zarra and Wright, 2010). The depositional setting of palustrine carbonates is characterized by very low gradients of the lake margin and low hydrodynamic energy. Under these conditions, fine-grained carbonates (mainly mud) formed in fresh water commonly contain the remains of biogenic particles e.g. encrusted charophytes stems and shells of mollusks and ostracods. These sediments are then subjected to subaerial exposure related to fluctuations in water level and are modified by pedogenic processes, giving rise to a variety of palustrine facies (Freytet and Verrecchia, 2002; Alonso-Zarra and Wright,

2010 and references herein). Many palustrine carbonates in the geological record are associated with shallow, hard-water perennial lakes and represent deposition on fluctuating vegetated wetland fringes (Alonso-Zarra and Wright, 2010). According to these authors, palustrine deposits can be recognized by identifying several sedimentary and diagenetic features such as nodulisation, pedogenic recrystallisation, desiccation cracks and traces of burrows and roots. Considering all the sedimentary and diagenetic features, Alonso-Zarra (2003) defined 12 types of palustrine facies assemblages (fig. 8).

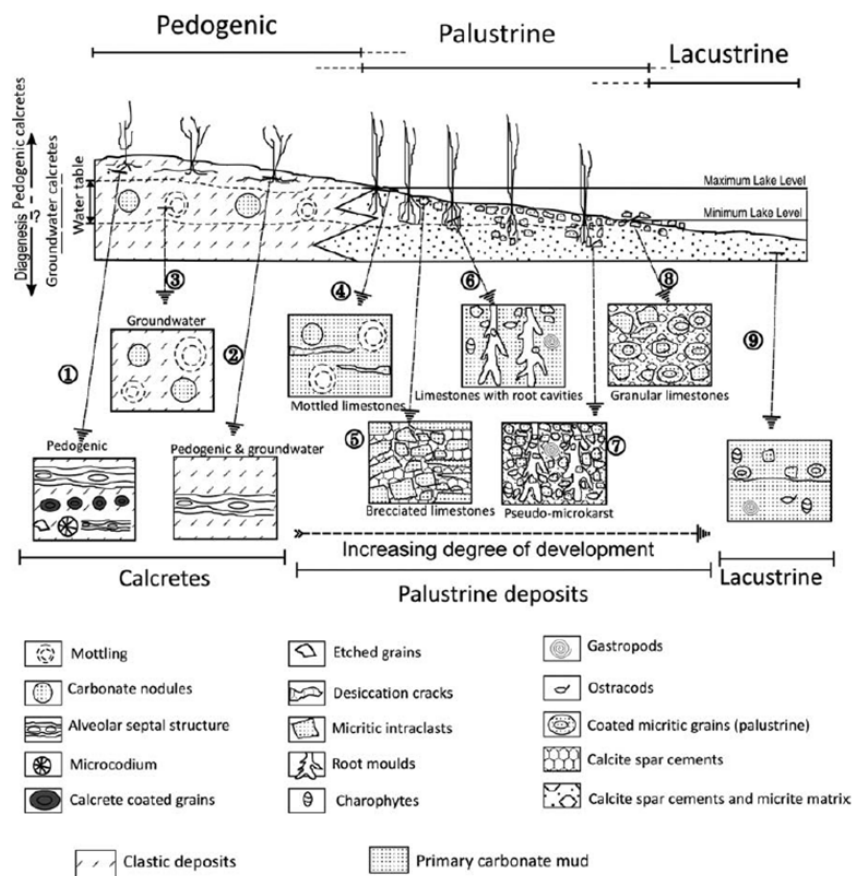


Figure 8: Palustrine-calcrete facies associations and their common petrographic aspect (Alonso-Zarra and Wright, 2010).

1.7 Micropaleontology

Micropaleontology is a branch of the paleontology that studies microfossils.

Microfossils are tiny tangible remains of organisms that lived thousands or millions of

years ago. In order to study the microfossil's morphology and characteristic details, the use of a microscope is a prerequisite. Microfossils are by far the most abundant of all fossils. Several groups of micro-organisms produce mineralized hard structures (shells, carapaces, tests or frustules) that fossilize (Javaux and Benzerara, 2009). These organisms can be so abundant that in some places they can form thick accumulations of pure fossil remains. For example the Chalk Cliffs of Dover (south of United Kingdom) is a hundreds of meter thick rock interval exclusively composed of microfossils.

Changes in the abundance and type of microfossils from year to year over millions of years of uninterrupted accumulations in sedimentary basins, makes a detailed record of climate change, plate tectonics and biological evolution (Moore and Echlos, 1979). Microfossil data reveals changes in the sea levels and temperature. Because of their size, high evolutionary ranges and abundance, many groups of microfossils are vital for oil exploration providing data about the relative age of sediments, source rock characteristics and organic matter origin (Moore and Echlos, 1979). According to these authors, microfossils are derived from five main parts of the organic world i.e. (1) complete skeletons of microorganisms such as foraminifera and ostracods, (2) individual elements from composite skeletons such as the plates or spines of echinoderms and coccoliths from coccolithophores, (3) spores and pollens from plants, (4) small but identifiable fragments of colonial organisms such as bryozoans or stromatoporoids and (5) immature individuals or minute adults of groups usually studied as microfossils such as mollusks or brachiopods.

Micropaleontologists and paleontologists rely on evidences such as fossil animals and plants to understand when has the fauna or flora existed, how did they look like, and how did they manage to survive and in which environment (Benton and

Harper, 2009). They draw hypotheses based on their knowledge of the geological time scale and fossil species. Then, they summarize and communicate precise data to statistically test these hypotheses and draw conclusions about evolution and extinction of various species.

1.7.1 *Microfossils in Lacustrine Deposits*

Microfossils extracted from lacustrine deposits near Zahle can be classified in 3 main groups: 1) charophytes, 2) ostracods and 3) mollusks. Minor amount of vertebrate remains have also been recovered from the studied sections.

1.7.1.1 Charophytes

Charophytes are submerged aquatic plants colloquially termed “stoneworts”. They grow forming dense meadows in freshwater or brackish water environments such as perennial or temporary lakes, ponds, estuaries and swamps (García, 1994; García and Chivas, 2006). Charophytes are of little direct importance to humans. However, they are essential for aquatic ecosystems providing food and habitat to many species of fish and other aquatic organisms. For example, several species of aquatic birds belonging to the Anatidae family (ducks) have their diet based on charophytes (Soulié-Märsche, 1989). Charophyte meadows frequently calcify and their remains accumulate as calcium carbonate deposits. These deposits may be so extensive that they form the major part of the calcareous marl of lakes (Gierlowski-Kordesch, 2010). The vegetative structure of charophytes superficially resembles some higher plants. They have root-like rhizoids and whorls of branches at regular intervals forming nodes and internodes (fig. 9). Charophyte stems or thalli can show certain degree of complexity being covered by

several types of vegetative structures such as cortical cells and spine cells located in the internodes and stipuloides located in the nodes (fig. 9).

During the sexual reproduction, the organs involved are the antheridium which contains one small biflagellate sperm and the oogonium (oosporangium) containing one large egg (Feist *et al.*, 2005) (figs. 9 and 10). The oogonium consists of five spiral cells (fig. 10). These cells are joined at the apex along a broken line, and the base of the oogonium is closed by one to three sister cells which constitute the basal plate. The apex is surrounded by one row of five coronular cells (fig. 10). After the fertilization process, the oogonium forms an organic resistant structure i.e. the oospore which is composed of sporopollenine and cellulose (Feist *et al.*, 2005). Overlying the oospore, the oogonium can produce a biomineralized layer termed gyrogonite. Gyrogonites are small calcified fructifications ranging in size from 0.25 mm to 2 mm. The gyrogonite consists of calcium carbonate that is deposited in both the enveloping cells (i.e., spiral cells) which spiral around and enclose the oospore, and the basal plate, representing the calcified sister cell of the oosphere (Feist *et al.*, 2005).

The calcine is the main constituent of the gyrogonite and the calcification process occurs inside the cell cytoplasm i.e. intracellular calcification (fig. 10). The calcine is differentiated into two zones, the internal one or endocalcine, having concentric organic lamellae, and the exterior ectocalcine which is massive and generally devoid of lamination (Feist *et al.*, 2005). A single plant can produce more than one hundred gyrogonites in one growing season. Thus, fossil gyrogonites are very abundant and easily recoverable microfossils in lacustrine and palustrine deposits. The applications of fossil gyrogonites are variable providing valuable insights into non-marine biostratigraphy, paleoecology, and paleobiogeography (Soulié-Märsche, 1989;

Garcia, 1994; Schneider *et al.*, 2015 and references herein). Gyrogonites frequently fossilize and have been traditionally used as biostratigraphic markers for non-marine deposits (Feist *et al.*, 2005). Moreover, they are known from the Silurian to the present (Soulié-Märsche, 1989). Thus, the classification of fossil charophytes is based on several parameters of the gyrogonite i.e. the general shape (fig. 11), number of convolutions, general dimensions (i.e. gyrogonite height and width), apical structure, basal structure (shape and type of basal pore and plate) and ornamentation of the spiral cells (Feist *et al.*, 2005 and references herein).

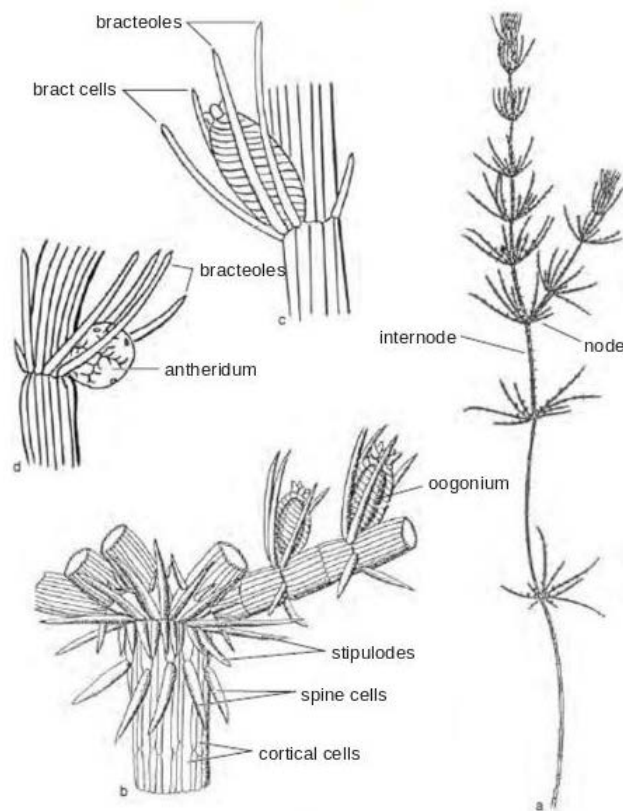


Figure 9: Vegetative parts of a charophyte. a) Complete charophyte showing the plant structure divided in nodes and internodes (real scale), b) Detailed draw of a node showing the stipulodes, the corticated cells, the female reproductive organ (oogonium) and spine cells (23 X magnifications), c) Detail of the oogonium (40 X magnifications). d) Detail of the antheridium being the male reproductive organ at 40 X magnifications (Feist *et al.*, 2005).

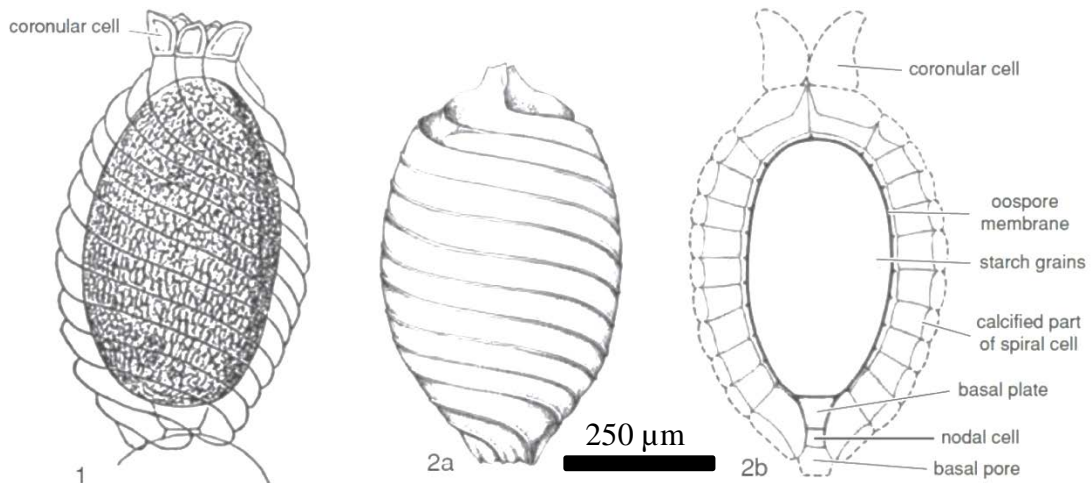


Figure 10: Female reproductive organs of a charophyte (40 X magnifications) 1) Oospore, 2a) Outer morphology of a gyrogonite (calcified oospore), 2b) Longitudinal section of a gyrogonite showing its internal structure; dotted lines represent the uncalcified parts of spiral and coronular cells that do not calcify (Feist *et al.*, 2005).

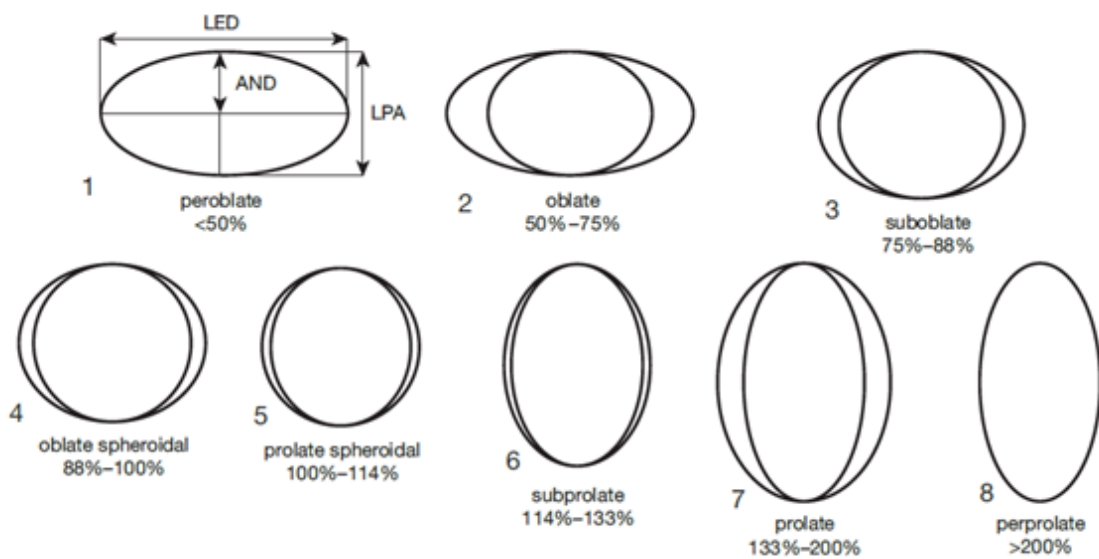


Figure 11: Terminology of gyrogonite shapes used in this master's thesis. Percentages represent the isopolarity index i.e. $LPA/LED \times 100$. *LPA*, length of polar axis; *LED*, largest equatorial diameter; *AND*, distance from apical pole to LED (Feist *et al.*, 2005).

1.7.1.2 Mollusks

Mollusks represent the second largest group of invertebrate animals after insects.

Fossils of mollusks have been recovered from very old sedimentary rocks dated as

Cambrian in age (Parkhaev, 2007; Sigwart and Sutton, 2007). Mollusks are aquatic or

terrestrial animals that extract calcium and magnesium from their surrounding environment to produce their shells (biomineralization). Shells of mollusks can be composed of calcite, aragonite and/or Mg-calcite (Marin and Le Roy, 2012).

Bivalves and gastropods represent the main type of mollusks currently thriving in lakes. They live in the littoral, sublittoral, and deeper aerobic settings. The soft body or mantle of gastropods and bivalves is rarely preserved in the fossil record. Hence, paleontological studies are based on their hard calcified shell. A Gastropod shell consists of a single and spiral calcified tube. It is helically coiled and composed of whorls (figs. 12 and 13). In most species, the whorl is cemented into the preceding whorl and simultaneously overlapping it (Savazzi and Sasaki, 2004). The gastropod systematics is based on several shell parameters i.e. the general shape (fig. 12), general dimensions (i.e. shell height and width), aperture shape, shell ornamentation, suture type and the umbilicus diameter. The larval shell or protoconch⁶ features are also considered in the classification of many gastropod groups (Smith, 2005). Several gastropod groups possess, attached to the upper surface of the foot (muscular structure of the mantle), an organic or calcified structure termed operculum that closes the aperture of the shell when soft parts of the animal retreats into it.

A bivalve shell is composed of two bilaterally symmetrical valves which are attached at the dorsal hinge (Coan and Valentich-Scott, 2006). The shells are simple and consist of two rigid valves free to rotate around a hinge axis (fig. 14). The valves can be closed by means of the adductor muscle and opened by an elastic ligament. Bivalves are classified in base on their shell shape, size (i.e. shell height and width) and ornamentation (Newel, 1969). According to this author, other key parameters used in

⁶ Protoconch: first or original shell of a mollusk. It represents the embryonic stage of the animal and may show features different from those of other parts of the adult shells.

bivalve systematics include the type and position of several internal features such as teeth, hinge and muscle scars.

In both gastropods and bivalves, the shell protects the soft animal parts from predators (Vermeij, 1977a, 1993; Bengtsson, 1994). Gastropods and bivalve's shells grow by marginal accretion or buildup (Sälgeback, 2006). Spines, knobs and ribs can cover different parts of the shells of both groups. Spines are often used by the animal as a protection against predators and to accumulate sediment and other debris on top of the shells for protection (Palmer, 1979; Sälgeback, 2006). Knobs often increase the stiffness of the shell, making it more resistant against deformation, especially compression (Vermeij, 1993).

Freshwater aquatic mollusks are very good environmental indicators and can be used to infer limnological⁷ and regional climatic conditions such as changes of temperature, seasonal changes, productivity and changes in depth and water chemistry (Udomkan *et al.*, 2003; Anadón *et al.*, 2008). Geochemical analyses based on stable isotopes and trace elements of non-altered carbonates in mollusk shells have been used to infer past environmental and climatic conditions (Johnson *et al.*, 2009; Eerkens *et al.*, 2013). Terrestrial mollusks have also been used as a paleoclimatological proxy to assess changes in relative humidity in specific areas (Balakrishnan *et al.*, 2005; Colonese *et al.*, 2007).

⁷ Limnology: the study of lakes.

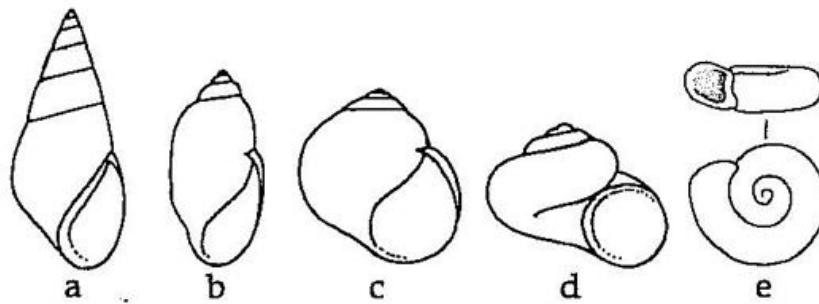


Figure 12: Lateral views of gastropod shells showing different shape types. a) Elongate conic, b) Elongate cylindrical, c) Globose, d) Depressed and e) Discoidal (Smith, 2005).

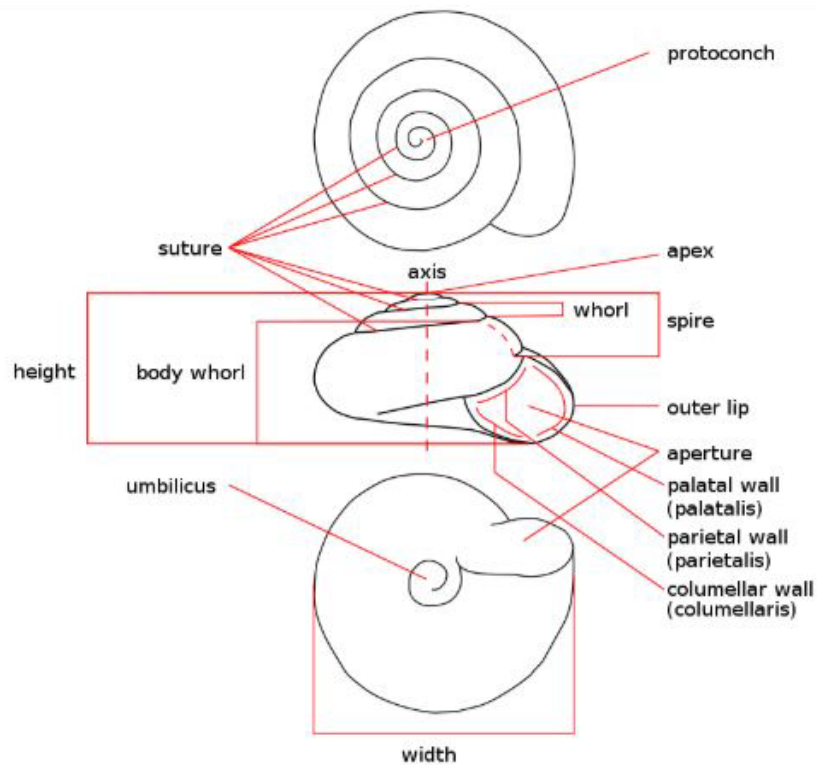


Figure 13: Morphological features of a gastropod shell. Upper image: dorsal view showing the whorls and the apex where the protoconch or larva shell is located. Central image: lateral view showing the profile of the shell and the aperture structure. Lower image: basal view showing the umbilicus in the center (from: <http://www.wikiwand.com/en/Gast>).

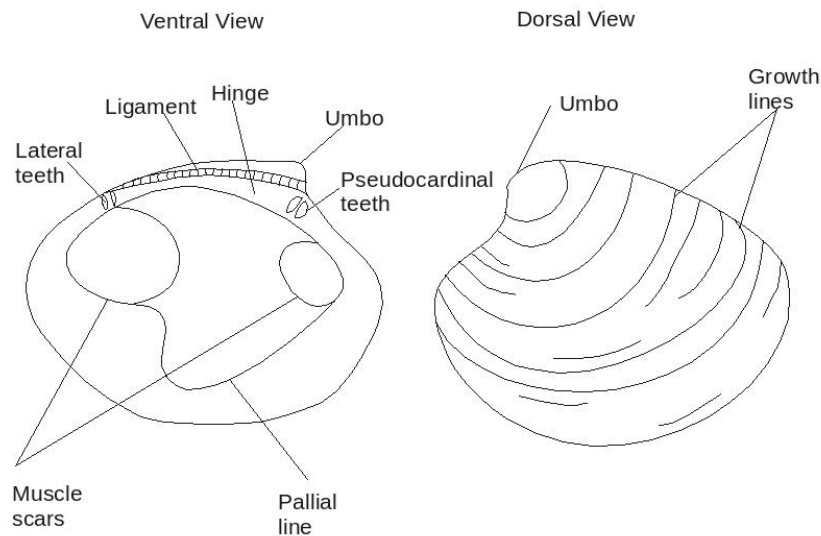


Figure 14: Sketch of a bivalve shell showing the main morphological features of the inner (left image) and outer (right image) shell (modified from Cesari and Pellizzato, 1990).

1.7.1.3 Ostracods

Ostracods are small bivalved crustaceans known colloquially named “seed shrimp” or “mussel shrimp”. They are a large class of mostly microscopic crustaceans ranging in size between 0.25 mm such as the species *Microcythere minuta* to 30 mm of some species of the genus *Gigantocypris* (Ruppert *et al.*, 2004). However, most species reach a size of about 1 mm in length (Ozawa, 2013). Ostracods live on or near the bottom of the sea/lake floor and are associated with aquatic vegetation. They are considered one of the most primitive groups of living crustaceans. Fossil ostracod carapaces have been recovered from sedimentary rocks as old as upper Cambrian (Meisch, 2000). Taking into account the current and fossil species, ostracods represent one of the invertebrate groups with highest diversity. About 60 thousand ostracod species are known (Meisch, 2000), most of which (over 50 thousand species) however, are fossil species (Karanovic, 2012). About 8000 living species have been described (Meisch, 2000); 2000 of the described species live nowadays in freshwater aquatic

environments (Raj, 2017). Because of their diversity, their wide ecological distribution in aquatic habitats and their extensive fossil record, ostracod shells have been used in a wide variety of scientific disciplines such as ecology/paleoecology, developmental biology, genetics, morphology and paleontology (Martens and Horne, 2000).

The ostracod carapace consists of a bivalve 'shell' enveloping the entire ostracod's soft body, making them look like small seeds or mussel (Ozawa, 2013). According to Namiotco *et al.* (2011b), the two main parts of the animal soft body are the anterior head (cephalon) and the posterior trunk (composed of the thorax and abdomen). Ostracods possess seven limbs (or appendages) being from the anterior to the posterior part: the antennula, the antenna, the mandibula, the maxillula and three trunk limbs that differ in structure and function between different taxa (Namiotco *et al.*, 2011b). The structure, shape and arrangement of these appendages are used by biologists as taxonomically diagnostic features. However, appendages and other soft body structures are rarely preserved in the fossil record. Hence, fossil taxonomy relies solely on the carapace features (fig. 15).

The two ostracod valves (carapaces) are articulated along the dorsal hinge (fig 15). Throughout their life, ostracods change their shells up to 9 times while changing their morphology from larva to adults (Ozawa, 2013). Moreover, several species of ostracods display a marked sexual dimorphism resulting in different shell morphology between males and females. For the taxonomic classification, micropaleontologists must take into account the interior and the exterior sides of the valve. The main taxonomic shell feature of the interior side of the valve is the adductor muscle scar. Adductor muscles are located in the centre of the body and are responsible for the closure of valves (Raj, 2017). These muscles are attached to the inside of the valves, forming a

characteristic scar on the central part (fig. 15). Other features such as the shape of the vestibulum (cavity housing reproductive or digestive organs), radial pore canals and the flange can also have taxonomic value. The exterior valve surface is usually covered in pores of tiny canals that cross the shell. The valve surface may be smooth or may carry ornamentations such as pits, spines, tubercles and ridges. In some groups such as *Ilyocypris*, the exterior valve surface displays conspicuous depressions known as sulci (fig. 72 G and H). Valve ornamentation is often sexually dimorphic (males normally show larger ornamentation features). Moreover, carapace features may vary greatly between individuals or populations, depending on environmental constraints (Meisch, 2000).

Many ostracod species are able to survive stressful environmental conditions in a dormant state or as drought-resistant eggs (Frisch *et al.*, 2007). This property enables ostracods to be easily dispersed by aquatic animals and birds, thus having a wide geographic distribution (Frisch *et al.*, 2007). However, some ostracod species have narrow environmental preferences representing a significant group for monitoring marine and freshwater conditions. Fossil ostracod valves have been used as paleohydrological and paleoclimatic indicators of water temperature and salinity (Gobert, 2012).

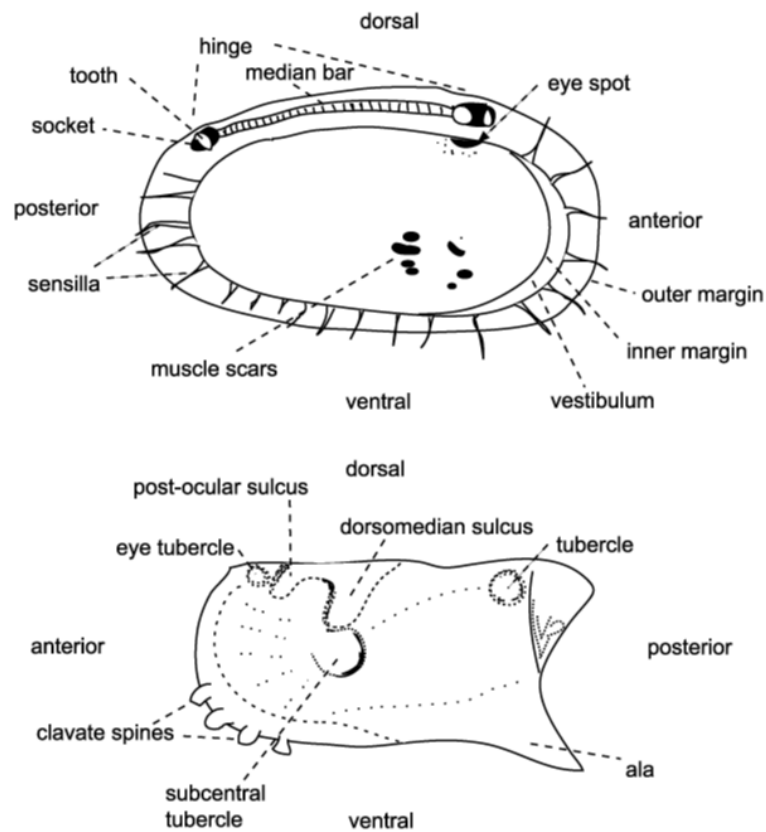


Figure 15: Sketch showing the main morphological features of two different idealized ostracod carapaces. The image located above represents an interior shell. The image below represents an exterior shell (Horne *et al.*, 1990).

1.7.2 *Paleoecology and Taphonomy*

Paleoecology is known as the ecology of ancient times (Carlton, 2008).

Palaeoecologists rely on empirical information extracted from fossils (biotic components) and their enclosing sedimentary rocks (abiotic components) to understand the relationships between different organisms of a certain community and their surrounding environments (Benton and Harper, 2009).

Two simultaneous analyses must be considered in a paleoecological reconstruction: 1) the study of the abiotic components (characterization of the depositional environment taking into account the rock lithology, sedimentary structures and rock textures) and 2) biotic components such as the fossil assemblage and the

taphonomical analysis (fig. 16). Taphonomy is the study of all processes (biological, physical and chemical) affecting an organism after its death until its fossilization (Lyman, 2010). Taphonomical analyses are essential in order to ascertain the origin of the fossil remains preserved within the sediments (Carlton, 2008). In fact, fossils are not always preserved in their original living environment and may suffer a complex history before their final fossilization (Benton and Harper, 2009). According to these authors, this history may include the decay of soft organic parts, transport, fragmentation as well as chemical and physical changes after the burial.

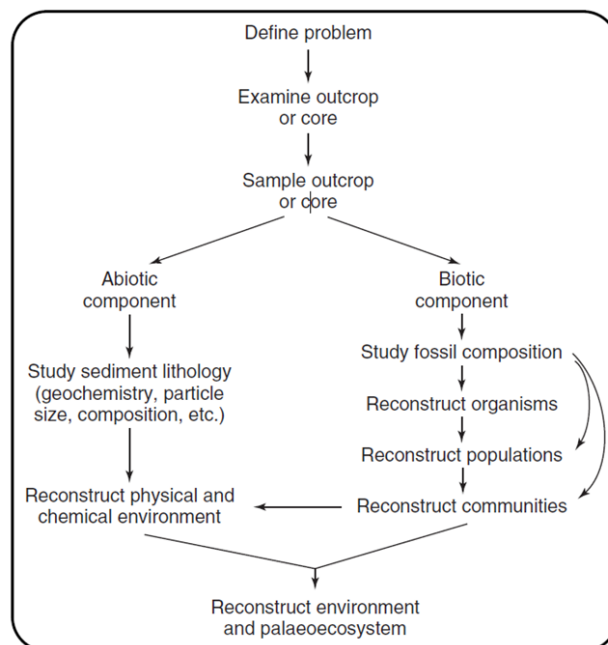


Figure 16: A flowchart showing the different steps of a paleoecological reconstruction (Birks and Birks, 1980).

Paleoecologists mainly aim to: reconstruct past environment in a specific area, infer the lifestyle of extinct organisms based on fossil taxonomy and taphonomy, understand ancient communities of organisms and their interaction with each other as well as with their environment, and document long-term changes in ecosystems (Carlton, 2008).

CHAPTER 2

METHODOLOGY

2.1 Planning and Outcrops Exploration

2.1.1 *Bibliography and Map Consultation*

Fieldtrip performed in the Bekaa Valley were carefully planned several days beforehand. Geologic and geographic maps were checked in order to access accessibility to studied outcrops. These maps were printed for later fieldwork. Specific and general scientific works including bibliography, existing maps and archives were also consulted. Required geological equipment and tools (hammer, shovel, magnifying lenses, Jacob bar, meter, plastic bags and permanent markers) were used for the purpose of stratigraphic logging and samples collection.

2.1.2 *Geologic Exploration*

Before the actual geological study of the selected outcrops near Zahle town, prior reconnaissance trips of the nearby areas were performed. Many paths were taken and many outcrops were assessed/evaluated to select the most representative ones for this work. Many difficulties were faced during exploration fieldtrips such as damaged, non-accessible or highly urbanized ones. It is also important to note that parts of the here-studied stratigraphic sections (several meters of the section 3) and the complete section 5 are no longer available since new buildings have been constructed since then.

2.2 Fieldwork

2.2.1 Field Tools and Equipment Used

The field equipment used during fieldtrips consisted of: 1) GPS to locate the outcrop on the map and record its coordinates, 2) a compass to measure bed orientation and inclination, 3) a hammer to collect soft and hard samples, 4) a tape-meter and Jacob staff to measure the height of the studied strata, 4) a magnifying lens to evaluate the grains size/texture and presence of microfossils, 5) an HCl bottle (HCl, 0.1 M) to test for calcite/limestone solubility upon effervesence, 6) regional geologic and geographic maps to locate specific outcrops and follow specific roads, 7) a notebook and pencils to draw the stratigraphic logs and take notes *in situ*, 8) plastic bags to fill in soft and hard samples for later laboratory work, 9) permanent markers to label the bags and the hard samples of rocks and 10) a camera (or phone camera) to take pictures of the complete outcrops, intervals within the outcrops, and sedimentary structures characteristic of specific layers.

2.2.2 Field Techniques and Fieldwork

A general sedimentological/stratigraphical approach at each outcrop was first performed with the aim to describe its general color, lithology and texture as well as strata orientation. Using the GPS, each exposure was located and its coordinates and elevation were noted down. Stratigraphic logs were then prepared and sketched in the field. First, the thickness of each stratum was measured using a meter or a Jacob staff. Then, a detailed sedimentological study considering the rock lithology, grains size and shape, fabric, sedimentary structures and fossil content was performed for each

stratigraphic section *in situ*. General and detailed photos were taken to illustrate different facies assemblages. The stratigraphic logs were later digitized using the Corel Draw software. In order to better describe the fabric and type of porosity of a thick limestone interval in section 1, one hard sample (ZL) was extracted and examined under the microscope. This sample was labeled and marked with an arrow showing the way up within the section (stratigraphic polarity). On the other hand, soft rock samples were treated in the laboratory with the aim to recover the microfossil assemblage. Accordingly, two kilograms of soft sediments were extracted using a hammer and a shovel placed inside plastic bags that were labeled using a permanent marker. In order to recover vertebrate remains, about 500 kg of sediments were extracted from samples Z-8 and Z-16 with the help of Drs. Raquel López-Antoñanzas, Fabien Knoll and George Kachacha. This large amount of sediment was extracted using a driller (fig. 17). Sediments were later washed and then dried in the Berdawni River near Zahle.



Figure 17: Picture of Drs. Fabien Knoll and George Kachacha extracting about 500 kg of sediments from sample Z-8 at section 3. Note that they are using a driller instead of a hammer to be able to extract large amount of sediments.

2.3 Labwork

2.3.1 *Soft Samples Treatment*

Collected soft samples (23 in total) underwent a long treatment process. This process took around a complete full-work week for each sample. Each plastic bag was first emptied inside a plastic container labeled with the appropriate sample's name. Afterwards, the indurated blocks of rocks were gently crashed and cleaned from organic debris, roots and other undesirable trash (fig. 18).



Figure 18: First stage of the sample treatment. Graduate students are removing the undesirable remains and crushing the indurated rock blocks.

Each sample container was filled with the sediment and a solution composed of water mixed with 100 ml of hydrogen peroxide (H_2O_2) and 3 grams of sodium carbonate (Na_2CO_3). This solution helped in the disintegration of the soft muddy rocks destroying the organic matter. For safety reasons, the sample manipulation was performed using a laboratory coat and plastic gloves. Each sediment and solution mixture was kept for at least three days. Samples were mixed several times each day to facilitate the sediment disintegration. Once samples were well disintegrated, they were sieved to separate the microfossils (shells, fragments of bones, carapaces) from the undesirable mud particles. Standard sieves of different mesh apertures (2mm, 0.8mm, 0.6mm, 0.3mm, and 0.2 mm) were first submerged in a blue tint solution (water and Methylene Blue Powder) and later washed. This process aims to identify contaminated grains from previous samples. The sieves were then placed on top of each other following the appropriate order from the finest to the largest mesh aperture. Each

sample was continuously washed with water to remove fine muddy particles which percolate through each sieve. After the sieving process, each sediment fraction was left to dry on a labeled newspaper. The process of water cleaning was repeated for the different sieves sizes. After few days, the dried sediment fractions (leavigates) were placed inside small plastic boxes labeled with the sample name and size. By the end of this process, samples were ready to undergo the next stage.

2.4 Microfossil Treatment

Dried sediment fractions (leavigates) were checked for biogenic structures such as microfossils and other remains. Few grams of sediments were scattered on a plate several times to extract the microfossils. Microfossils were picked out using a wet thin brush under a binocular light microscope (fig. 19). For the so called “picking process” a high degree of precision is required. The extracted shells were placed inside small special boxes (sample carrier) that were labeled with the sample number and fraction size (fig. 19).

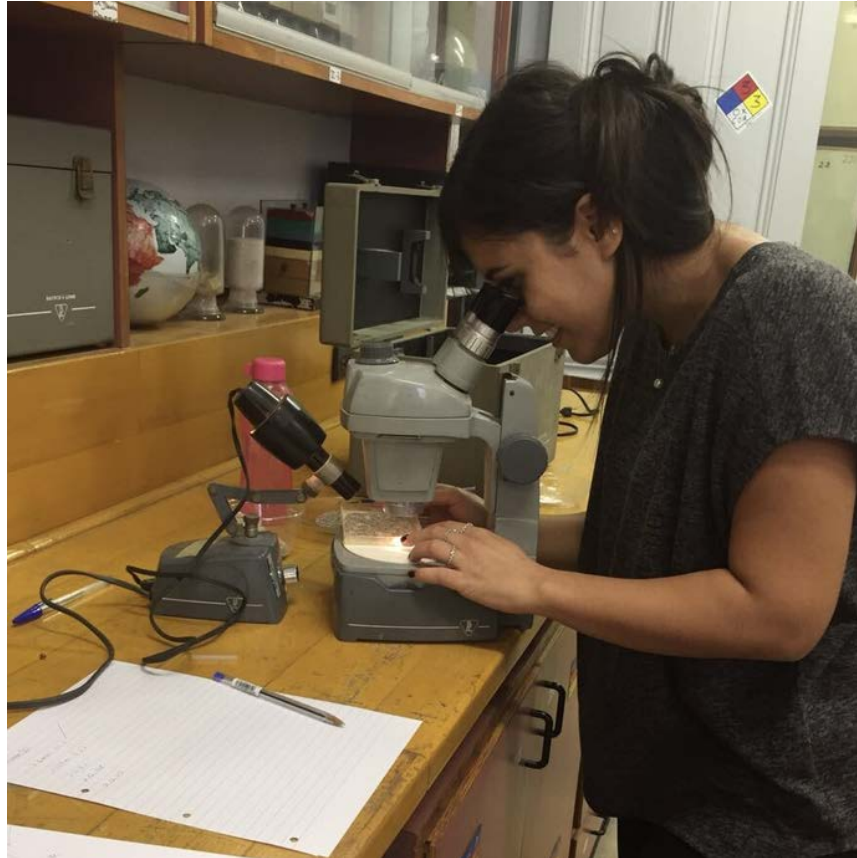


Figure 19: Picking process using binocular of microfossils from the scattered grains placed on a plate with a fine brush while light is directed towards the grains.

This process was repeated several times for each leavigate (minimum 3 times) and for each sample. The relative amount of microfossils picked out from the 23 samples is based on a semi-quantitative visual estimation (Tables 1 and 2). This process took by far most of the sample treatment time. Many hours a day after a complete year were required to pick out all microfossils studied in this thesis. After the picking process, selected microfossils were prepared for the SEM (Scanning Electronic Microscope) study. For this purpose, the most representative and best preserved microfossils were selected and later glued on a bio-adhesive stick placed on a circular stub. Several individuals were selected for each species in order to study all the 3D features. For

example in case of the charophytes, 3 different views (apical, basal and lateral) are required for the taxonomic classification.

Once in the AUB Central Research Science Laboratory (CRSL) facilities, each stub was placed in the metal coater equipment Quorum Q150T. A gold coating program (Gold PTF, 2 μm) was selected for each sample. After the coating process, stubs were placed in the SEM MIRA 3LMU. With the help of the CRSL technician Rania Shatila, the microfossil assemblage was examined in great detail and many morphometrical parameters were studied. Many images were taken for each recovered taxa (fig. 20).

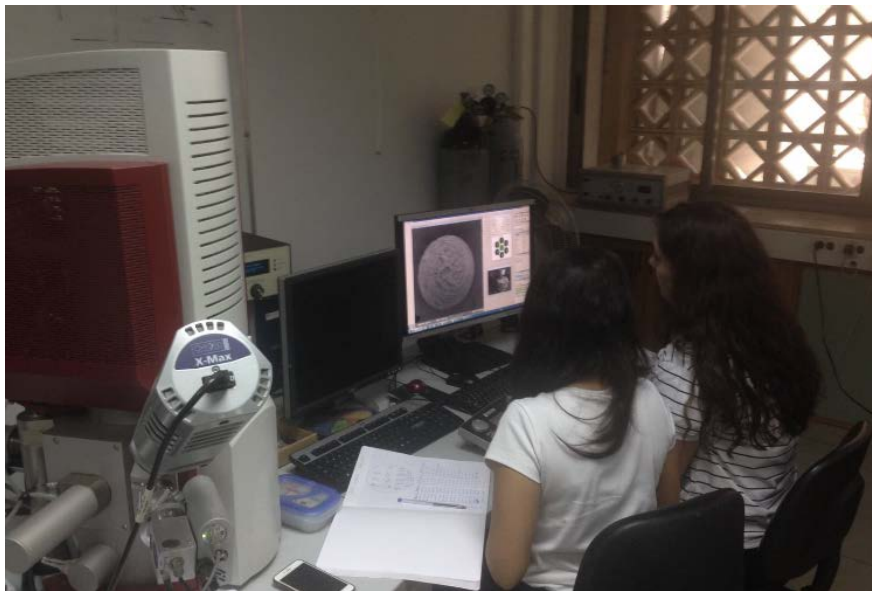


Figure 20: Graduate students describing microfossils and taking photographs during a SEM session in the CRSL.

Selected SEM photos were later edited using specific softwares such as Adobe Photoshop and/or Corel Draw. Several specimens of each species were photographed and later measured. A large number of charophyte gyrogonites were measured by Dr. Sanjuan during his research stay in Barcelona University. He used the software Motic Images Plus 2.0 ML in a stereomicroscope Motic BA310 housed in the Department of

Earth and Ocean Dynamics (Barcelona University). Several plates were later prepared to illustrate the fossil assemblage recovered.

The classification of the microfossil assemblage was performed using specific bibliography, taxonomic books and expert opinion. Many problems were faced regarding microfossil taxonomy because of a lack of accessible literature and few taxonomic keys and books for the correct identification. Besides the problem of a lack of literature, these groups of microfossils often display intraspecific variations. Hence, three micropaleontologists from different European institutions were consulted i.e. Dr. Thomas Neubauer who is an authority in freshwater mollusk taxonomy and ecology, Dr. Jonathan Holmes who is an expert in Neogene ostracod taxonomy and Dr. Raquel López-Antoñanzas who is an authority in Neogene micromammals taxonomy and phylogeny.

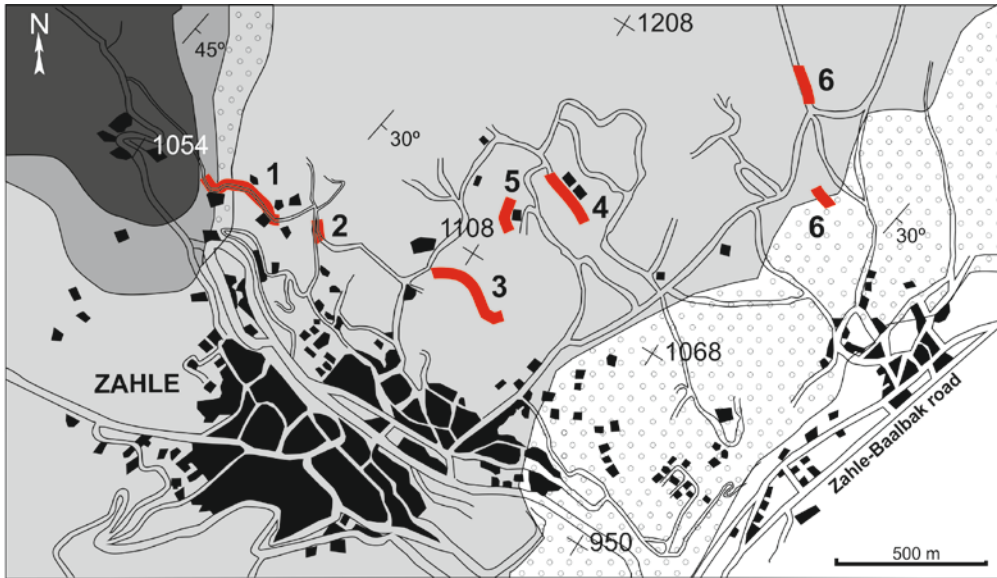
2.5 Cabinet

On a regular basis during the whole thesis work, meetings with the advisor were designed. The cabinet meetings were essential to manage and organize the entire work, meet the deadlines and organize all the fieldtrips. The advisor helped in the clarification of many concepts and techniques regarding fossil taxonomy and communicated with external authorities. These regular meetings successfully contributed to the accomplishment of this work and the completion of the thesis aims.

CHAPTER 3

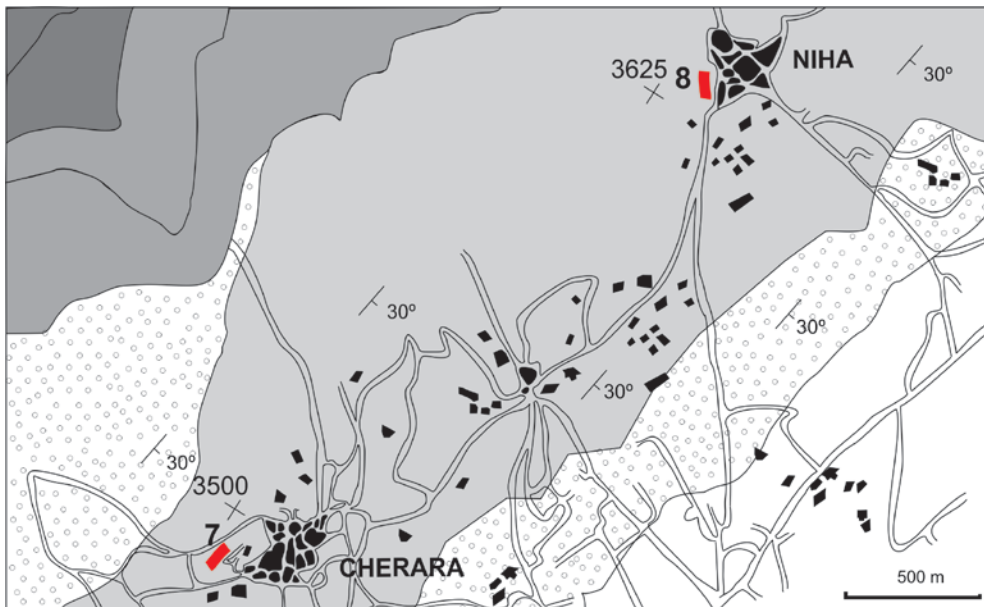
STRATIGRAPHY

Eight stratigraphic sections were constructed from different areas near the town of Zahle and villages of Niha and Cherara (east margin of the Bekaa Valley) following the basic stratigraphic principles i.e. original horizontality, superposition, strata continuity and cross-cutting relationships. The first three sections (section 1, 2 and 3) are stratigraphically arranged on top of each other and can be tentatively correlated (fig. 40). The section 1 is located at the base and lies directly above an Eocene Nummulitic limestone bed (fig. 24). Sections 4, 5, 6, 7 and 8 were performed from different stratigraphic positions within the Miocene nearby deposits (fig. 21). Section 6 represents the uppermost log showing the contact with the upper Pliocene fluvial conglomerates. Sections 7 and 8 are located northwards from the previous sections, near the villages of Niha and Cherara (fig. 22).



Legend

- | | |
|--|---------------------|
| Pliocene - Recent (Alluvial) | Buildings |
| Lacustrine marls, limestone and lignites (Miocene) | Sections |
| Conglomerate and red mudstone (Miocene and Pliocene) | Road/streets |
| Nummulitic limestone (Eocene) | Faults |
| Limestone (Cretaceous) | Dipping |
| | Elevation point (m) |



Legend

- | | |
|--|---------------------|
| Pliocene - Recent (Alluvial) | Buildings |
| Lacustrine marls, limestone and lignites (Miocene) | Sections |
| Conglomerate and red mudstone (Miocene and Pliocene) | Road/streets |
| Nummulitic limestone (Eocene) | Faults |
| Limestone (Cretaceous) | Dipping |
| | Elevation point (m) |

Figure 22: Geologic map showing the location of sections 7 and 8 at Cherara and Niha villages (modified from Dubertret, 1955).

3.1 Section 1

This stratigraphic section is located near the town of Zahle (figs. 24 and 30). The base of the section is precisely located next to the Monte Alberto hotel resort (Base 33°51'22.2"N, 35°53'39"E; Top 33°51'15.12"N, 35°53'49"E). This section overlies an Eocene fossiliferous limestone bed dominated by *Nummulites* dipping 50° east (fig. 23). It consists of 95 m of clastic and carbonate biogeneous deposits dipping 30° east. Facies change from a massive conglomerate interval passing upwards to silt and marls alternated with marly limestone layers and few lignite horizons.

3.1.1 Detailed Description from Base to Top

- 20 m thick massive matrix-supported oligomict conglomerates (fig. 25). Deposits are poorly sorted and lack sedimentary structures. Clasts are subrounded in shape and variable in size ranging between 5 and 40 cm in diameter (fig. 25). All clasts are composed of Nummulitic limestone suggesting that the clasts' source rock corresponds to the underlying Eocene limestone interval.



Figure 23: Detailed image of the Eocene Nummulitic limestone at the basal part of section 1. Note the axial sections of *Nummulites* shells.



Figure 24: Field picture facing the west showing the upper part of the massive conglomerate interval (Co) and the overlying lacustrine marls (Lm) located at the base of the section 1, next to Monte Alberto hotel.

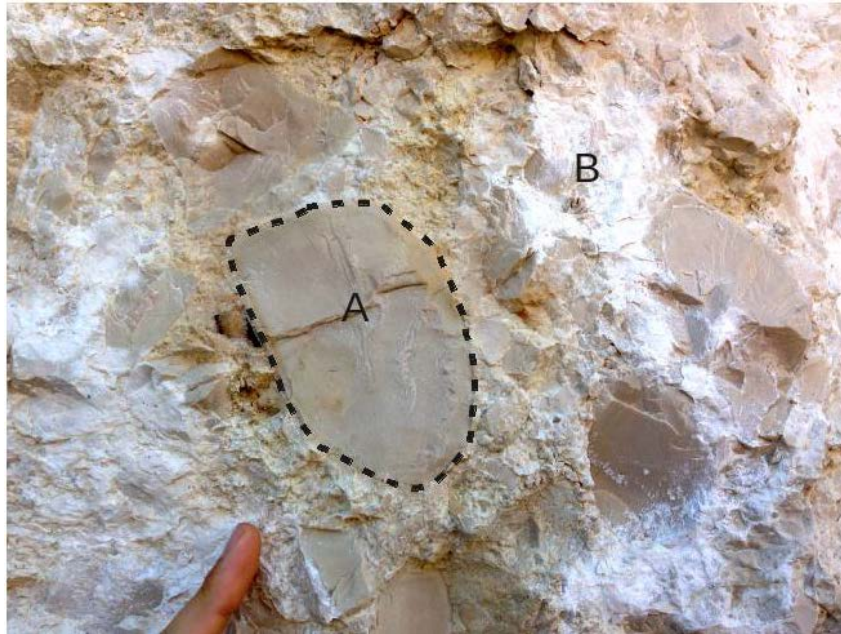


Figure 25: Detailed photograph of the basal conglomerates at section 1. A) Nummulitic limestone clasts and B) Marly matrix surrounding the clasts.

- 10 m of metric conglomerate beds alternated with yellowish-creamy siltstone intervals (fig. 26). Conglomerate beds are decametric in thickness showing a normal grain size grading. Each bed displays erosive bases where clasts are more concentrated (clast-supported). Clasts are subrounded in shape ranging in diameter between 5 and 60 cm. A soft sample (Z-0) extracted from one of the siltstone intervals provides few ostracod shells belonging to genus *Cyprideis*.

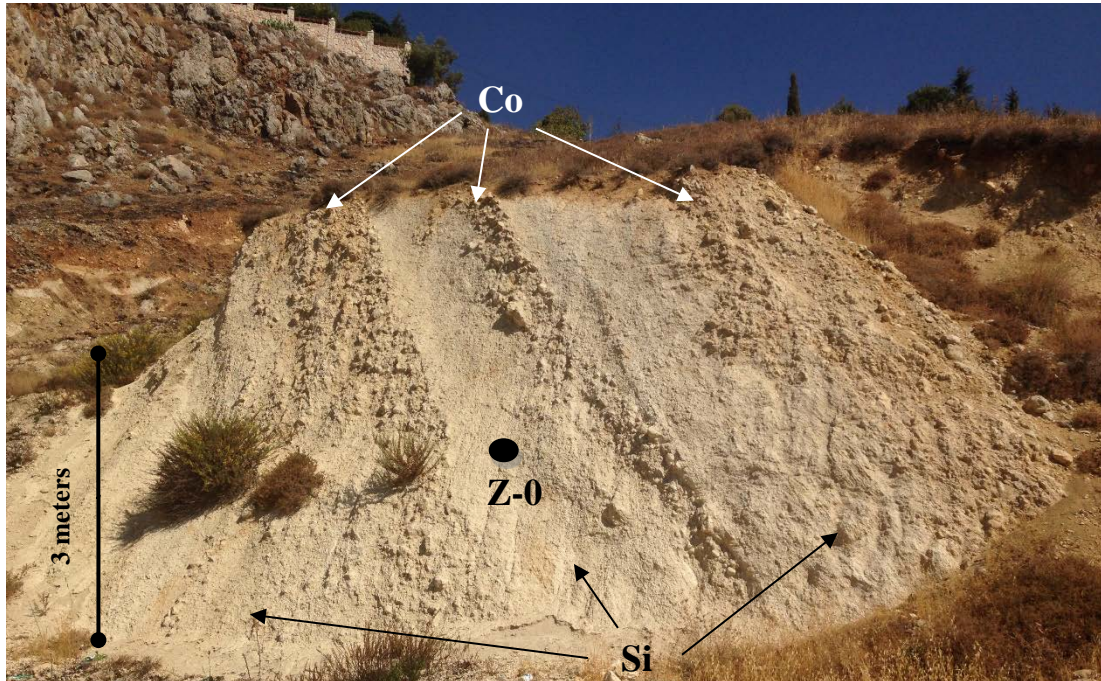


Figure 26: Field photo showing the alternation between conglomerate (Co) and siltstone (Si) intervals at the base of section 1. Note the stratigraphic location of the sample Z-0.

- 3 m of light grey marls with diffuse planar lamination very rich in microfossils. A sample recovered from this interval (Z-1) provided a rich assemblage of aquatic gastropods, charophytes and ostracods (Table 2).
- 0.6 m of brown claystone rich in gastropod shells.
- 1.5 m of dark grey marlstone very rich in gastropod shells. At the top of this interval, shells appear broken. This interval shows root marks (rhizoliths) and it is topped by an organic-matter rich interval of about 10 cm thick forming a thin layer of lignite and providing plant debris.
- 5 m of light grey marly limestone alternated with thin limestone layers very rich in gastropod shells (packstone of gastropods).
- 4.5 m of monotonous yellowish marls with diffuse parallel laminations. Gastropod shells are very abundant throughout this interval.

- 4 m of light grey marls alternated with a 30 cm thick limestone layer (wackestone of gastropods).
- 1 m thick bed of light grey limestone representing a packstone of gastropods.
- 5 m of variegated yellowish to pale green marls rich in microfossils. A soft sample extracted from this interval (Z-2) provides a rich microfossil assemblage composed of charophytes, aquatic gastropods and ostracods. A crocodile tooth has been recovered from this sample.
- 10 cm dark grey marl interval topped by a lignite layer of 5-10 cm in thickness.
- 7 m of yellowish marls with parallel lamination topped by 2 metric limestone beds (packstone of gastropods).
- 30 m of yellowish-creamy marls with parallel lamination and rich in microfossils (fig. 27). Two limestone beds (about 0.5 meters each) representing a wackestone have been observed within this interval. One organic matter rich layer with comminute plant fragments occurs in the meter 75 of the section. A soft sample has been extracted at the top of this interval (Z-3) providing a large amount of charophyte gyrogonites and aquatic gastropods.



Figure 27: Field image facing the northeast showing the middle part of section 1.

- 15 m of light grey marls passing upwards to metric limestone beds. A soft sample extracted from the marl layers (Z-4) is composed of charophyte gyrogonites and aquatic gastropods. Limestone beds are generally light grey in color and forming irregularly tabular beds of 20–50 cm in thickness (fig. 28). A hard rock sample (ZL) has been recovered from two of these intervals (fig. 29). Facies consist of low-cemented wackestone–packstone. The most common components of this limestone interval are gastropods shells, frequently dissolved and forming a secondary moldic porosity⁸.

⁸ Secondary moldic porosity: porosity (rock empty spaces) produced by dissolution of pre-existing rock constituents,



Figure 28: Field picture showing the alternation of marl and limestone layers at the top of section 1. Note the stratigraphic location of the hard sample ZL.

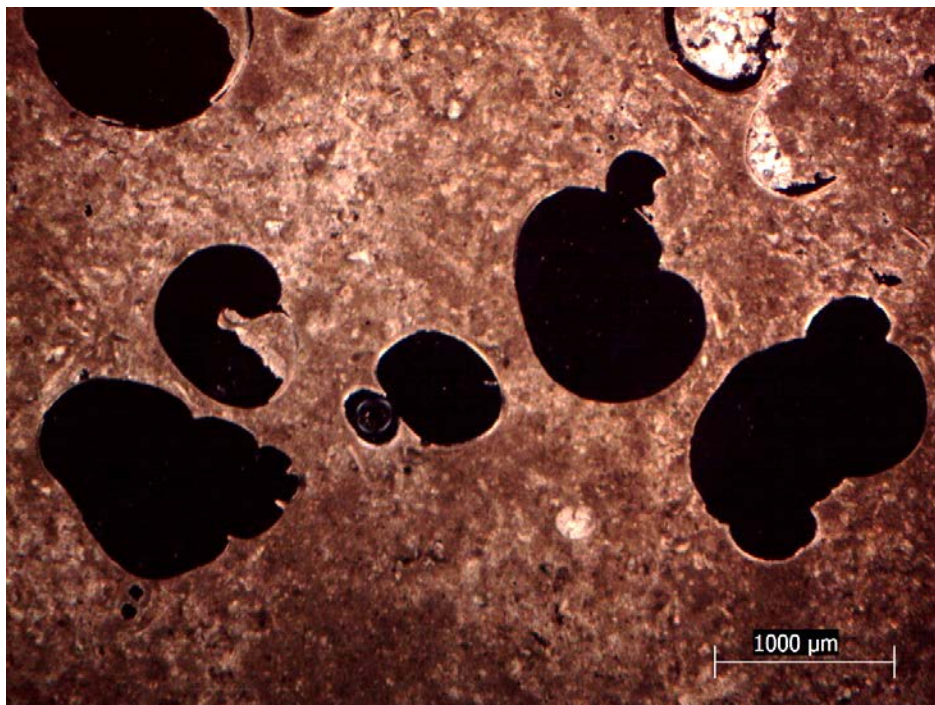


Figure 29: Detailed photograph of the thin section of sample ZL. Note the dissolved gastropod shells at the center of the figure (secondary porosity) and the precipitated calcite crystals within the dissolved shells to the upper right corner of the picture.

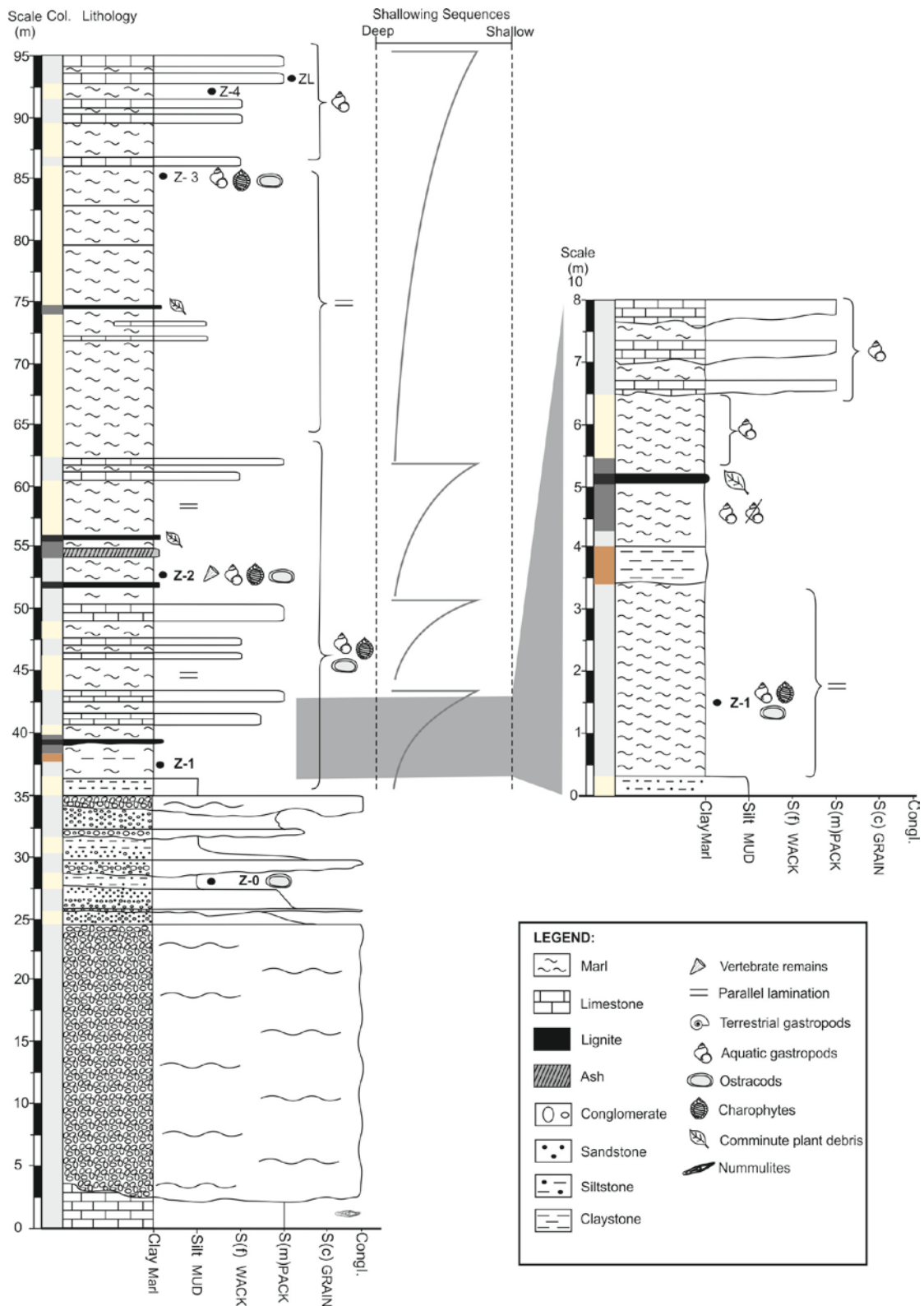


Figure 30: Stratigraphic log for section 1 showing a detail of a shallowing sedimentary cycle. Z-0 to Z-4 represent the stratigraphic position of samples extracted for microfossils. ZL represents the location of the extracted hard sample for microfacies analysis.

3.2 Section 2

This stratigraphic section (fig. 33) is located 152 m east from the top of the previous section 1 (Base 33°51'14.69"N, 35°53'55.65"E; Top 33°51'13.1"N, 35°53'55.69"E). Deposits exposed in this section are located stratigraphically above the section 1. It consists of 20 m of marls alternated with marly limestone and siltstone layers (figs. 31 and 32).

3.2.1 Detailed Description from Base to Top

- 6 m of yellowish marls with parallel lamination very rich in aquatic gastropods. Large gastropod shells of *Melanopsis* can be easily observed. Two limestone intervals (wackestone) of 0.3 m thick can be distinguished.
- 30 cm thick dark grey-colored ash interval rich in fossils. A soft sample (Z-5) has been recovered from this layer. This sample provides a diverse fossil assemblage composed of several species of aquatic gastropods, charophyte gyrogonites, ostracods and bivalves (Table 2).



Figure 31: Field image (facing the east) showing the basal strata of the section 2.

- 7 m of yellowish marls with parallel lamination and very rich in aquatic gastropods. Within this interval, three marly-limestone beds (wackestone-packstone of gastropods) ranging in thickness between 10 and 50 cm were distinguished.
- 6 m thick yellowish marl interval very rich in fossil content. One sample was extracted from this interval (Z-6) which provided a very rich fossil assemblage mainly composed of gastropods and ostracods.
- An 80 cm marly limestone bed rich in caliche can be distinguished at the top of the previous interval. Nodules are whitish to creamy in color, irregularly rounded with a knobby surface. They are large (about 4 mm in diameter) and display a branching irregular shape (fig. 32).
- 1 m dark reddish marl interval rich in gastropod shells.

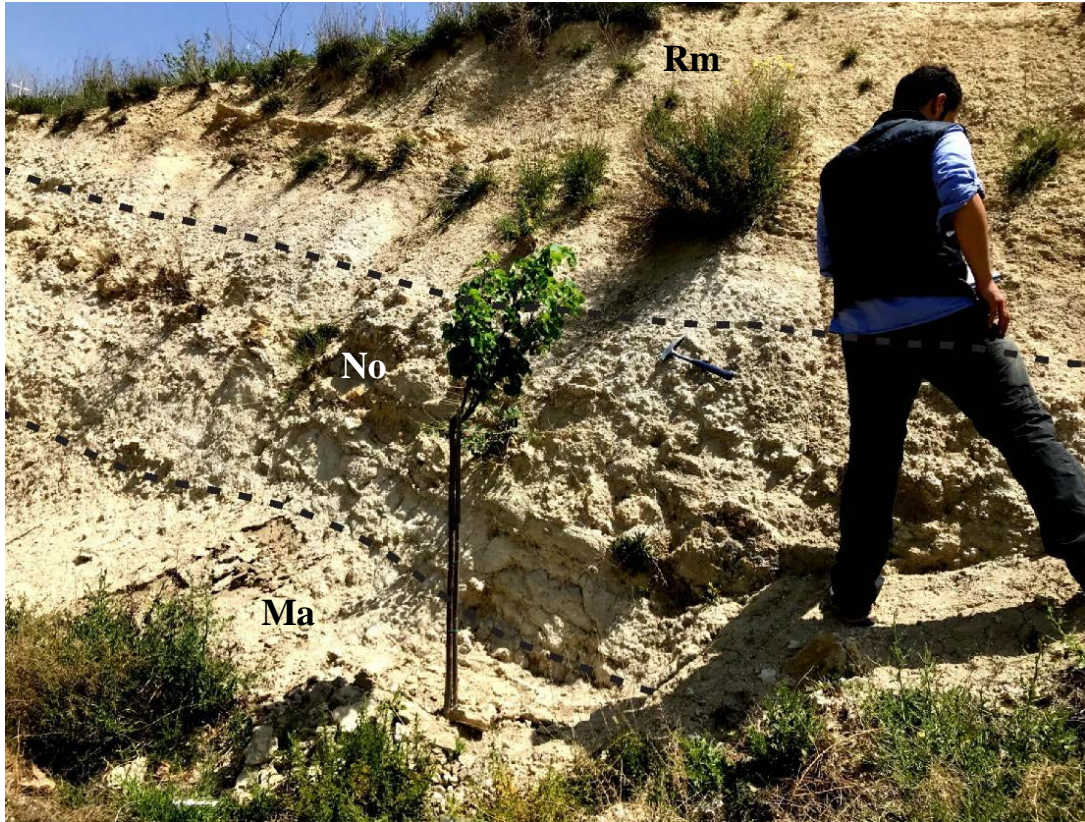


Figure 32: Field picture (facing the east) of the uppermost part of section 2. Lower marl strat (Ma) are overlain by marly limestone (No) pedogenic structures (caliche). Pale red marl interval (Rm) occurs at the top of these layers.

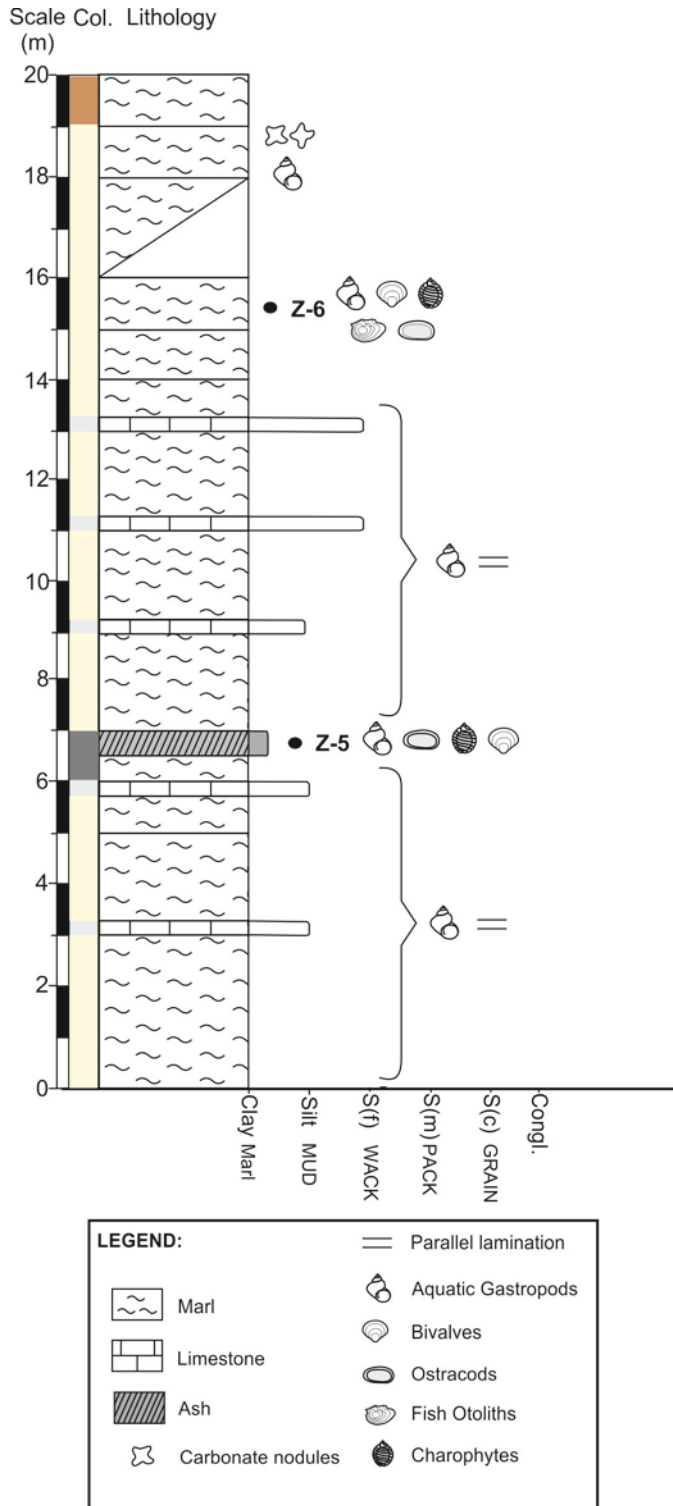


Figure 33: Stratigraphic log for section 2. Z-5 and Z-6 represent the stratigraphic position of samples extracted for microfossils.

3.3 Section 3

This stratigraphic section (fig. 39) is located about 540 m SE of the previous section in a path (Base 33°51'05.95"N, 35°54'14.95"E; Top 33°51'02.77"N, 35°54'22.96"E). From the stratigraphical viewpoint, rocks studied in this section are located above the section 2. Materials from this section comprise 54 m of fossiliferous marls passing upwards to organic matter rich marls and clays with lignites and edaphic features (fig. 34).



Figure 34: Photograph of the upper part of the section 3 showing the organic-rich marl deposits.

3.3.1 Detailed Description from Base to Top

- 24 m of yellowish creamy colored marls with parallel lamination and rich in aquatic gastropods. A metric silty bed rich in fossils can be distinguished within this interval. This interval has been sampled for microfossils (Z-7). Fossil assemblage is mainly composed of aquatic gastropods and ostracods. Charophytes and fish teeth occur in a small proportion within this interval.

- 19 m of yellowish marls extremely rich in fossils and edaphic sedimentary structures such as rhizoliths and caliche. Rhizoliths are located towards the top of the marly layers. They extend vertically and most of them show branching shapes (fig. 36). The caliche or nodules are large (about 5 cm in diameter) showing irregular shapes sometimes branching downwards. They are creamy white in color. Four metric intervals of dark-grey brownie clays can be easily distinguished in the section (fig. 35). Two of those intervals (the lower, Z-8 and the upper, Z-9) were sampled for microfossils (fig. 39). The lower sampled bed yields abundant ostracods, aquatic and terrestrial gastropods, with a smaller proportion of charophytes, bivalves, broken shells, as well as vertebrate and fish teeth. The upper interval provided large amount of aquatic and terrestrial gastropod shells which sometimes are broken. Minor amount of charophytes, bivalves and fish teeth occur within these beds (Table 2).



Figure 35: Detailed picture of the lignite layers recently excavated directly below the sample Z-9 in the section 3.



Figure 36: Detailed photograph of the rhizoliths in sample Z-9.

- 11 m of variegated marls and siltstone changing in color from dark to light grey occasionally pale orange. These deposits are organised in beds ranging in thickness from 0.3 to 0.5 m. They are mostly made of tabular beds, sometimes with erosive bases (fig. 37). Some intervals contain abundant organic matter occasionally forming lignite layers of 5–10 cm in thickness (figs. 37 and 38). Vertical burrowing structures can be distinguished in some intervals. They are relatively small, elongated in shape and are directed vertically. Abundant rhizoliths can be observed at the bed surfaces of organic matter-rich marl interval (fig. 38). They show a distinguished orange color and in some intervals they are about 30 cm long. Soft samples extracted from these intervals (Z-10 and Z-11) provided a high diversity of fossils. Aquatic gastropods and charophytes occur in large number. Other abundant fossils recovered from these intervals include terrestrial gastropod shells and fish

remains (teeth and otoliths). Characteristic 5-10 cm thick coquina layers can be observed within this interval. Coquinas show large number of concentrated reworked shells. Large broken gastropod shells belong to the species *Melanopsis buccinoidea*, which occasionally forms thicker accumulations.



Figure 37: Detailed photograph (facing the east) at the upper part of section 3. Note the alternation between the marl layers and organic rich interval, separated by an erosive base (marked by the dashed line).



Figure 38: Detailed image showing the contact between a yellowish fossiliferous marl bed and an organic-matter rich interval at the top of the section 3. Note the rhizolites located at the top of the marl interval.

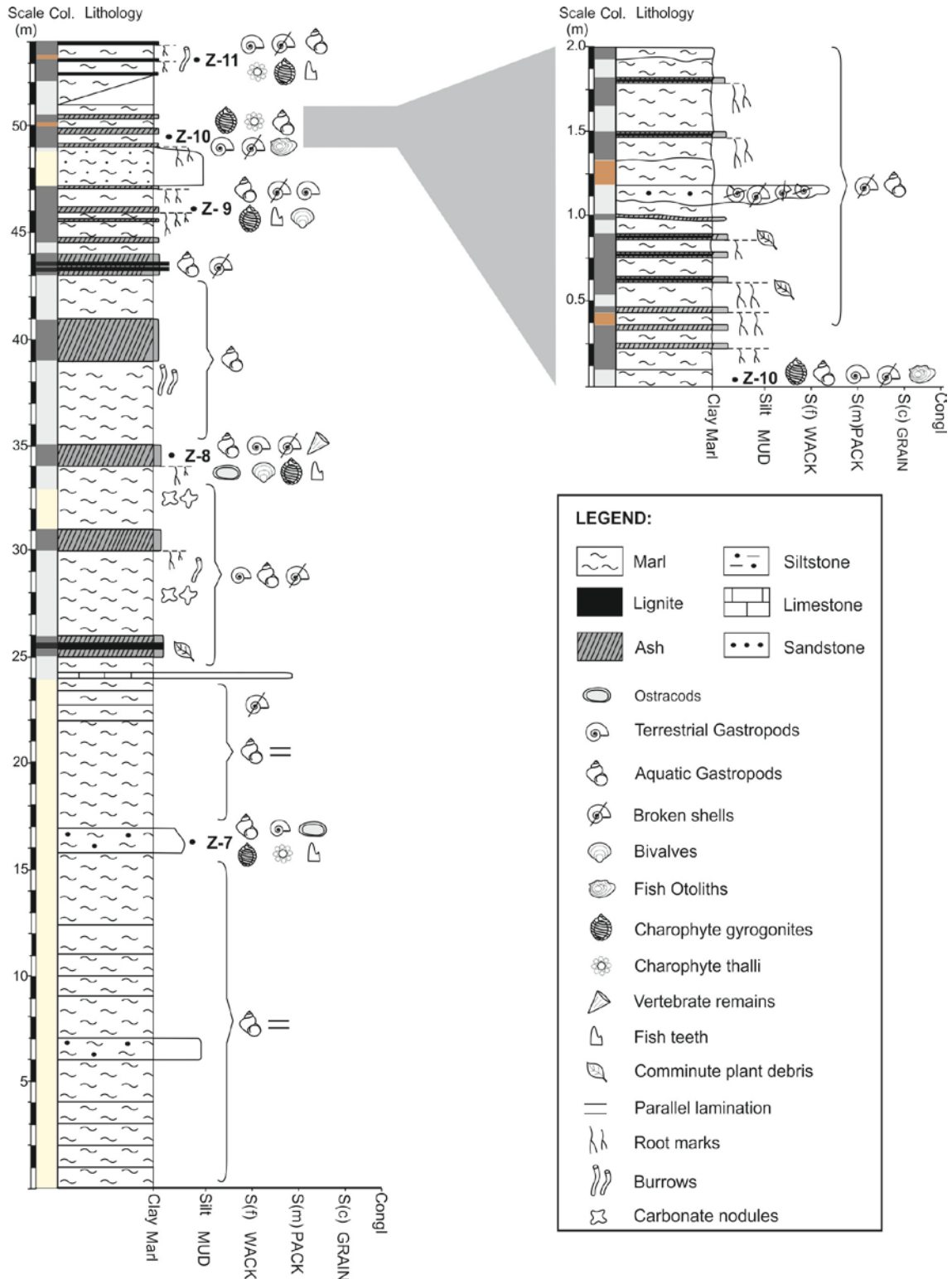


Figure 39: Stratigraphic log for the section 3 showing a detail facies assemblage at its top. Z-7 to Z-11 represent the stratigraphic position of samples extracted for microfossils.

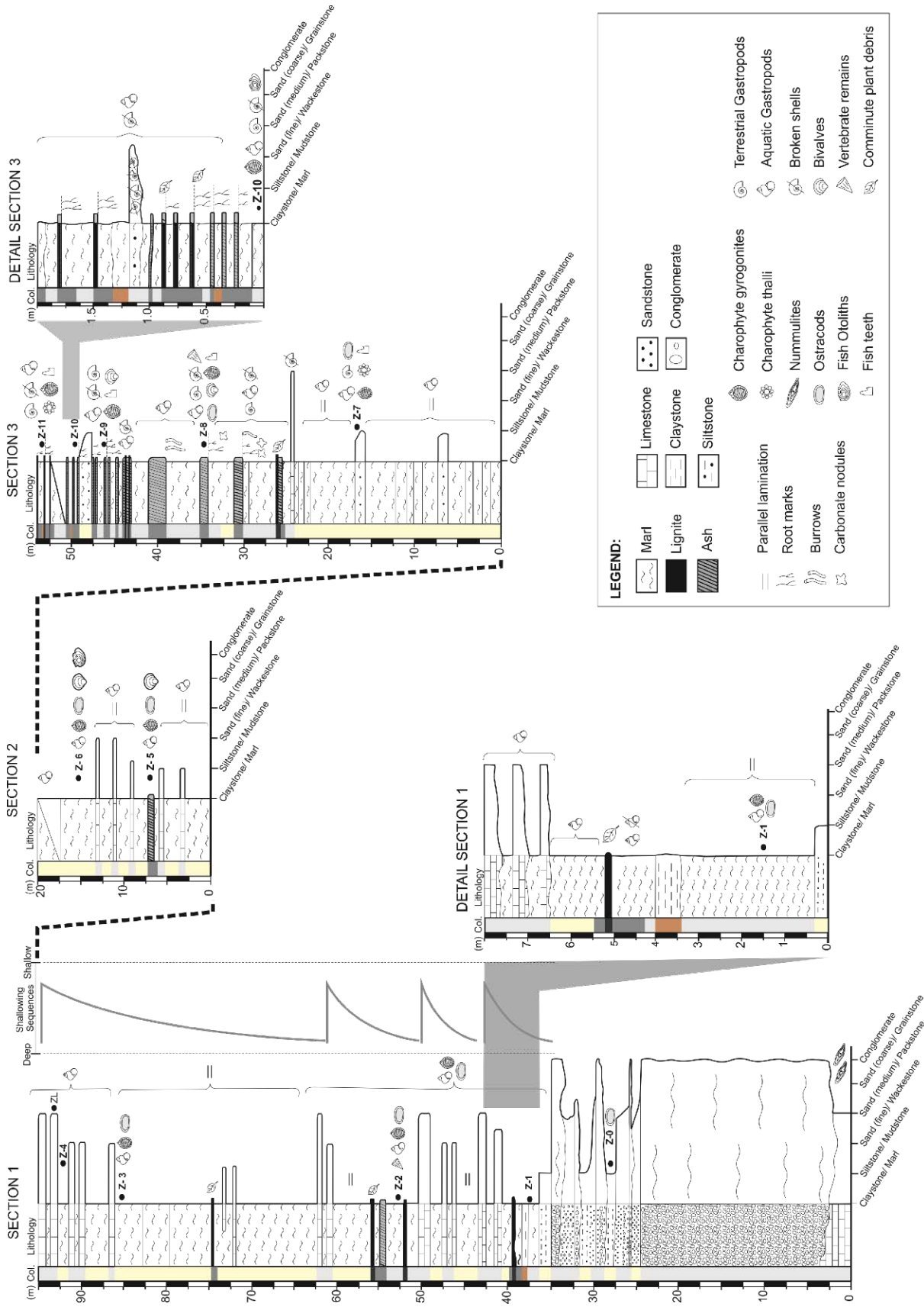


Figure 40: Stratigraphic logs for sections 1, 2 and 3 of the lacustrine deposits of Zahle showing their correlation and their facies associations. Z-0 to Z-11 represent the stratigraphic position of microfossils. ZL refers to the stratigraphic position of the sample recovered for microfacies analysis.

3.4 Section 4

This section is located 1 km to the north of Zahle town (Base: 33°51'19.95"N, 35°54'30.80"E; Top: 33°51'18.04"N, 35°54'31.57"E). It is composed of 24.5 meters of semicovered yellowish fossiliferous marls (fig. 42).

3.4.1 Detailed Description from Base to Top

- 1 meter of dark marl with root marks. A soft sample (Z-12) extracted from this layer provided a large number of charophyte gyrogonites and thalli as well as fewer aquatic gastropods, ostracods and broken shells (fig. 41).



Figure 41: Field photograph (facing the east) showing the semicovered dark grey marl layers at the base of section 4. Note the hole in the section representing the stratigraphic location of the sample Z-12.

- 7.5 meters of semicovered yellowish marls. Large amount of aquatic gastropod shells can be distinguished in this interval.

- 1 meter of marls whose lower part consists of 50 cm of whitish marl interval with small rhizoliths. A soft sample extracted from this marl interval (Z-13) provided many charophyte remains as well as fewer aquatic gastropods, ostracods and broken shells. The upper part of the marls has a yellowish color and no edaphic structures were observed.
- 1 meter of yellowish marls with no apparent structures.
- 4.5 meters of yellowish marls rich in gastropod shells.
- 1 meter of dark-toned grey marls. A soft sample (Z-14) from this dark layer yielded abundant fossils such as charophytes, aquatic gastropods and ostracods.
- 1 meter of semicovered dark marls.
- 7.5 meters of semicovered marl interval. The upper part of this interval is partially indurated showing and alternation of limestone (packestone) and marl layers (fig. 42).

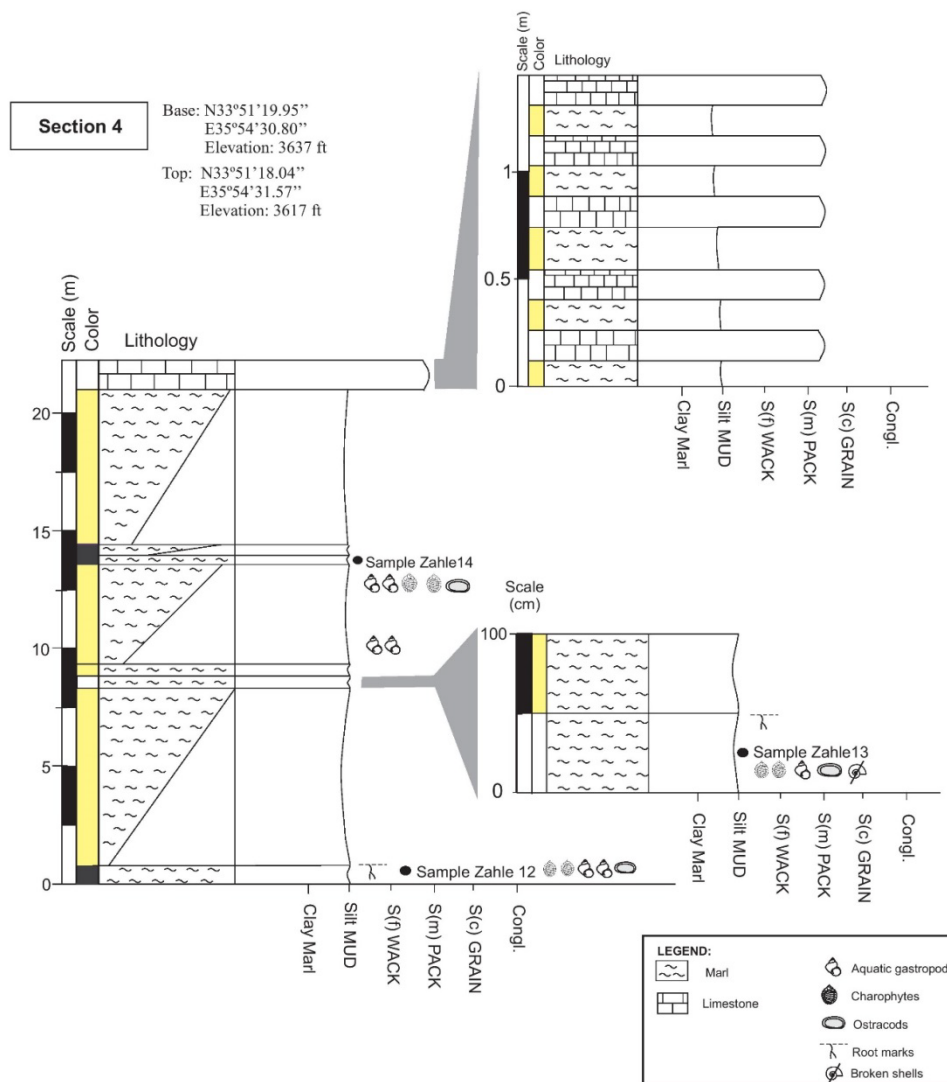


Figure 42: Stratigraphic log for section 4 showing a detail of two intervals. Z-12, Z-13 and Z-14 represent the stratigraphic position of the studied samples.

3.5 Section 5

The section 5 is located facing the previous section 4 to the north-west of Zahle (Base: 33°51'13.85"N, 35°54'24.70"E; Top: 33°51'12.70"N, 35°54'24.41"E). More specifically, this section is located behind a recently built apartment block. Excavation works recently performed in the area have created an exceptional fresh outcrop for sedimentological and micropaleontological studies (figs. 43, 44 and 48). This section is composed of 24 meters of marls, claystones and silty marls (figs. 53 and 54).



Figure 43: General field photograph (facing the west) showing the basal part of the section 5. Note the stratigraphic location of samples Z-15 and Z-16.

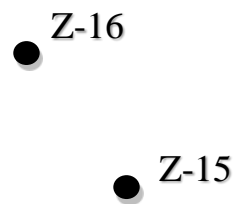


Figure 44: General field photograph (facing the northwest) showing the basal part of the section 5. Note the stratigraphic location of samples Z-15 and Z-16. Drs George Kashasha and Fabien Knoll are extracting soft rocks from the organic-rich marl interval (Z-16).

3.5.1 Detailed Description from Base to Top

- 0.5 m of light grey marls with rhizoliths rich in ostracods and fewer aquatic gastropods.
- 0.3 m of yellowish marls rich in carbonized plant remains.
- 0.7 m of light beige marls with small rhizoliths towards its top rich in ostracods and broken shells.
- 0.4 m of light beige silty marls with parallel laminations and some plant remains.
- 0.4 cm of dark grey marls exhibiting rhizoliths rich in broken shells and aquatic gastropods. An erosive layer is located at the top of this bed.
- 1 m of light beige silty marl interval rich in carbonized plant fragments.
- 3.1 m of yellowish marls with edaphic structures such as rhizoliths towards its top (fig. 45). A soft sample extracted from this interval (Z-15) provides a large amount of ostracods and charophyte thalli as well as fish teeth and plant remains.



Figure 45: Detailed photograph (facing the west) showing the marl layers of sample Z-15 in section 5. Note the presence of rhizoliths.

- 1 m of dark grey marls showing rhizoliths at its surface (fig. 46). A soft sample from this interval (Z-16) yielded an abundant population of aquatic gastropod shells and gastropod opercula, charophytes, ostracods, broken shells and bone fragments. This soft sample provided also bivalve shells and large amount of vertebrate remains such as many mammal and fish teeth and crocodile osteoderms⁹. The large number of fossils recovered from this sample suggests that this organic-rich interval has a strong potential in further paleontological works.



Figure 46: Detailed photograph (facing the west) of the sample Z-16 in section 5. Note the dark color of this fossiliferous marl interval.

- 5 cm thick lignite layer. Undefined plant fragments were observed at the top of this layer.

⁹ Crocodile osteoderm: bone tissues located in the skin of a crocodile. The osteoderm has a defensive and temperature regulation functions.

- 0.75 m of white marls very rich in shells of aquatic gastropods.
- 0.2 m of green/grey claystone extremely rich in ostracod shells.
- 1.1 m of dark grey marl with irregular caliche and few ostracod carapaces.
- 1 m of whitish marls bed with little fossil content (ostracods) and with reduced size rhizoliths located at its upper surface.
- 30 cm thick interval of dark marls rich in organic matter and containing a lignite horizon.
- 1.3 m of light grey marl bed containing few shells of ostracods and centimetric irregular carbonate concretions or caliche at its top (fig. 47).



Figure 47: Detailed photograph of the caliche in section 5.

- 0.9 m of dark grey silty marl with erosive base exhibiting rhizoliths at its upper surface. A soft sample from this interval (Z-17) provided large amount of well-preserved fossils such as aquatic gastropod shells, ostracods (showing their valves

connected), charophytes, fish otoliths, gastropod opercula as well as few bivalve shells (fig. 48).

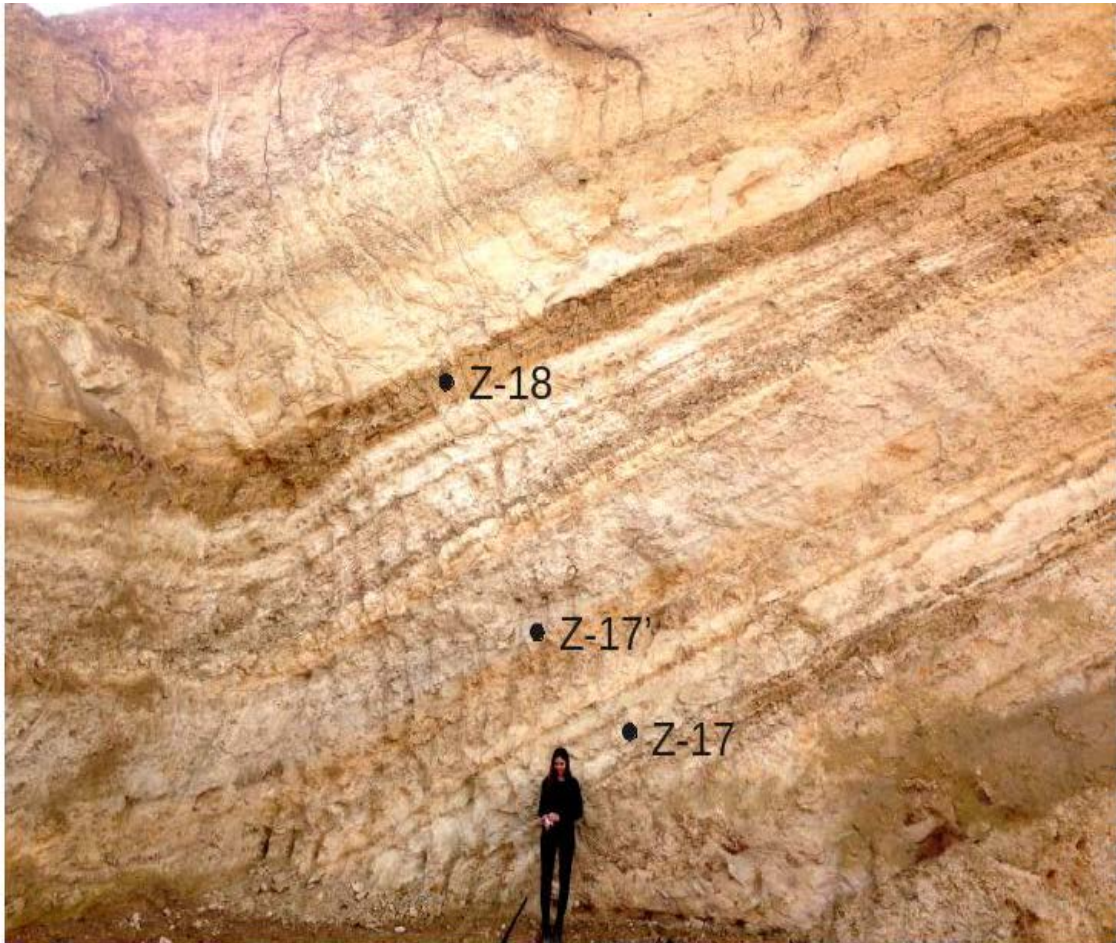


Figure 48: General field photograph (facing the west) showing the upper part of section 5. Note the thicknesses and colors of different strata and the location of samples Z-17, Z-17' and Z-18.

- 0.8 m of light beige marls with rhizoliths at the upper surface. Abundant gastropod and ostracod shells occur in this interval (fig. 49A).
- 1.5 m of grey marls with gastropod and ostracod shells. The upper bed surface appears truncated.
- 5 to 20 cm of dark grey marly shell and bone debris siltstone made of shells and bone fragments (coquina) (fig. 49). A sample extracted from this fossiliferous interval (Z-17') yield a large diversity of fossils. Gastropod shells display a wide

range of sizes reaching 5 cm in case of *Melanopsis* (fig. 50). Monospecific ostracod carapaces occur largely in this interval. Mollusk and ostracod shells may appear broken and the complete specimens usually preserve the original shell coloration. Bone fragments and teeth related to fishes also occur in large number within this bed.

- 0.2 m thick light beige marl layer. At its surface several elongated leaf impressions of reed-like plants can be observed (fig. 51).

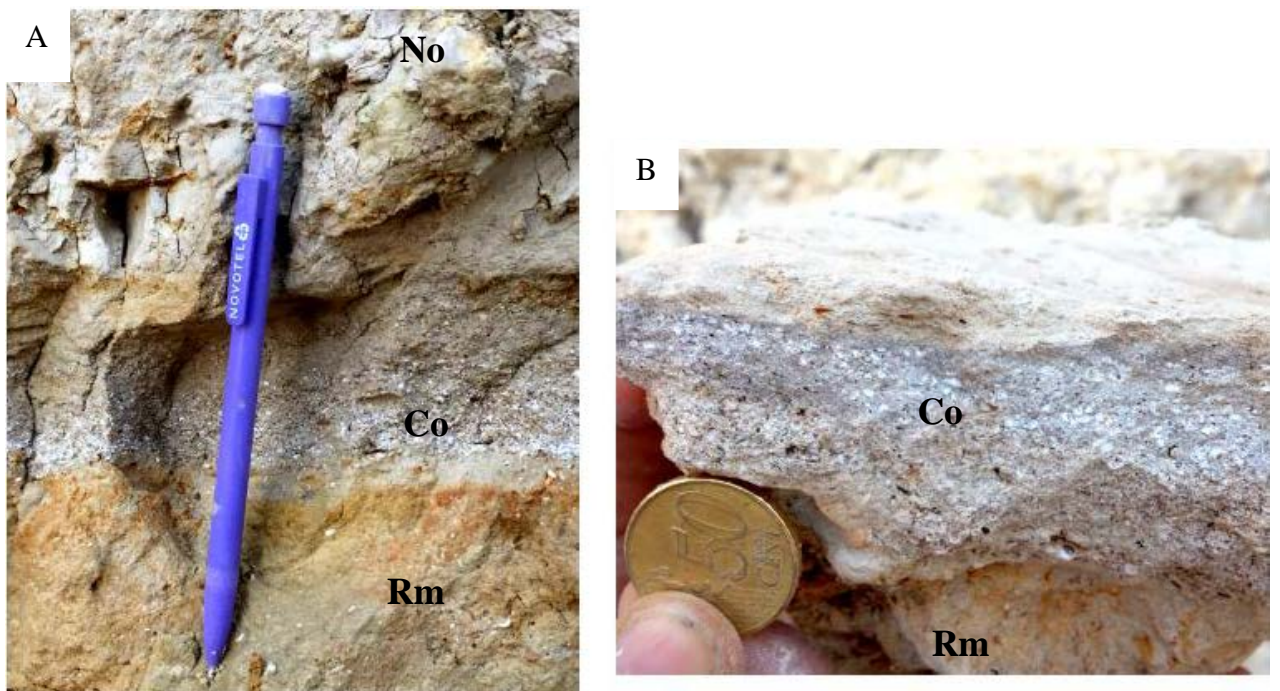


Figure 49: Detailed photograph (facing the west) showing a coquina interval. A) From base to top: yellowish marl layer showing rhizoliths (Rm), a coquina interval (Co) from where the sample Z-17' was recovered, and the grey marl interval showing caliche (No). B) Detailed photograph of a coquina.



Figure 50: Detailed photo showing a large shell of *Melanopsis buccinoidea* from sample Z-17'. Note the original coloration preserved.



Figure 51: Detailed photograph of reed-like leaf impressions above the sample Z-17'.

- 0.15 m interval of dark silty marls mainly made of aquatic gastropod shells (coquina)

- 0.3 m light beige marls.
- 0.15 m yellowish marls interval rich in caliche ranging in size between 5 and 10 cm in diameter. The caliche may show branching shapes and may appear joined forming a more resistant horizon (fig. 52).



Figure 52: Detailed photograph showing the nodular structures (caliche) located above the sample Z-17'. The dashed line outstands some caliche.

- 0.4 m light beige marl interval exhibiting some rhizoliths at its upper surface.
- 0.7 m thick yellowish marl bed. No apparent structures have been recognized within this layer.
- 0.15 m lens of yellow marls rich in caliche. This interval mainly contains small aquatic gastropod shells.
- 0.65 m thick yellow marls with root marks, showing an erosive contact with the overlying beds.

- 1 m of reddish silty marl interval showing an erosive base (fig. 47). A soft sample (Z-18) from this bed provided a large amount of ostracod carapaces and shells of aquatic gastropods.
- 1.4 m reddish marl.
- 0.1 m dark silty marls with ripple marks.
- 1.2 m of light beige marls.
- 1.5 m of yellow marls.

Section 5

Base: N33°51'13.85"
 E35°54'24.70"
 Elevation: 3583 ft
 Top: N33°51'12.70"
 E35°54'24.41"
 Elevation: 3580 ft

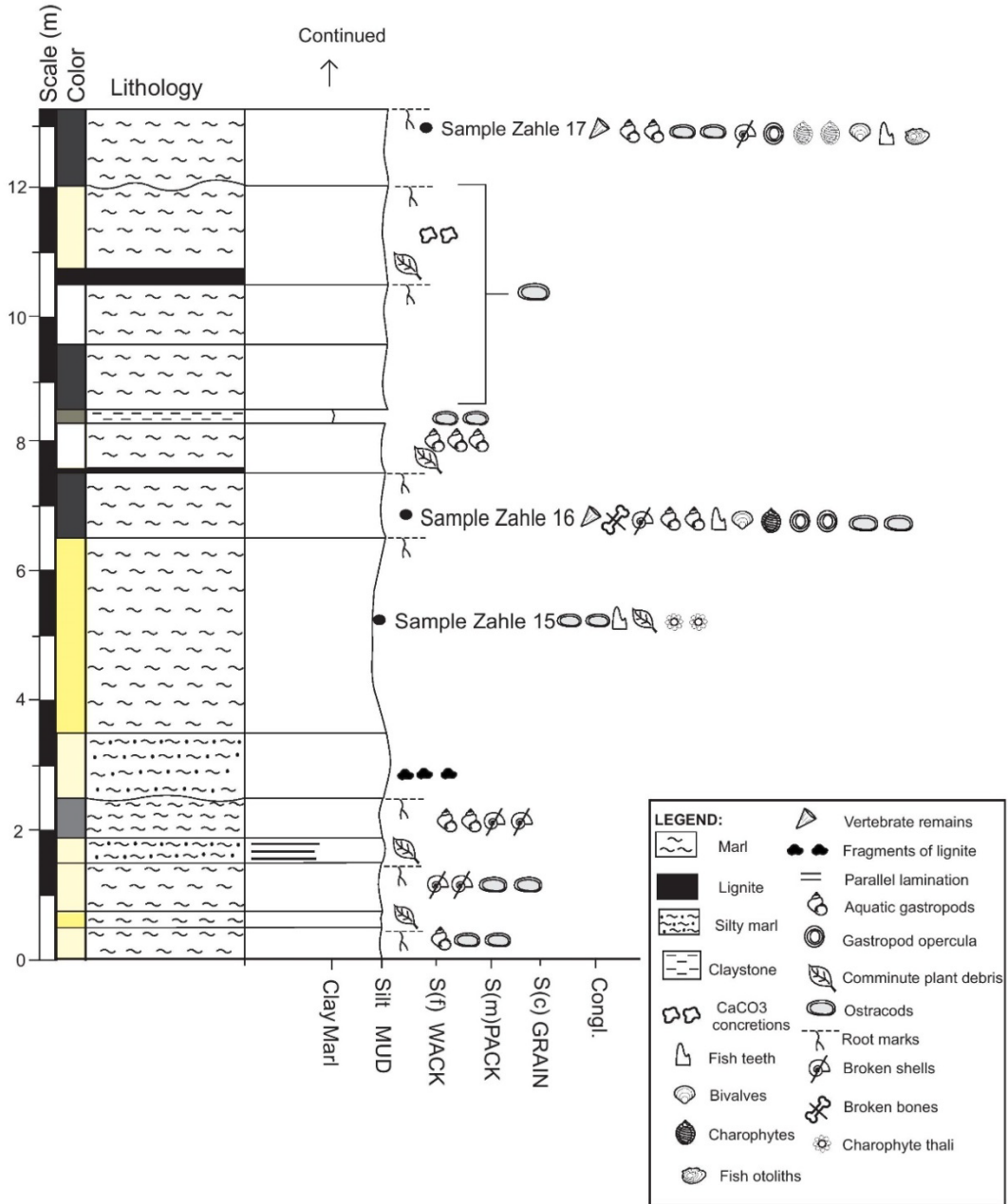


Figure 53: Stratigraphic log for the base of the section 5. Zahle 15 (Z-15) to Zahle 17 (Z-17) represent the stratigraphic location of the samples extracted for microfossils.

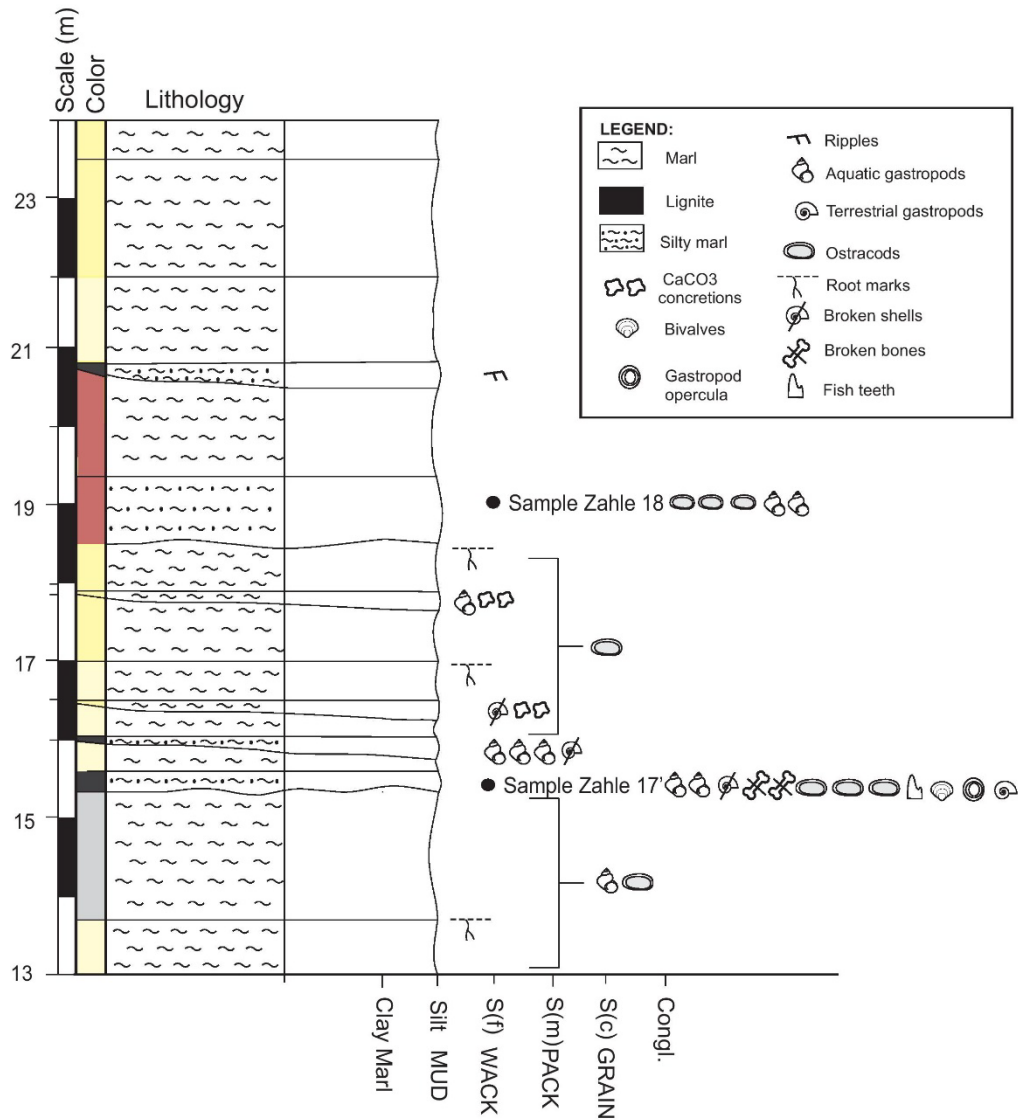


Figure 54: Stratigraphic log for the top of the section 5. Z-17' and Z-18 represent the stratigraphic location of the samples extracted for microfossils.

3.6 Section 6

This section is composed of two sub-section (fig. 58). The lower section (Base: 33°51'29.30"N, 35°55'11.50"E; Top: 33°51'28.74"N, 35°55'11.68"E) includes 14 meters of monotonous marls (fig. 55), while the upper section (Base: 33°51'14.09"N, 35°55'01.57"E; Top: 33°51'14.68"N, 35°55'01.64"E) is only 2.5 meters thick and it is composed of red claystone and conglomerates (figs. 56 and 58).



Figure 55: Field photograph (facing the north) showing the basal part of section 6. Note the location of the samples Z-20.

3.6.1 Detailed Description from Base to Top

- 0.3 m of dark grey marl with no apparent structures. One sample has been recovered from this layer (Z-19) yielding abundant ostracod carapaces and gastropod shells. Ostracod carapaces are connected.
- 0.3 m of dark grey marls with parallel laminations.
- 1.1 m thick light beige marls showing parallel laminations.

- 5.8 m of light beige marls with increasing abundance of ostracod shells from base to top.
- 0.5 m of dark grey marls with root marks at its surface. Parallel laminations can be observed within this layer.
- 0.6 m of semicovered light beige marls. A soft sample extracted from these marl interval (Z-20) shows a large number of charophyte gyrogonites and ostracod carapaces. Fish otoliths and broken gastropod shells also occur in this layer (fig. 55).
- 0.1 m of semicovered dark grey marl layer.
- 1.8 m of semicovered light beige marl bed.
- 1 m thick light beige marl layer. Ostracod carapaces have been observed within this layer.
- 2.5 m thick semicovered non-fossiliferous light beige marl interval that can be laterally correlated with the upper section described below.

The upper section (fig. 56) is located around 450 meters to the south-west of the previous section. It shows a dramatic change of facies. A large temporal gap existed between the basal and upper part of the section. This gap is represented by a covered interval between the basal marls on one side and the upper reddish conglomerates on the other side.



Figure 56: Field photograph of the upper part of section 6 showing the reddish clay and conglomerates.

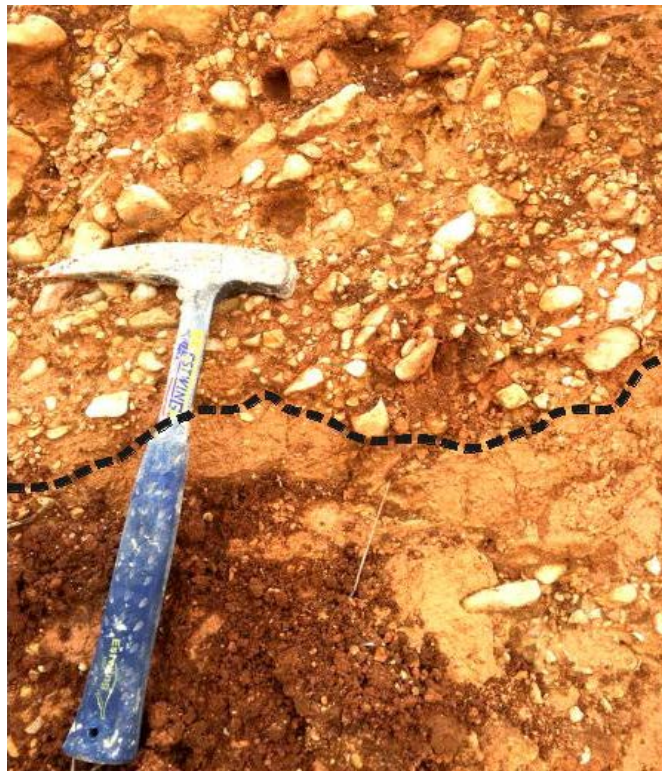


Figure 57: Conglomerate contact showing imbrication fabrics and erosive base (marked with a dashed line).

- 0.25 m thick reddish conglomerate. Pebbles of this interval are imbricated and point in the north direction. Ripple marks are prominent towards the top of this interval.
- 0.5 m of dark grey claystones. This layer is separated from the upper layers by an erosive surface (fig. 57).
- 0.38 cm of reddish conglomerates with imbrications towards the bottom and ripple mark structures in the upper part (fig. 57).
- 0.62 m thick dark grey claystones.
- 0.5 m layer of semi covered dark claystones.

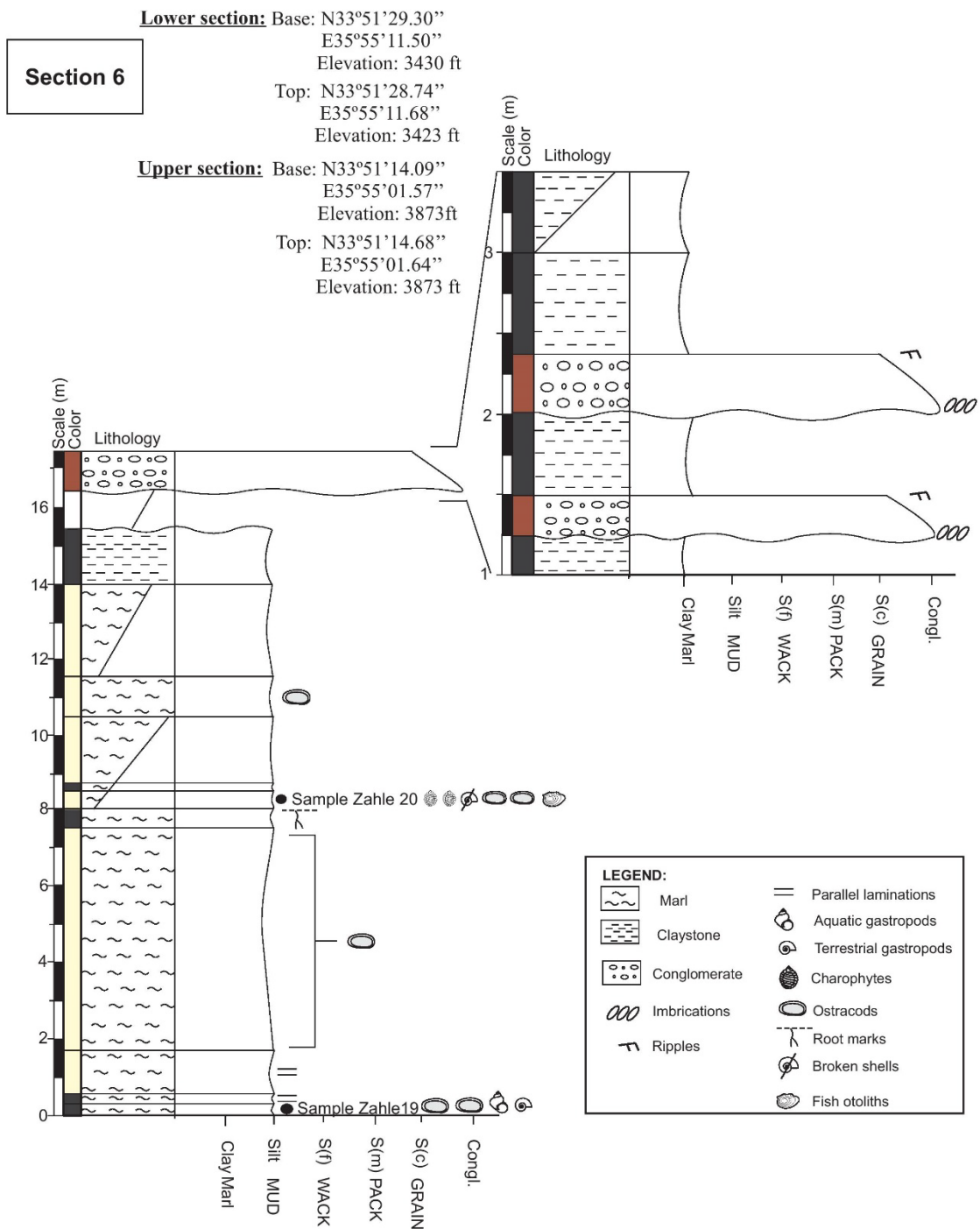


Figure 58: Stratigraphic log for the section 6. Z-19 and Z-20 represent the stratigraphic location of the samples extracted for microfossils.

3.7 Section 7

This section is located in the Cherara village (Base: 33°52'26.36"N, 35°56'23.03"E; Top: 33°52'27.09"N, 35°56'23.09"E) (figs. 59 and 61). It is composed

of 6.5 meters of monotonous marls alternated with marly limestones and silty marls (fig. 61).



Figure 59: General field photograph of the section 7 at Cherara.

3.7.1 Detailed Description from Base to Top

- 2 m of white marly limestones showing parallel lamination. Little amount of fossils was observed in this strata. Caliche and small rhizoliths occur at the upper part of this interval.
- 0.8 m of whitish marly limestones with irregular caliche.
- 0.6 m of white marly limestone. No apparent structures have been recognized.
- 0.8 m thick light beige marls. Carbonate nodular features (caliche) can be recognized in this interval.
- 0.2 m of light beige silty marls showing low-angle cross-bedding.
- 0.8 m of light beige marls showing irregular caliche.

- 0.2 m thick white marly limestone layer, with rhizoliths at the surface. Few aquatic gastropods occur in this interval.
- 0.6 m of alternated white marls and marly limestones devoid of any apparent sedimentary structures. A soft sample from the marl layers (Z-21) contains a large proportion of ostracod shells. Fish otoliths occur in a restricted amount within this layer (fig. 60).



Figure 60: Field photograph of the upper part of section 7. Note the alternation between the marls and whitish marly limestone layers. The star represents the location of the sample Z-21.

- 0.2 m of white marly limestones showing rhizoliths towards its top.
- 0.3 m of semi-covered white marly limestones. No clear structures can be seen in this interval.

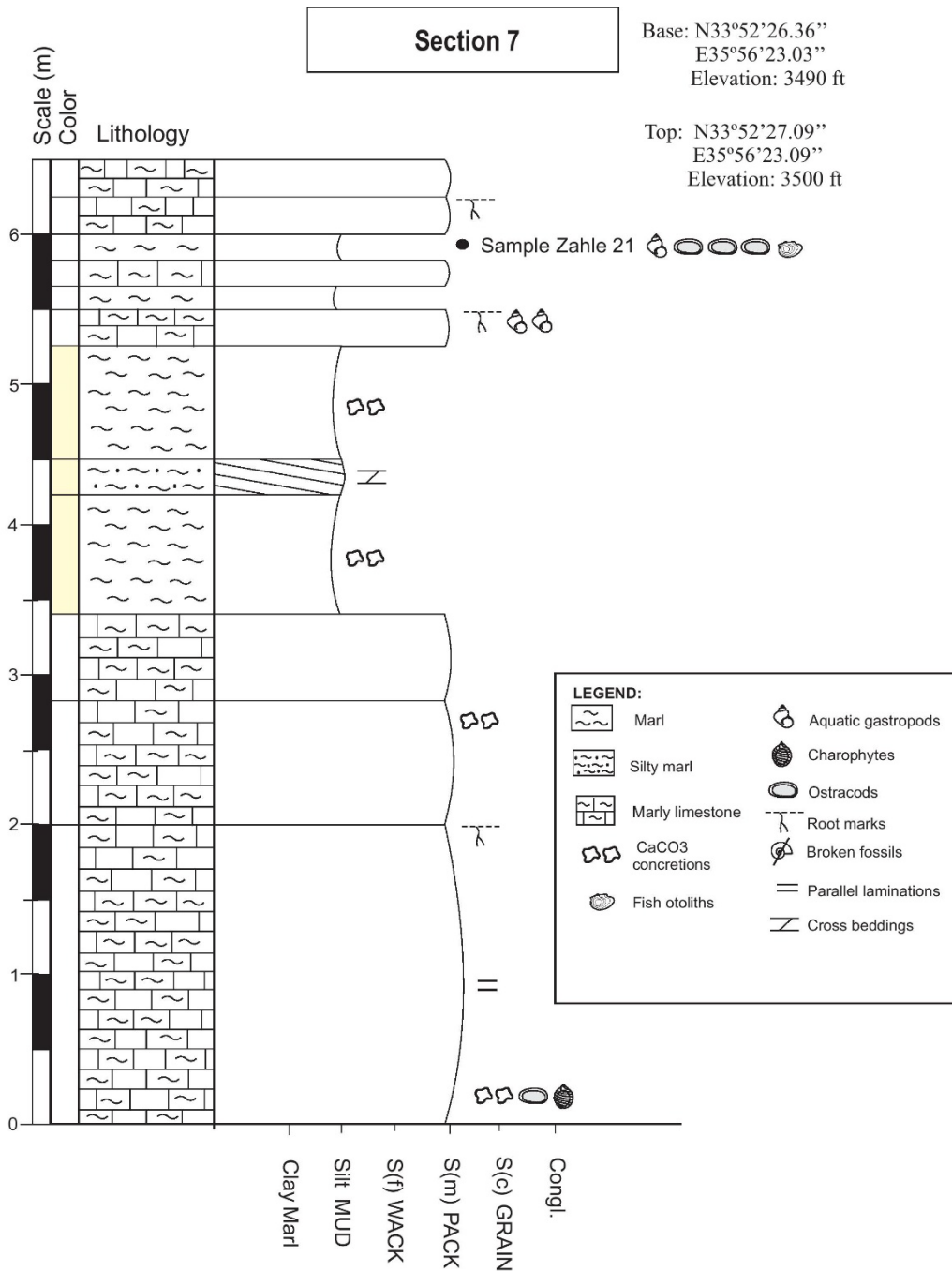


Figure 61: Stratigraphic log for the section 7. Z-21 represents the stratigraphic location of the sample extracted for microfossils.

3.8 Section 8

This section was raised in the Niha village, in a parking next to the ruins of the lower Roman temple (Base: 33°53'40.10"N, 35°57'46.49"E; Top: 33°53'40.02"N, 35°57'46.63"E). This section is composed of 17.8 meters of marls and marly

limestones (figs. 62 and 64).



Figure 62: Field photograph of section 8 near the Niha ruins. The star represents the location of the sample Z-22.

3.8.1 Detailed Description from Base to Top

- 4.2 m of light beige marly limestones with aquatic gastropod shells.
- 0.6 m whitish marls with no apparent structures.
- 1.3 m of white marls corresponding to the soft sample Z-22. This interval is very rich in gastropod shells (fig. 63).



Figure 63: Field photograph showing the basal portion of section 8. Note the location of the sample Z-22.

- 5-20 cm thick lignite layer with comminute plant remains.
- 0.5 m of whitish marls. This layer is devoid of fossils and shows no apparent structures.
- 5.5 m of yellowish marly limestone bed with few gastropod shells.
- 20 cm thick light beige marly limestone layer. Few gastropod shells occur in this interval.
- 20 cm structureless white marls devoid of fossils.
- 1 m of yellow marly limestones exhibiting few gastropod shells.
- 0.6 m thick yellowish marl layer.
- 2.4 m of yellow marly limestones with few gastropods.
- 0.4 m thick yellowish marls.
- 0.8 m of yellow marly limestones.

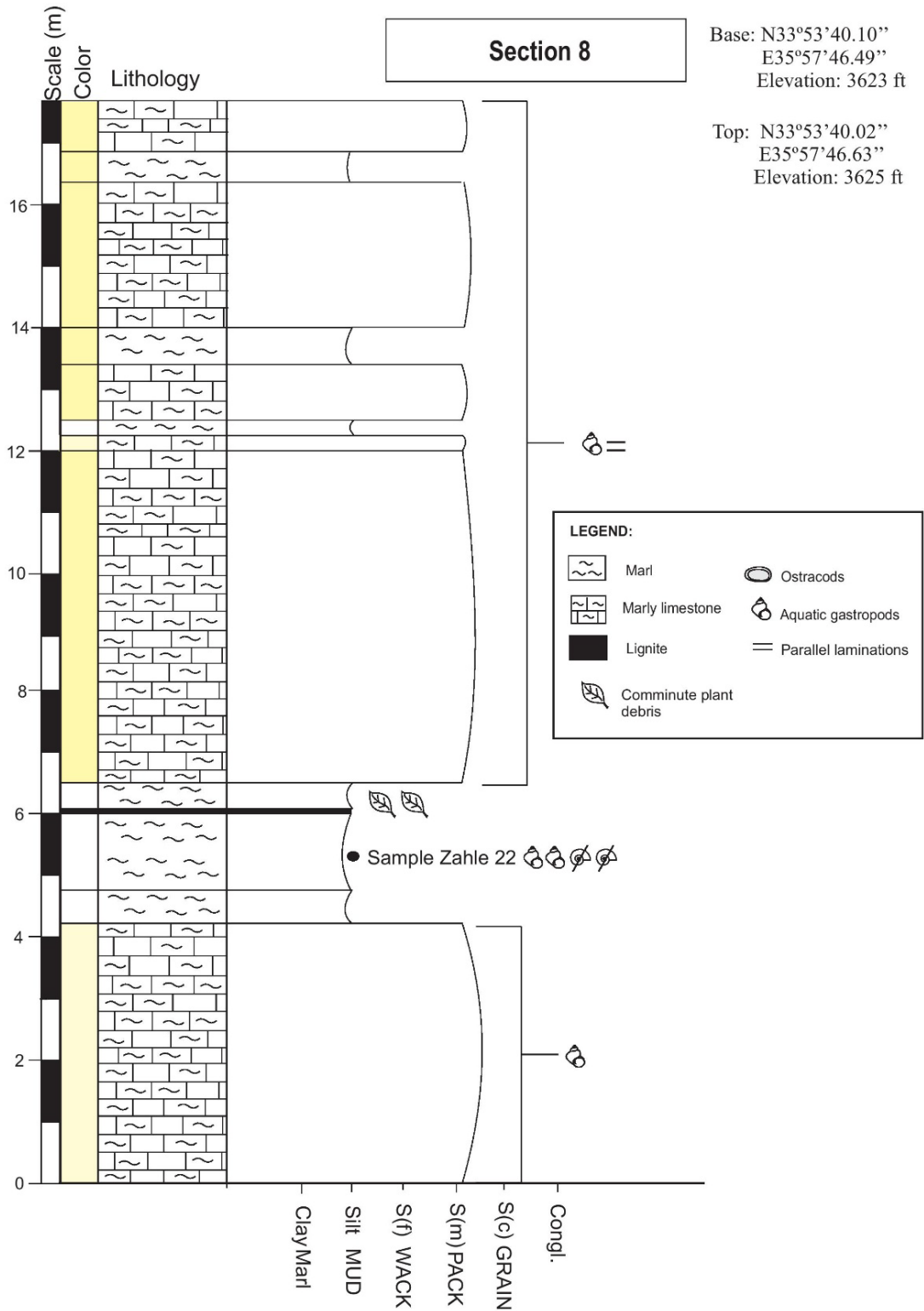


Figure 64: Stratigraphic log for the section 8 showing the stratigraphic location of sample Z-22 that was extracted for microfossil analysis.

CHAPTER 4

FACIES ASSEMBLAGES AND INTERPRETATION

Four types of facies assemblages related to four sedimentary environments can be identified in the studied sections.

4.1 Alluvial

This facies type basically composed of matrix-supported massive limestone conglomerates (limestone pebbles) occurring at the base of the section 1 (fig. 30). The massive and structureless bad sorted conglomerates located at the base of section 1 are related to debris flow deposits in an alluvial fan context (Boggs, 2011). The increase of clast concentration at the upper part of the interval together with the presence of silty layers suggests a progressive change from debris to stream flow sedimentary processes. Upper conglomerates show clear erosive bases and normal graded bedding suggesting that more water is involved into the sedimentary processes. Moreover, the presence of freshwater ostracods within the silty beds (sample Z-0) indicates that sedimentary processes occurred in subaquatic conditions. The abundant supply of clastic sediment in the area may be related to the high tectonic activity, i.e. fault displacement, during the first stages of the lacustrine system.

4.2 Lacustrine Facies

These are by far the dominant type of facies assemblage in the studied area. Marls, silty marls and marly limestone facies with a high diversity of fossils occur in the

upper part of the section 1, the base of the section 3 and the complete sections 2, 4, 6, 7 and 8. These facies can be related to stable lacustrine conditions at different bathymetries.

Characteristic facies succession related to shallowing cycles can be interpreted at the upper part of the section 1. The vertical succession of facies changing from monotonous fossiliferous marls with some lignite horizons grading upwards to wackestone–packstone marly limestone intervals can be interpreted as the increasing abundance of calcareous organisms in the shallower and well-illuminated lacustrine environments. The marls were probably deposited in more distal and deeper lacustrine facies than the limestones. Despite the relatively high content of fossils in these lacustrine deposits, facies from these sections show some intervals of diffuse lamination and they contain a few organic-matter rich horizons with comminute plant fragments suggesting that the lake bottom was occasionally anoxic, hindering bioturbation and preserving the plant remains (Gierlowski-Kordesch, 2010). Moreover, no edaphic features have been observed underlying these organic rich layers indicating that plant remains were probably transported from the lakeshore and sank in the deeper areas forming an allochthonous assemblage on the lake bottom. Microfossils are generally well-preserved and do not show signs of fragmentation. Left and right ostracod carapaces occurred frequently attached suggesting that fossils were buried *in situ* or after minor or no transport. Fossils occur in both marls and limestones and from the sedimentological viewpoint they correspond to biogenic carbonate producers. The presence of charophyte gyrogonites and thalli suggest that the lake bottom was well-oxygenated and probably well-illuminated. Dissolved gastropod shells observed from thin sections are related to secondary diagenetic processes. The absence of ripples and

broken shells in almost all the sections showing this facies assemblage implies that the depositional environment was relatively quiet, without the action of strong waves or currents. The presence of wackestone and packstone textures from marly limestone beds also suggest that low to moderate sedimentation energy prevailed (Boggs, 2011). The presence of few marl horizons with caliche and small rhizoliths together with low angle cross bedding in section 7 indicates shallower lacustrine conditions prevailed subjected to occasional subaerial exposures.

Then, we can conclude that the monotonous succession of marls and limestones studied in these sections are related to lake sedimentary processes under fully lacustrine conditions.

4.3 Palustrine Facies

This facies assemblage is consisting in variegated organic matter rich marls (dark grey, yellowish and pale orange) and siltstone showing erosive bases, edaphic structures and lignite horizons. This facies assemblage mainly occurs at the top (upper 25 m) of the section 3 and the complete section 5.

Dark-grey colored marls and silty marl intervals with abundant lignite horizons suggest that high concentration of organic matter (plant remains) prevailed within the depositional environment. Marls and clays are not laminated suggesting that organic and burrowing activity destroyed the original lamination (Alonso-Zarza, 2003). The presence of edaphic structures, which are particularly abundant below the lignite horizons, indicate that plant remains were not transported and the plant community grew *in situ* in the lake shores. Leaf fragments of helophytic-like plants (plants adapted to grow in marshes, partly submerged in water) preserving leaf impressions probably

related to reeds e.g. *Typha* have been observed in some intervals. Sedimentological characteristics suggest that sedimentary rocks from section 3 and 5 were deposited under extremely shallow lake conditions probably in a vegetated lake margin (palustrine).

Small shells are well-preserved, while large gastropod shells are partially fragmented occasionally concentrated forming coquina lenses or horizons. Coquina horizons show erosive bases and may have high lateral continuity. The presence of coquina interval suggests that shells were subjected to an energetic selective environment, probably related to re-working episodes due to water level fluctuation and/or lake currents activity (waves or longshore currents). The abundance of well-preserved ostracods, usually showing the two valves in anatomical connection indicates that larger shells were accumulated under subaquatic conditions. However, evidences of subaerial exposure can be tentatively inferred in these sections due to the presence of marl horizons rich in branching carbonate nodules (caliche). The caliche are normally forms within calcium bicarbonate-rich lake margins. Caliche tend to form under very low gradients of freshwater lake margins subjected to low energy. The caliche source are fine-grained biogenic carbonate particles containing remains of charophytes, ostracods and mollusks that has been subaerially exposed due to fluctuations of the water table. Pedogenic (soil forming) processes then change these fine-grained carbonates (Freytet and Verrenchia, 2002). According to Freytet (1973), nodular shape is mainly due to dessication and subsequent filling of the planar to curved fissures under the vadose and phreatic zones. The abundance of ash intervals at the top of the section 3 section may indicate an increase of the volcanic activity in the area.

4.4 Fluvial

This facies assemblage is composed by clast supported conglomerates alternated with red claystone intervals which occur at the top of section 6. The presence of imbricated clast-supported fabrics is related to channel-fill deposits in a fluvial context (Boggs, 2011). The upward transition of these conglomerates into fine-grained claystones suggests a change from channel to floodplain deposits.

Section	General Description	Facies Analysis
0-35 m of section 1	Lithology: oligomict conglomerates and siltstone. Structures: erosive bases and normal grading. Color: creamy white-whitish	Alluvial facies (Debris flow at base-Stream flow to the top)
Upper section 1, base of section 3 and the complete sections 2, 4, 6, 7 and 8	Lithology: marls, marly limestones, lignites, limestones (wackestone-packestone). Structures: parallel laminations, few plant remains, some caliche and low angle cross bedding. Color: grey-yellowish.	Lacustrine facies
Upper section 3 and complete section 5	Lithology: organic rich marls, claystones, coquina, organic rich marlstones, lignites and ash intervals. Structures: abundant caliche, abundant rhizoliths and erosive bases. Color: reddish-dark grey.	Palustrine Facies
Upper section 6	Lithology: conglomerates and claystones. Structures: erosive bases, imbrications and ripples. Color: reddish.	Fluvial Facies

Table 1: Table summarizing the facies description in sections 1 till 8 and their associated environment.

CHAPTER 5

MICROPALEONTOLOGY

A large number of microfossils belonging to 7 different Classes have been recovered from the studied sections i.e. shells of Gasteropoda, Bivalvia and Ostracoda and fragments of vertebrate bones and teeth such as Actinopterygii (fishes), Reptilia and Mammalia. Fructifications of plants belonging to the Class Charophyceae also occur in large number within the studied sections. All the recovered microfossils are here described and illustrated for the first time in Lebanon. Their relative abundance within each sample is listed in tables 1 and 2. Moreover, the ecological/paleoecological and geographical/paleogeographical distributions are here discussed.

Gastropod shells represent by far the most dominant microfossil in all the studied sections.

5.1.1 *Aquatic Gastropods*

Family: **Valvatidae**

Species: *Valvata saulcy* Bourguignat, 1853

(figs. 67 A-C and 68 A-B)

Material: More than 100 specimens were recovered from samples Z-8, Z-13 and Z-17, while 25-100 shells were found in samples Z-12 and Z-14. Few specimens were recovered from samples Z-1, Z-9 and Z-16 (Tables 2 and 3). Ten specimens were measured in this study (fig. 65).

General description: flat, depressed shell. It has a width of about 1.4 mm in average (ranging between 0.84 and 2 mm) and an average height of 0.87 mm, ranging between 0.6 and 1 mm (fig. 65). The shell consists of 2 circular whorls with the last whorl expanding more rapidly than the others. Shells have low spire and a blunt apex. The surface is densely covered by regular silky ribs. The sutures between whorls are incised. The aperture is rounded. The inner aperture lip is slightly curved while the outer lip is rounded. The umbilicus is broad with an average diameter of 0.3 mm.

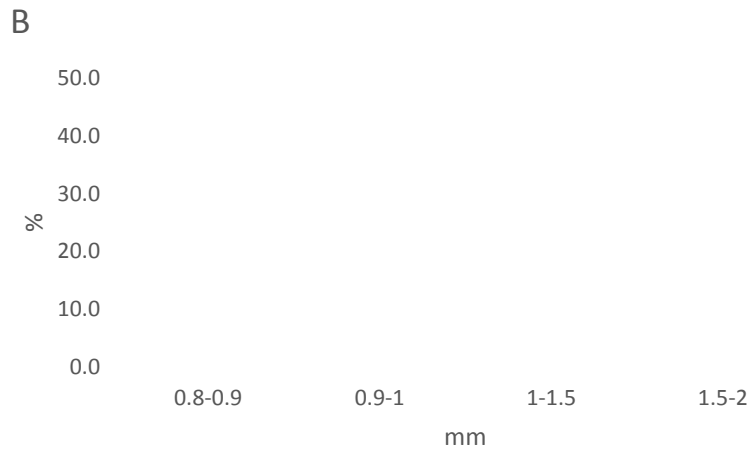


Figure 65: Biometric values of *Valvata saulcyi* (n = 10 shells). A) Shell height (mm) and B) Shell width (mm).

Ecology/Paleoecology: This living species thrives in slowly running headwaters of rivers, ponds, springs, channels and lakes on muddy-sandy bottoms to hard grounds, as well as in ditches with stagnant water, preferably with aquatic vegetation. *V. saulcyi* is tolerant of (slight) salinity increases and eutrophication (Şereflişan *et al.*, 2009; Bößneck, 2011; Van Damme and Kebapçı, 2014).

Biogeography/Paleobiogeography: According to Tchernov (1979), *V. saulcyi* is widespread in the Levant regions since the Pliocene on. The range of distribution of living populations includes several Middle East aquatic environments from Jordan,

Syria, Palestine, Lebanon, Turkey and Egypt (Amr *et al.*, 2014). According to these authors, *V. saulcy* has also been reported in wetlands from the island of Sicily (Italy). Mienis (1987) reported this species in freshwater springs and ponds from Lebanon during a faunal survey in 1983. No fossil populations of this species has been previously cited. This species is considered as recent taxa (www.molluscbase.org).

Family: **Bithynidae**

Species: *Bithynia* sp.

(figs. 67 D-E and 68 C)

Material: Many opercula belonging to *Bithynia* were retrieved from different samples many from sections 1, 2, 3, 4 and 5 (Tables 2 and 3). Seven opercula were measured.

General description: The operculum is a calcareous structure common in many groups of gastropods that acts as a trapdoor. Animals use the operculum to close the aperture of the shell when its soft parts are retracted. *Bithynia* opercula are oval or teardrop in shape and they can be classified as concentric type according to the opercula taxonomy developed by Panha and Burch (2004). The average diameter of 7 measured opercula is 1.48 mm.

Ecology/Paleoecology: Species of *Bithynia* dwell in moving and standing water bodies, also in temporarily drying water bodies, on muddy bottoms, rock or plants (Welter-Schultes, 2012).

Biogeography/Paleobiogeography: Remains of *Bithynia* shells (main shells and operculum) have been recovered from lacustrine and shallow marine deposits in Eurasia ranging in age from Jurassic (China) to Quaternary in Europe (www.fossilworks.org and references herein). However, the Mesozoic attributions to this genus are uncertain (pers. comm. Dr. Thomas Neubauer).

Family: **Melanopsidae**

Species: *Melanopsis buccinoidea* Olivier, 1801

(figs. 50 and 67 F)

Material: A large number of specimens were found in sample Z-17 and Z-17', whereas less than 25 shells were retrieved from several samples in sections 2, 3, 4 and 5 (Tables 2 and 3). Ten shells were measured.

General description: Shells are elongated showing a conical shape (figs. 49, 65, 66 F). They are very variable in size. Juvenile specimens range in width (SD) from 1.2 to 1.5 mm and in height (SH) from 2.1 mm and 2.5 mm. Shells belonging to adults are up to 32 mm in height and 22 mm in width (fig. 50). The shell is composed of up to 7 whorls. It is smooth and has a pointed spire. The whorls are flattened and separated by very shallow sutures. The spire is located within the upper part of the shell while the body whorl occupies more than half of the shell. The shell aperture or mouth is located within the body whorl. It is oblique, elongated and sharply edged, with a mouth diameter (MD) about 0.6 mm and a mouth height (MH) of 1.2 mm (fig. 66). The inner lip is nearly straight while the outer lip is oblique to nearly curved.

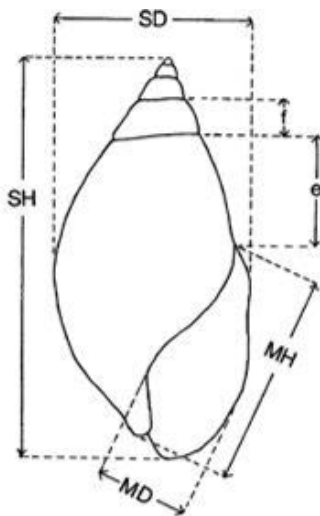


Figure 66: Schematic draw of a *Melanopsis* shell. Shell conchometric's abbreviations: SH, shell-height; MH, mouth-height; SD, shell-diameter; MD, mouth-diameter; f, whorl; e, last whorl. (Heller *et al.*, 2005).

Ecology/Paleoecology: This species, nowadays native to the Middle East, dwells in various freshwater habitats, including streams, ponds, springs, pools and swamps (Van Damme, 2014).

Biogeography/Paleobiogeography: *Melanopsis buccinoidea* is today a widely spread aquatic snail living throughout the Levant area and Turkey. Beyond the Levant, populations of *M. buccinoidea* have been reported in the Iberian Peninsula and in north-west Africa (Brown, 1994). Little is known about the paleobiogeographic distribution of this species. Fossils of *M. buccinoidea* have been recovered from Pleistocene lacustrine deposits in the Jordan Rift Valley at the north of Jordan and in Miocene and Pliocene deposits of Palestine (Tchernov, 1979; Alhejoj and Bandel, 2013). According to Neubauer *et al.* (2016), *Melanopsis* species cannot be easily differentiated due to their shell polymorphism in response to environmental conditions. This genus has an Eurasian origin. Fossils of *Melanopsis* have been recovered from many Miocene and Pleistocene Eurasian lacustrine basins (Van Damme, 1984 and references herein).

Family: **Hydrobiidae**

Species: *Semisalsa* sp.

(figs. 67 G-H and 68 D-E)

Material: Gastropod shells of *Semisalsa* sp. were found in almost all the sections (Tables 2 and 3). Ten specimens were measured in this study.

General description: Small elongated, conical shell with a width ranging between 0.9 and 1.8 mm (mean 1.33 mm) and a height ranging between 1.7 and 3.8 mm (mean 2.71 mm). The spire occupies half of the shell while the body whorl occupies the other half. The aperture is sub rounded about 500 µm in diameter. It is slightly elongated with

sharp edged upper part and rounded bottom. The inner lip is nearly straight while the outer lip is oblique to nearly curved.

Ecology/Paleoecology: This genus has a broad ecological amplitude occurring in brackish water environments, estuaries, salt lakes and non-tidal lagoons, coastal rivers, as well as in freshwater springs, wells, ponds and lakes (Bank and Butot, 1984; Glöer, 2002).

Biogeography/Paleobiogeography: The oldest record of the genus dates back to the latest Oligocene of Germany (Kadolsky, 2008). Fossil shells of *Semisalsa* were recorded from middle-upper Miocene (12.7-11.6 Ma) rocks in Austria (pers. comm. Dr. Thomas Neubauer).

Species: *Pseudamnicola* sp.

(fig. 67 E)

Material: More than 100 specimens were found in sample Z-16. A reduced number of shells were recovered from sections 1, 2 5 and 8 (Tables 2 and 3). Five fossils were measured.

General description: Shells are conical in shape with a diameter size ranging between 0.9 and 1.2 mm (mean 1.08 mm) and height ranging in size between 1.5 and 2.4 mm (mean 1.95 mm). Shells have 4 whorls showing inclined and moderately incised sutures. The spire occupies half of the shell while the body whorl occupies the other half. The aperture extends beyond the spire. It is circular with sharply edged upper parts and rounded bottom. The inner and the outer lips are rounded and the umbilical area is oblique and broad.

Ecology/Paleoecology: Species of *Pseudamnicola* dwell in coastal streams, lakes, ponds, low river courses, springs and thermal springs (Szarowska, 2006; Glöer *et al.*, 2010; Delicado *et al.*, 2015).

Biogeography/Paleobiogeography: Fossils belonging to this genus date back into the early Paleocene of Belgium (Glibert, 1973). Fossil shells of *Pseudamnicola* were reported from Eocene and Oligocene deposits in France and United Kingdom. However, their attribution to the genus *Pseudamnicola* is very doubtful (pers. comm. Dr. Thomas Neubauer).

Species: *Islamia* sp.

(figs. 67 J-K and 68 F-G)

Material: *Islamia* sp. represents the most abundant gastropod species occurring in almost all the samples. Shells of *Islamia* are extremely abundant in samples Z-5, Z-6, Z-8, Z-10 and Z-11. A smaller shell assemblage was recovered from samples Z-1, Z-2, Z-7 and Z-17', while few shells were found in samples Z-3, Z-9, Z-12, Z-16 and Z-17 (Tables 2 and 3). Fifteen shells were measured in this study.

General description: Shells are small and depressed in shape ranging in diameter between 0.6-1.6 mm (mean 1.19 mm) and height between 0.8 and 1.6 mm (mean 1.05 mm). The shell consists of 3 whorls. The sutures between the whorls are inclined and deeply incised. The aperture has a circular shape of about 0.79 mm in diameter. It is circular with rounded upper and bottom areas. The inner and the outer lips are rounded and the umbilical area is inclined and broad.

Ecology/Paleoecology: Living species of *Islamia* are found in subterranean waters and springs, occasionally also in rivers and lakes (Bodon *et al.*, 2001; Arconada and Ramos, 2006; Radea *et al.*, 2017). *Islamia* inhabits non-polluted springs, rich in water and

aquatic vegetation. Many species of *Islamia* have a very narrow distribution being endemic from their type localities (Beran *et al.*, 2016). These authors reported that the narrow distribution of several *Islamia* species makes them vulnerable to water pollutants and their populations are threatened by human activities.

Biogeography/Paleobiogeography: The fossil record of *Islamia* is quite patchy probably due to the difficulties in identifying the genus in the fossil record. According to Thomas Neubauer (pers. comm.), some fossil attribution might be mistaken for *Valvata* or similar valvatiform hydrobiids. Fossil shells of *Islamia* were extracted from the upper Miocene (Tortonian and Messinian) lacustrine deposits of Italy (Esu and Girotti, 2015). Esu (1984) reported fossil *Islamia* shells from the Pliocene deposits of Italy.

Family: **Lymnaeidae**

Species: *Radix* sp.

(fig. 67 L)

Material: A reduced number of shells were recovered from samples Z-10 and Z-17 (Tables 2 and 3). Three shells were measured.

General description: Elongated subovate shell with an average diameter of 1.4 mm and an average height of 2.3 mm. Individual shell is composed of around 3 whorls. The sutures between the whorls are straight and moderately incised. The spire is located within the upper part of the shell while the body whorl occupies 3/4 of the shell. The aperture is much extended beyond the spire. It has a characteristic ear shape with narrow upper part and broad bottom. The inner lip is straight and the outer lip has a curved shape. The umbilical area is oblique and broad.

Ecology/Paleoecology: Species of the genus *Radix* are found in standing or slowly moving freshwaters often rich in vegetation (Welter-Schultes, 2012).

Biogeography/Paleobiogeography: Species of *Radix* thrive in freshwater environments across the Palearctic realm¹⁰ (Pfenninger *et al.*, 2006). Fossil populations of *Radix* have been found in early-middle Miocene deposits located at the northern margin of the Molasse basin in southern Germany (Salvador *et al.*, 2017).

Family: **Planorbidae**

Species: *Gyraulus* cf. *hebraicus* Bourguignat, 1852

(fig. 67 M)

Material: Few shells were recovered from samples Z-1, Z-8, Z-11 and Z-17' (Tables 2 and 3). Only one specimen was measured.

General description: flat, depressed and smooth planispiral shell with helical form. It has a width of 1.56 mm and a height of 1.05 mm. The shell consists of 3-4 regular whorls with constant and slightly incised sutures. The top and the bottom of the aperture coincides with the spire. The inner aperture lip is nearly straight while the outer lip is strongly curved.

Ecology/Paleoecology: This species thrives in ponds and vegetated rivers (Seddon, 2014).

Biogeography/Paleobiogeography: Living populations of this species has been reported in ponds from Turkey, Syria, and Lebanon (Meier-Brook, 1983). Fossils of *G. hebraicus* have been extracted from Pleistocene lacustrine deposits in southern Turkey (Glöer and Girod, 2013). Fossils of the genus *Gyraulus* were found in many localities worldwide from different sedimentary rock ages including Jurassic layers from China

¹⁰ Palearctic: biogeographic realm including Europe, Asia north of the foothills of Himalayas, North Africa, northern and central parts of Arabian peninsula and the Mediterranean.

and France to recent deposits in the Palearctic realm (www.fossilworks.org and references herein). However, the Mesozoic and Paleogene attributions to this genus are unclear.

Species: *Gyraulus* cf. *piscinarum* Bourguignat, 1852

(figs. 67 N-O and 68 J)

Material: About 25-100 specimens were recovered from samples Z-8, Z-10 and Z-16. A reduced number of gastropod shells occur in several samples from sections 1, 2, 3, 4, 5 and 6 (Tables 2 and 3). Ten specimen were measured in the study.

General description: The shell is flat, depressed and planispiral. The surface of the shell is densely covered by regular ribs. It is ranging in width between 1.4 and 3 mm (mean 1.9 mm) and ranging in height between 0.5 and 0.9 mm (mean 0.66 mm). The shell consists of 3-4 whorls with incised sutures. Differences between *G. piscinarum* and *G. hebraicus* are based on the whorl diameter and accretion. The shell of *G. piscinarum* shows wider whorls relative to its total diameter. Moreover, the whorl accretion in *G. piscinarum* is much slower than the former *G. hebraicus*.

Ecology/Paleoecology: This species dwells in swamps and slowly flowing, vegetated waters (Heller, 2009).

Biogeography/Paleobiogeography: The range of distribution of living populations of *G. piscinarum* includes lacustrine environments from Bulgaria, Iran, Palestine, Lebanon, Syria and Turkey (Amr *et al.*, 2014). Fossils of this species have been reported in Quaternary deposits from Palestine (Tchernov, 1979).

Family: **Thiaridae**

Species: *Melanoides* cf. *tuberculata* Müller, 1774

(fig. 69 A-C)

Material: About 25 to 100 specimen were recovered from the sample Z-17' (Table 3). Three specimen are measured in the study.

General description: The shell is elongated and conical in shape. Its width ranges between 2.56 and 4.26 mm (mean 3.16 mm) and a height ranging between 4.35 and 9.28 mm (mean 6.39 mm). The spire occupies half of the shell while the body whorl occupies the other half. Six to seven regularly increasing, inflated whorls with well-rounded periphery can be distinguished. Between each whorl, shell surface is covered by a characteristic ornamentation composed of 5 horizontal ribs and many vertical ribs. The aperture is oval and slightly elongated with sharp edged upper part and rounded bottom. The inner lip is nearly straight while the outer lip is oblique to nearly curved. The apertures of many shells appear broken suggesting that they were buried after some transport from their original living locality.

Ecology/Paleoecology: This species lives in all types of permanent fresh water in warm temperate to tropical climates. This species can thrive in small springs or vast lakes such as the Lake Victoria (Tanzania), and from oligotrophic to eutrophic waters (Brown, 1994). *M. tuberculata* is a browser of microalgae and a detritivore, feeding on detritus, plant leaves and dead animals (Madsen, 1992). This aquatic snail is able to survive in relatively alkaline and saline waters. This species is parthenogenetic¹¹ and it is spread by aquatic birds. (www.iucnredlist.org and references herein).

Biogeography/Paleobiogeography: *Melanoides tuberculata* thrives in lakes from Africa, Middle East and east of Asia (Brown, 1994; Neubert, 1998). This species was also found in the Greek islands of Rhodes and Kos (Heller, 2007). Moreover, it is an exotic invader to America. *M. tuberculata* was reported in several Miocene lacustrine

¹¹ Parthenogenetic: natural form of asexual reproduction in which growth and development of embryos occur without fertilization. Parthenogenesis occurs naturally in some plants, some invertebrate animal species and a few vertebrates.

basins from both African and Asian continents, suggesting that its distribution range have not changed very much (Van Damme & Pickford, 2003; Songtham *et al.*, 2005). Moreover, it has been reextracted from Quaternary lacustrine deposits from south of Italy and Spanish Balearic Islands (Giusti *et al.*, 1995). *M. tuberculata* also occurs in Pliocene lacustrine deposits in Palestine (Tchernov, 1979).

5.1.2 *Terrestrial Gastropods*

Family: **Vitrinidae**

Species: *Phenacolimax* sp.

(fig. 68 H-I)

Material: Only two specimens were extracted from sample Z-19 (Table 3).

General description: The shells are flattened showing a subglobose shape. They are 2.1 mm high and 1.3 mm wide in average. Individual shells are smooth consisting of three whorls that enlarge rapidly. The body whorl is extremely enlarged. The aperture is wide and the umbilicus is small.

Ecology/Paleoecology: This species has no specific ecological requirements.

Biogeography/Paleobiogeography: The fossil record of this genus is composed of 3 species. i.e. *P. intermedius* from the early Miocene (19.1-17.65 Ma) of Czech Republic (Harzhauser *et al.*, 2014); *P. crassitesta* from the middle Miocene (14.9-13.8 Ma) of Poland (Harzhauser and Neubauer, 2018) and *P. suevica* from the latest early to middle Miocene (c. 16.8-13.8 Ma) of Germany (Salvador *et al.*, 2016).

Family: **Crychiidae**

Species: *Carychium* sp.

(fig. 67 P)

Material: dozens of shells have been extracted from samples Z-8, Z-9 and Z-11 (Table 2). Four specimens were measured in this work.

General description: Shells are elongated with an angular narrow apex, ranging in width between 0.6 and 0.9 mm (mean 0.813 mm) and in height between 1.5 and 2 mm (mean 1.8 mm). The shell consists of about 4-5 whorls with deeply incised nearly horizontal sutures. The aperture is elongate oblique with nearly symmetrical inner and outer lips extending beyond the aperture. Two characteristic denticles can be observed inside the aperture.

Ecology/Paleoecology: *Carychium* species live in humid or wet habitats in tropical and temperate forests, meadows and swamps, where they comprise the decomposer community of the leaf litter of ecologically stable environments. (Welter-Schultes, 2012).

Biogeography/Paleobiogeography: Species of this tiny terrestrial snail thrive in 3 large biogeographic realms i.e. Nearctic¹², Palearctic and Indomalayan¹³ (Weigand *et al.*, 2013). *Carychium* is found at high northern latitudes (Sweden) as well as lower latitudes such as Indonesia (Weigand *et al.*, 2013; Jochum *et al.*, 2017). Fossil populations of *Carychium* have been extracted from Paleocene, Miocene and Pleistocene non-marine deposits from many European basins (Wenz, 1923-1930 and references herein).

Family: **Vertiginidae**

Species: *Vertigo* cf. *antivertigo* Draparnaud, 1801

(fig. 67 Q)

¹² Nearctic: biogeographic realm including North America, Greenland, central Florida and highlands of Mexico.

¹³ Indomalayan: biogeographic realm including south and Southeast Asia as well as south parts of east Asia.

Material: a reduced number of shells have been extracted from samples Z-8, Z-10 and Z-11 (Tables 2 and 3). Two fossils were measured and described.

General description: Shells are subovate in shape with a rounded broad apex. They have an average width of 1.2 mm and an average height of 1.75 mm. Each shell consists of 3 whorls with moderately incised, slightly inclined sutures. The aperture is nearly circular with curved inner and outer lips showing three denticles.

Ecology/Paleoecology: This hygrophilous¹⁴ species dwells in swampy meadows, along river and lake margins and in regularly flooded areas, mainly among rotting plant material. This species needs permanent moist habitats and it cannot thrive in places subjected to temporary droughts (Welter-Schultes, 2012).

Biogeography/Paleobiogeography: This species has a Palaearctic distribution pattern living nowadays widespread in almost all of Europe and large parts of Asia (Ložek, 1964; Kerney *et al.*, 1983; Shileyko, 1984; Pokryszko, 1990). In Europe, this species was not recorded at elevations higher than 900 above the sea level while in Asia, it was reported by Shileyko (1984) from the Asian tundra and in Pakistan (Pokryszko *et al.*, 2009). This tiny terrestrial snail is a characteristic species of early and middle Pleistocene ages in east Europe. Fossils of this species have been reported from early to late Pleistocene in Hungary (Krolopp and Sümegei, 1993). Shells belonging to *Vertigo* genus were found in Paleocene, Eocene, Oligocene, Miocene and Pliocene terrestrial deposits of Europe, North Africa and Turkey (Wenz, 1923-1930 and references herein).

Family: **Strobilopsidae**

Species: *Strobilops* sp.

(fig. 67 R)

¹⁴ Hygrophilous: organism living in wet or very moist ground.

Material: A reduced number of specimens have been recovered from the sample Z-11 (Table 2). One specimen has measured and described in this study.

General description: The shell is trochiform and dome-shaped. It has a width of 1.2 mm and a height of 2.1 mm. The shell is composed by 4 enlarging whorls with horizontal and deeply incised sutures. The shell surface exhibits a characteristic striation. Striations extends obliquely between the sutures. The aperture is small with a straight inner lip and curved outer lip. One denticle is located within the inner lip.

Ecology/Paleoecology: Extant species of *Strobilops* live in decaying logs and dead leaves in moderately humid forests (Pilsbry, 1927).

Biogeography/Paleobiogeography: Species of *Strobilops* are thriving in west North America and Canada areas (Forsyth and Oldham, 2014). Fossil shells of this terrestrial snail have been recovered from Quaternary sediments in Florida, Texas and Virginia counties in USA. However, older fossil of *Strobilops* (up to 26 species) have been reported in upper Eocene to Pliocene deposits from several terrestrial European basins (Wenz, 1923-1930 and references herein). No record of this genus has been found after the Pliocene in Europe since it became extinct before the first major glaciation.

5.2 Mollusca (BIVALVIA)

Family: Sphariidae

Species: *Piscidium* cf. *moitessierianum* Paladilhe, 1866

(figs. 67 S-U and 68 K)

Material: a reduced number of shells have been extracted from samples Z-5, Z-6, Z-8, Z-9, Z-16, Z-17 and Z-17' (Tables 2 and 3). Five valves were measured and described.

General description: The long-oval and oblique wedge-shaped shell is thick with a height ranging between 1 and 1.7 mm (1.38 mm) and width between 1.5 and 2.5 mm (mean 1.95 mm). The outer shell surface is silky and sculptured with coarse, concentric, uniformly-spaced striae. The inner part of the shell is characterized by a long and arched hinge. The umbo and pallial line are prominent. The hinge plate is narrowed at the pseudocardinal teeth and becomes thicker toward the lateral teeth (fig. 14).

Ecology/Paleoecology: This species requires slowly moving, well-oxygenated hard water over clean, unpolluted substrates varying from fine mud to sand. It dwells in lowland rivers, canals and large lakes with moderately moving water and amongst macrophytes (Welter-Schultes, 2012). It occurs from 0.5–20 m depth in the littoral zone of lakes. It usually favors oligotrophic water with oxygen content over 50% saturation but it can tolerate some anoxic conditions over winter. *Pisidium moitessierianum* is relatively thermophilic¹⁵ and can tolerate an annual water temperature range of 1–20°C (Grigorovich *et al.*, 2000).

Biogeography/Paleobiogeography: This freshwater aquatic clamshell occurs in many European perennial lakes becoming frequent at higher latitudes (Kuiper *et al.*, 1989). This species is native in north Europe. However, *P. moitessierianum* has been reported in North American Great lakes from 1890s probably introduced into the new continent through ships (Grigorovich *et al.* 2000; Cummings and Graf, 2010). Fossils of *Pisidium* genus have been recovered from Neogene European and North American lacustrine deposits (pers. comm. Dr. Thomas Neubauer).

¹⁵ Thermophilic: organism able to survive at high temperatures.

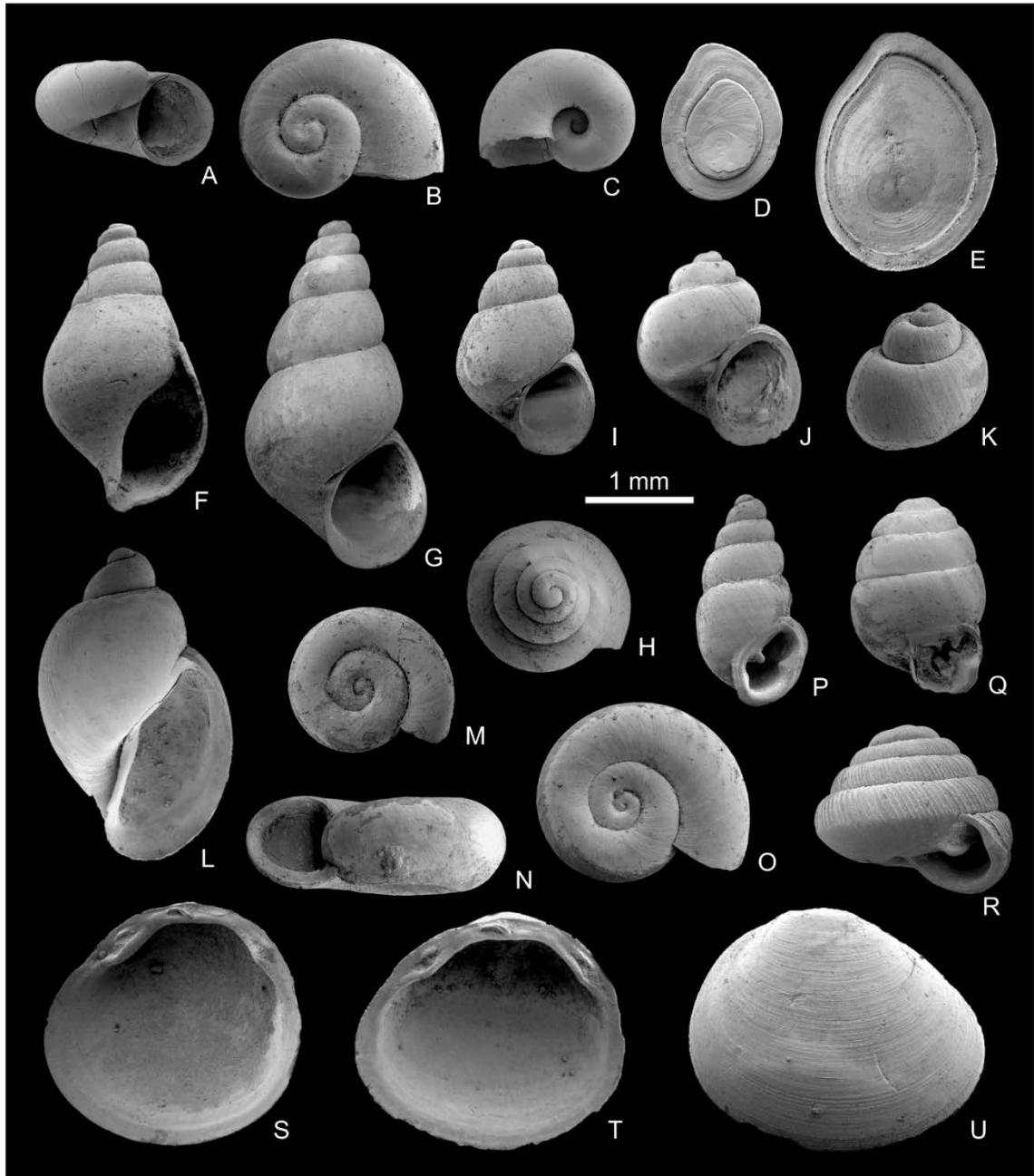


Figure 67: Mollusks recovered from Miocene lacustrine deposits near Zahle. A-C) *Valvata saulcyi*, sample Z-8. D-E) *Bithynia* sp. (opercula), sample Z-8. F) *Melanopsis buccinoidea*, sample Z-6. G-H) *Semisalsa* sp., both from sample Z-5. I) *Pseudamnicola* sp., sample Z-4. J) *Islamia* sp., sample Z-5. K) *Islamia* sp., sample Z-1. L) *Radix* sp., sample Z-10. M) *Gyraulus* cf. *hebraicus*, sample Z-8. N) *Gyraulus* cf. *piscinarum*, sample Z-5. O) *Gyraulus* cf. *piscinarum*, sample Z-1. P) *Carychium* sp., sample Z-8. Q) *Vertigo* cf. *antivertigo*, sample Z-8. R) *Strotilops* sp., sample Z-11. S-U) *Pisidium* cf. *moitessierianum*, sample Z-6.

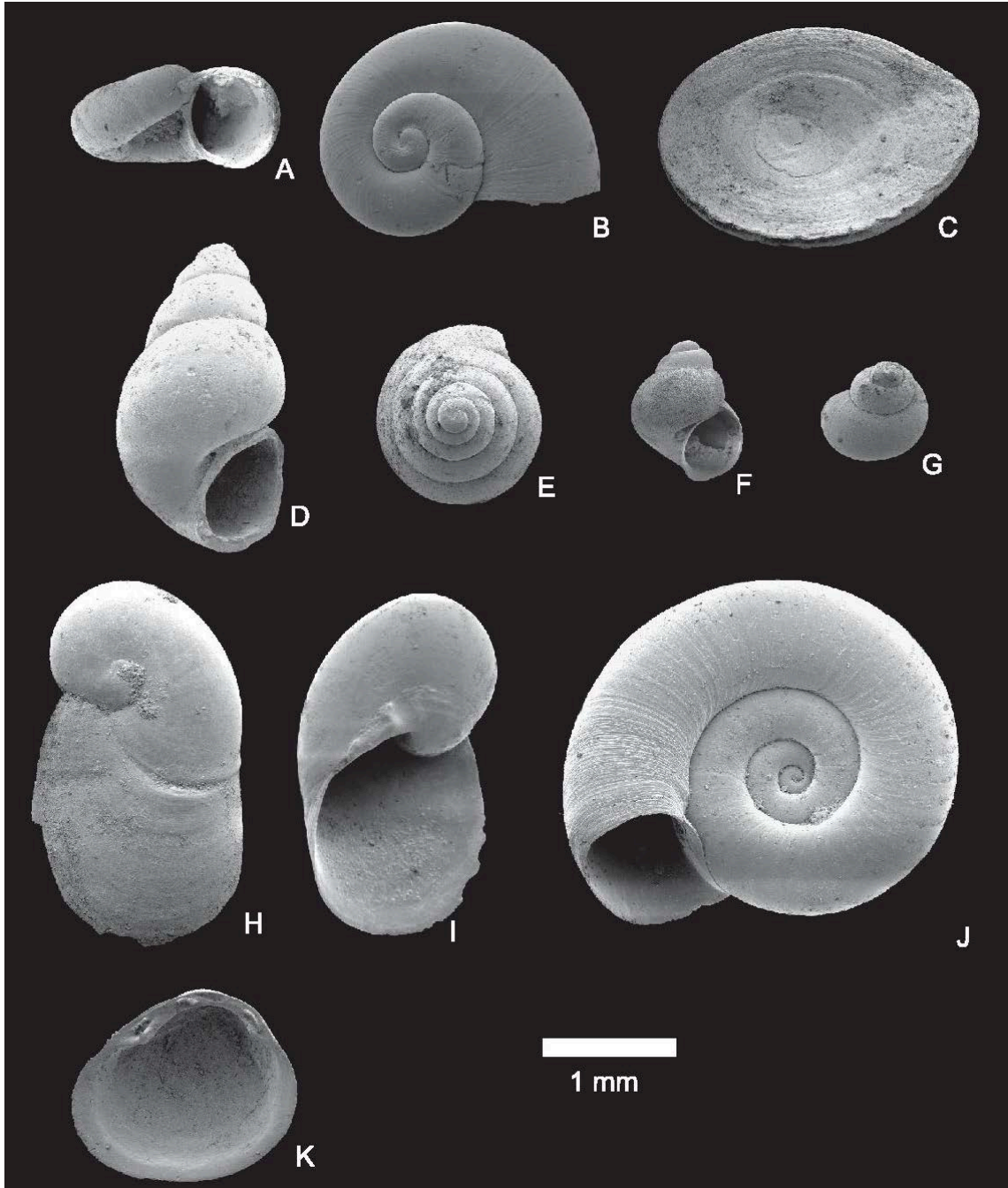


Figure 68: Mollusks recovered from Zahle. A) *Valvata saulcy*, sample Z-13. B) *Valvata saulcy*, sample Z-16. C) *Bithynia* sp. operculum, sample Z-13. D) *Semisalsa* sp. (broken aperture), sample Z-19. E) *Semisalsa* sp., sample Z-14. F-G) *Islamia* sp., sample Z-17. H-I) *Phenacolimax* sp. sample Z-19. J) *Gyraulus* cf. *piscinarum*, sample Z-16. K) *Piscidium* cf. *moitessierianum*, sample Z-16.

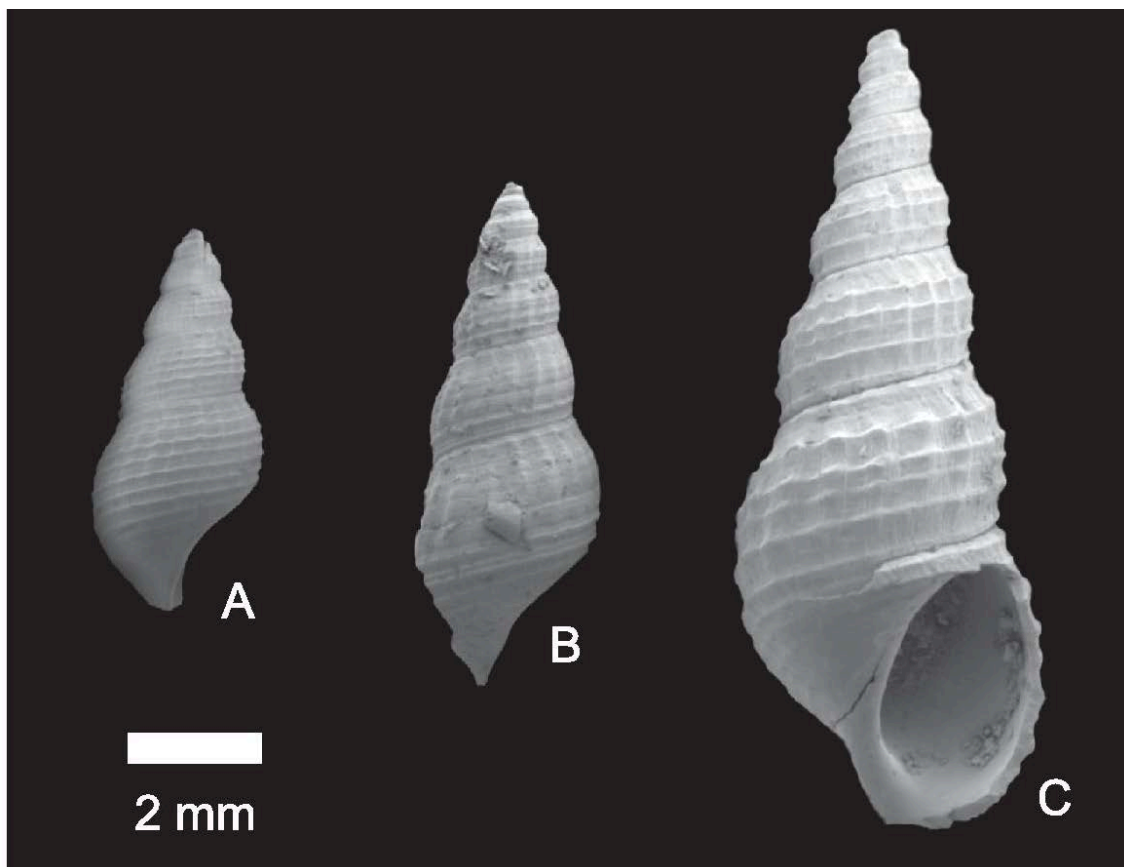


Figure 69: SEM images of *Melanoides* cf. *tuberculata* from sample sample Z-17'. Shells show their last whorl broken.

5.3 Crustacea (OSTRACODA)

Five ostracod species have been recovered from the studied sections, i.e.

Cyprideis sp., *Cypris pubera* Müller, 1776, *Candona* cf. *angulata* Müller, 1900, *Strandesia* sp. and *Ilyocypris* sp.

Family: **Cytherideidae**

Species: *Cyprideis* sp.

(figs. 71 A-N and 72 C-F and I)

Material: This species is the dominant ostracod which occurs in a large number of samples (Tables 2 and 3). A reduced number of shells have been recovered from samples Z-0, Z-1, Z-2, Z-12 and Z-13 (Tables 2 and 3). Forty-eight shells were measured (fig. 70).

General description: carapaces are very variable in size ranging in length between 620 and 1135 μm (mean 841 μm) and between 400 and 650 μm (mean 501 μm) in height (fig. 70). Either side of the dorsal hump are almost straight. Anterior and posterior margins are equally rounded and the ventral margin is straight. The surface of the carapace is very variable being smooth, pitted or ornamented with large nodules. Nodded carapaces are frequent in some sample (fig. 71 K-N). The specimens from Zahle closely resemble the widespread and well-known polymorphic species *Cyprideis torosa* (Jones, 1850).

Ecology/Paleoecology: Living species of *Cyprideis* thrive in a wide range of aquatic habitats from freshwater oligohaline¹⁶ athalassic¹⁷ lakes (low salinity inland lakes) to brackish coastal flooded areas and have a diverse salinity range (Sandberg, 1964; Keyser, 1978). Shells of this genus show a strong polymorphism linked to its ecophenotypical¹⁸ plasticity such as increased shell nodding with decreased salinity (Sandberg, 1964; Van Harten, 1975, 2000). The species *Cyprideis torosa* evolved in the Neogene or early Pleistocene and is at present common in marginal marine and athalassic saline waters (Gliozzi *et al.*, 2017). It is extremely euryhaline¹⁹, tolerating a wide range of salinities from around 0.5 to 60 psu²⁰ or more, although its optimum ranges appear to be in more dilute waters, from about 17 to 20 psu (Wouters, 2016). The species is generally found in shallow waters, <10 m deep (Pint *et al.*, 2012), and is tolerant of a wide range of dissolved oxygen concentrations, with the ability to tolerate

¹⁶ Oligohaline: characterized by very low salinity.

¹⁷ Athalassic: permanent or temporary, brackish, saline or hypersaline water body isolated from the sea.

¹⁸ Ecophenotype: non-heritable modifications of the organism's observable characteristics or traits, produced in response to factors in the environment or habitat.

¹⁹ Euryhaline: organism able to adapt to a wide range of salinities.

²⁰ Psu: practical salinity unit, equals to ‰.

dysaerobic²¹ conditions (Pint and Frenzel, 2016). The species is able to tolerate water temperatures from at least 5 to 20°C, although it is more productive at higher end of this range (Ruiz *et al.*, 2013). *Cyprideis torosa* shows strong salinity-driven ecophenotypic response in valve size (Boomer *et al.*, 2017), nodding (Frenzel *et al.*, 2012) and sieve pore morphology (Frenzel *et al.*, 2017). Variations in these characteristics in fossil shells have been used for paleosalinity reconstructions (De Deckker and Lord, 2017).

Biogeography/Paleobiogeography: The genus *Cyprideis* appeared in the late Oligocene or early Miocene with *Cyprideis traisensis* from the Mainz basin in Germany (Malz and Triebel, 1970). Since the Miocene, *Cyprideis* genus became widespread both in Eurasian and American continent (Ligios and Gliozzi, 2012). Fossils of *Cyprideis* were recorded in Miocene lacustrine deposits of Europe and Asia, in Pliocene layers of North Africa, south Europe and North America, Pliocene/Pleistocene deposits of North Africa, as well as the Quaternary of North and South America, North Africa and south Europe (www.fossilworks.org and references herein). Nowadays, *Cyprideis* species can be found in the Middle East, Europe, Africa, Asia, Australia as well as North America (Sandberg, 1964; Wouters, 2016). According to Decima (1964), *Cyprideis torosa* was derived from *Cyprideis tuberculata* during the Messinian (late Miocene), while Van Harten (1990) suggested its Pliocene origin from the Mediterranean species *C. agrigentina*. *Cyprideis torosa* displays the largest geographical distribution among all *Cyprideis* species, thriving mainly in coastal brackish waters of Europe, Asia and Africa (Meisch 2000; Wouters 2002, 2016). According to Van Harten (1990), the wide dispersal area of *C. torosa* is mainly due to the passive dispersal by aquatic birds feeding on them. This author stated that the shallow water preferences and the ability of

²¹ Dysaerobic: low oxygen levels.

C. torosa to survive temporary hostile conditions while transported make its dispersion even more efficient.

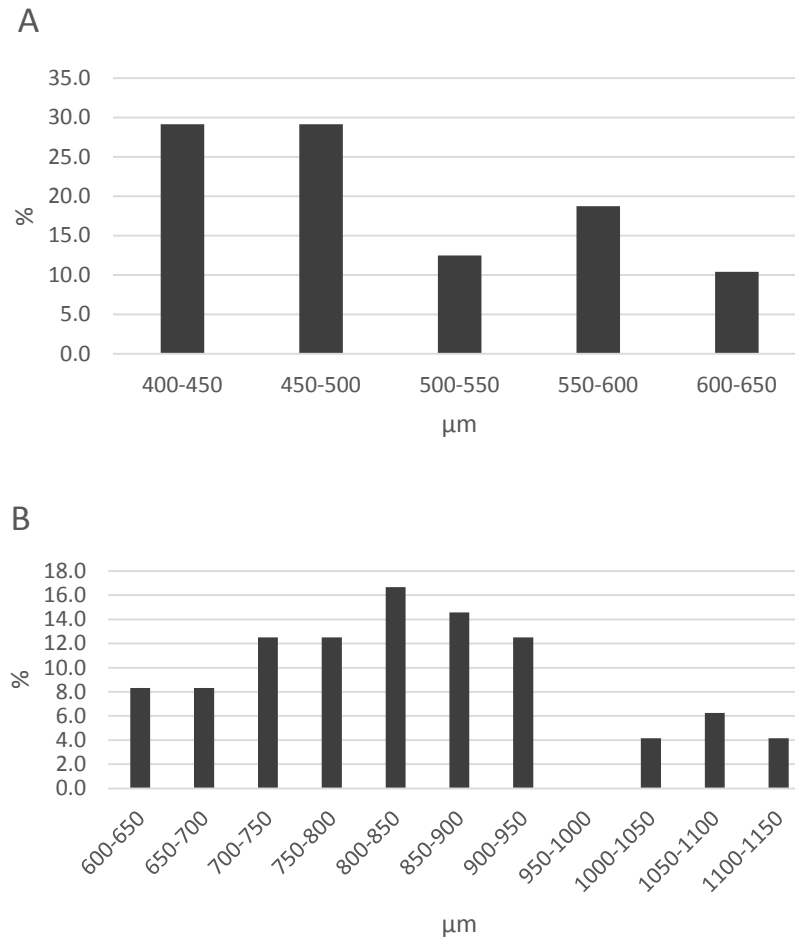


Figure 70: Biometric values of *Cyprideis* sp. (n = 48 carapaces). A) Carapace's height (µm) and B) Carapace's length (µm).

Family: **Candonidae**

Candona cf. *angulata* Müller, 1900

(figs. 71 Q and 72 A-B)

Material: Few specimens were recovered from samples Z-3, Z-5, Z-12, Z-15 (Tables 2 and 3). Five carapaces were measured.

General description: the carapace is 960 to 1280 µm long (mean 1088 µm) and 500 to 620 µm high (mean 550 µm). The dorsal hump is straight, and the right valves are larger compared to the left valves. The anterior margin is broadly rounded while the posterior margin is characterized by the presence of an angular apex. The ventral margin is strongly concave near the mid part of the shell. The surface of the valves is smooth and devoid of ornamentation.

Ecology/Paleoecology: *Candona angulata* prefers brackish water and is often found in coastal lakes with some input of seawater: it is found in waters with salinity from 0.2 to 14 psu and often co-occurs with *Cyprideis torosa* (Meisch, 2000).

Biogeography/Paleobiogeography: this species is mainly found nowadays in several European lakes and coastal flooded areas (Belgium, UK, France, Italy and Germany) (www.fauna-eu.org and references herein). Fossils of *Candona angulata* were reported in the upper Miocene deposits from eastern Anatolia (Turkey) (Nazik *et al.*, 2008) and late Pleistocene lacustrine deposits in Palestine (Kalbe *et al.*, 2015). Fossilized carapaces of *Candona* genus have been recovered from very old non-marine sedimentary rocks as old as Carboniferous from Germany, Mesozoic rocks from North America, South America and Asia and Cenozoic sediments from Europe, North America, Turkey and Asia (www.fossilworks.org and references herein).

Family: **Cyprididae**

Species: *Cypris pubera* Müller, 1776

(fig. 71 O)

Material: Few carapaces have been recovered from samples Z-5 and Z-6 (Table 2). Three shells were measured.

General description: large carapaces with an average length of 957 μm and average height of 663 μm . The valve surface is smooth. Greatest height is situated at dorsal hump. Ventral margin is straight. Anterior margin of dorsal hump is broadly rounded while the posterior margin is slightly angular with small angular spines.

Ecology/Paleoecology: This species is most commonly found in shallow water; it can tolerate elevated salinity up to about 4 psu (Meisch, 2000). According to this author, this species can live in both temporary and permanent aquatic environments.

Biogeography/Paleobiogeography: *Cypris pubera* is common in central and western Europe but rare in southern Europe (Meisch, 2000 and references herein). According to this author, this species has a Holarctic²² distribution. Fossil populations belonging to this species were reported in upper Miocene, Pleistocene and Quaternary deposits in several European basins (Meisch, 2000).

Species: *Strandesia* sp.

(fig. 72 P)

Material: One specimen has been recovered from sample Z-1 (Table 2).

General description: The shell is 970 μm long and 582 μm high. Anterior and posterior margins are equally rounded. The ventral and dorsal margins are straight along the entire carapace length while the dorsal margin is characterized by the presence of a spine (dorsal process). Surface of the valve is smooth devoid of ornamentation.

Ecology/Paleoecology: This specimen could not be identified to species level.

Biogeography/Paleobiogeography: Ostracods of the genus *Strandesia* thrive nowadays in North and South America, Europe, as well as west Australia, Africa and Asia (Karanovic, 2005).

²² Holarctic: biogeographic realm including Europe, central Asia, China, Africa, Turkey, the Middle East, North Africa and North America.

Family: **Ilyocypridae**

Species: *Ilyocypris* sp.

(fig. 72 G and H)

Material: Very few carapaces were extracted from samples Z-13 and Z-14 (Table 3).

Two shells have been measured and described.

General description: The carapaces have an average length of 780 μm and an average height of 480 μm . The anterior margin is broadly rounded compared to the posterior margin. The dorsal margin is straight along the entire length while the ventral margin is strongly concave near the middle part of the carapace. The surface of the shell is roughly ornamented with dense shallow pits and circular nodules. A characteristic depression (sulci) can be easily distinguished in the central part of the external shell.

Ecology/Paleoecology: Species of *Ilyocypris* live in vegetation-rich, temporary and permanent running waters. Moreover, they occur in shallow lakes, springs, marshes and rice-fields (Meisch, 2000). *Ilyocypris* can stand high salinity levels (Do Carmo *et al.*, 1999).

Biogeography/Paleobiogeography: *Ilyocypris* is a globally distributed genus and has been recorded from all continents except Antarctica (Karanovic and Lee, 2013). Fossils belonging to the genus *Ilyocypris* were recovered from lower Miocene sediments of Turkey, upper Miocene rocks of Turkey and France (Nazik *et al.*, 2008), Pleistocene and Holocene deposits in eastern Germany (Meisch *et al.*, 1996), Pleistocene layers of northern Palestine (Kalbe *et al.*, 2015) and Quaternary sediments in western China (Yang *et al.*, 2002).

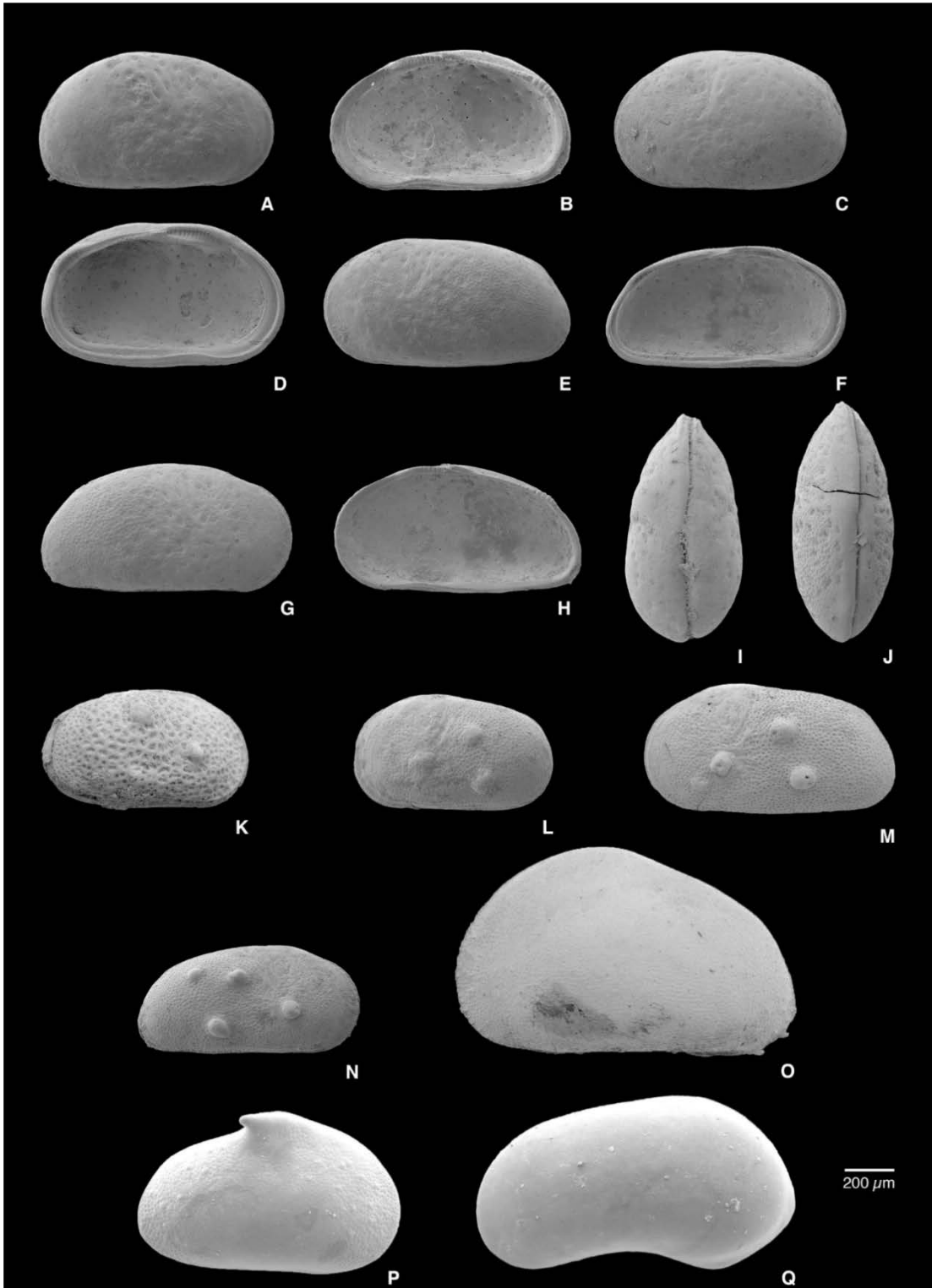


Figure 71: Ostracods from lacustrine deposits of Zahle in section 1, 2 and 3. A-J) *Cyprideis* sp., sample Z-7. K) *Cyprideis* sp., sample Z-0. L) *Cyprideis* sp., sample Z-5. M) *Cyprideis* sp., sample Z-8. N) *Cyprideis* sp., sample Z-5. O) *Cypris pubera*, sample Z-6. P) *Strandesia* sp., sample Z-1. Q) *Candona* cf. *angulata*, sample Z-5.

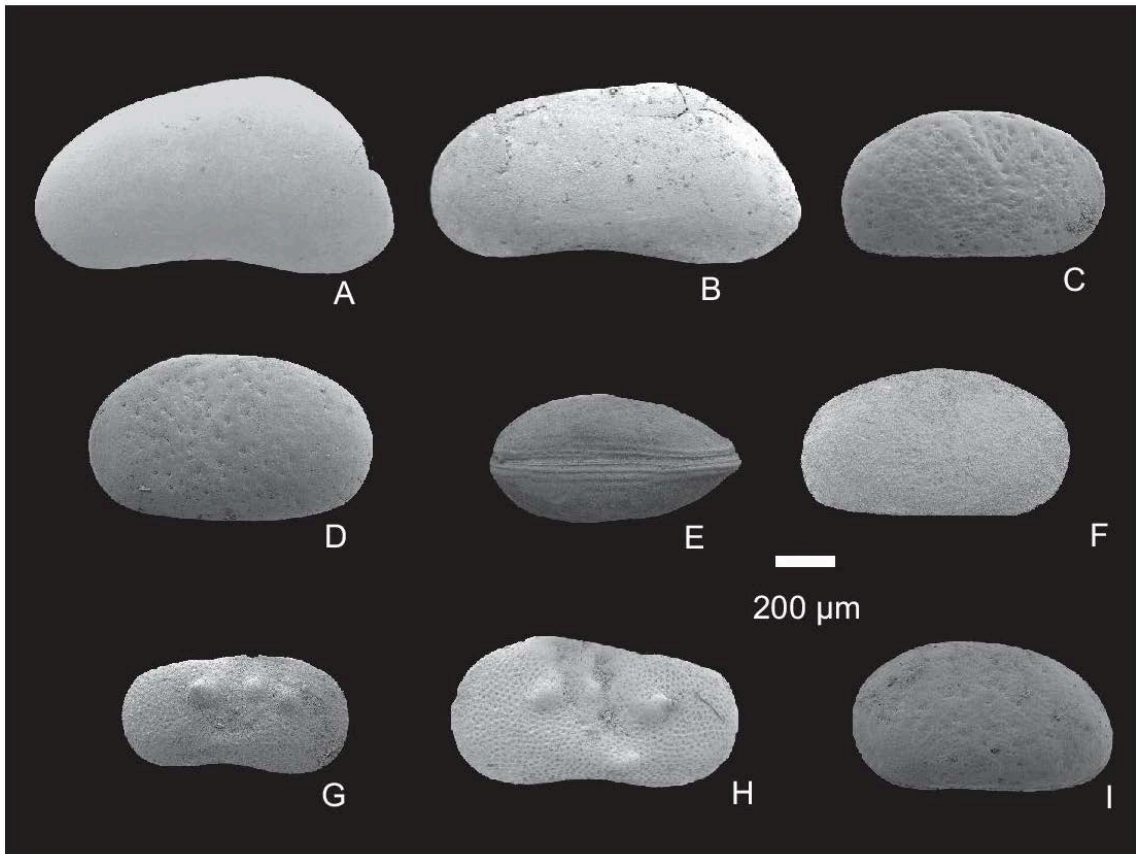


Figure 72: Ostracod assemblage recovered from sections 4, 5, and 7 near Zahle. A) *Candona* cf. *angulata*, sample Z-12. B) *Candona* cf. *angulata*, sample Z-15. C-D) *Cyprideis* sp., sample Z-17. E) *Cyprideis* sp., sample Z-21. F) *Cyprideis* sp., sample Z-14. G) *Ilyocypris* sp., sample Z-14. H) *Ilyocypris* sp., sample Z-13. I) *Cyprideis* sp., sample Z-14.

5.4 Charophyta (CHAROPHYCEAE)

Charophyte gyrogonites belonging to five taxa have been recognised in the lacustrine deposits of Zahle, i.e. *Nitellopsis (Tectochara) merianii*, *Lychnothamnus barbatus* var. *antiquus*, *Chara microcera*, *Chara* cf. *globularis* and *Sphaerochara* sp.

Family: **Characeae**

Species: *Chara* cf. *microcera* Grambast & Paul, 1965

(fig. 74 G-J)

Material: Several well-preserved gyrogonites (25-100) have been recovered from samples Z-1 and Z-2 (Table 2). Thirty-nine *gyrogonites* have been measured in this work.

General description: Small to medium sized gyrogonites, very variable in size, 475-720 μm high (mean 617 μm) and 340-474 μm wide (mean 414 μm), elongate, prolate to perprolate in shape, with an isopolarity index ranging from 120% to 179% (mean 144%). Ten to thirteen (frequently eleven) convolutions are visible in lateral view (52 μm high in mean value). Spiral cells are generally concave. Many gyrogonites display a characteristic ornamentation consisting in isolated small tubercles irregularly arranged along the spiral cells following one or two rows. The apex is psilocharoid (Feist *et al.*, 2005 taxonomy), prominent, sometimes ornamented with isolated small tubercles. The base is rounded or slightly pointed showing a shallow pentagonal basal pore.

Ecology/Paleoecology: Although there is no living representative of this species, previous micropalaeontological studies suggested that this extinct species grew in perennial freshwater lakes (Sanjuan *et al.*, 2014).

Biogeography/Paleobiogeography: *Chara* aff. *microcera* has been recorded from a large number of west European localities in many Paleogene/Neogene basins i.e., France (Paris, Aquitaine, Provence), Switzerland (Swiss Molasse), Germany (Rhine Graben) and Spain (Ebro and Tajo), (Sanjuan and Martín-Closas, 2014 and references herein). The occurrence of *Chara* aff. *microcera* in lacustrine deposits from Zahle represents its easternmost locality.

Species: *Chara* cf. *globularis* Thuiller, 1799

(figs. 74 K-N and 75 J-L)

Material: Many specimens of *Chara cf. globularis* have been recovered from a large number of samples through the sections (Tables 2 and 3). Ten specimens have been measured.

General description: Small to medium sized gyrogonites, 486-637 μm high (mean 555 μm) and 375-456 μm wide (mean 416 μm), elongate and prolate in shape, with an isopolarity index ranging from 120% to 144% (mean 130%). Nine to eleven convolutions are visible in lateral view in mean value). Spiral cells flat to concave and without ornamentation. Apex psilocharoid and prominent (Feist *et al.*, 2005 taxonomy). Base rounded to slightly pointed showing a small pentagonal basal pore.

Ecology/Paleoecology: *Chara globularis* lives in permanent or temporary shallow bodies of water. This species has a strong tolerance to eutrophication and is able to survive in areas with low light irradiance and very cold water temperatures, even resistant to lakes with frozen surfaces (Bailly and Shaefer, 2010).

Biogeography/Paleobiogeography: *Chara globularis* represents a cosmopolite species living in a large number of wetlands and lakes in all the continents except Antarctica (Bailly and Shaefer, 2010).

Species: *Lychnothamnus barbatus* var. *antiquus* Soulié-Märsche, 1989

(figs. 74 D-F and 75 D-G)

Material: Large gyrogonite proportions were recovered from sample Z-17. About 50-100 well-preserved gyrogonites have been recovered from samples Z-2, Z-12, Z-13 and Z-20. Few specimens were extracted from samples Z-5, Z-8 and Z-14 (Tables 2 and 3). Forty specimens were measured in this study.

General description: Gyrogonites are large, very variable in size, 619-901 μm high (mean 773 μm) and 521-739 μm wide (mean 613 μm), ellipsoidal in shape

with an isopolarity index ranging from 108% to 144% (average 125%). Spiral cells in the apical zone show a remarkably constant width, which results in a flat apex (figs. 73 E and 74 D-E). The base is tapered with a star-shaped basal pore, about 80 μm in diameter. Nine to eleven (frequently ten) cells are visible laterally. These are normally concave, non-ornamented and separated by prominent sutures, sometimes bicarinated.

Ecology/Paleoecology: The typical depth range of the living species *Lychnothamnus barbatus* in Europe is from 2 to 8 m where it forms dense meadows of up to 1 m high plants (Krause, 1985). This species has been traditionally related to cold and oligotrophic freshwaters usually associated to phreatic origin from northern Europe (Krause, 1997; Soulié-Märsche and Martín-Closas, 2003). However, recent studies performed in central-western Poland concluded that *L. barbatus* can also thrive under eutrophic conditions (Pelechaty *et al.*, 2017).

Biogeography/Paleobiogeography: *Lychnothamnus barbatus* var. *antiquus* has hitherto been recorded from numerous Miocene European localities i.e., Spain (González-Pardos, 2012; Suárez-Hernando *et al.*, 2013), southern France (Soulié-Märsche, 1989), Portugal (Antunes *et al.*, 1992), Montenegro (Krstić *et al.*, 2010) and Turkey (Mazzini *et al.*, 2013). The extant representative i.e., *L. barbatus* is a common species of the moraine lakes of northern Europe (Karczmarz, 1967). It was formerly known from Germany, Poland, France, Italy and Austria (Migula, 1897; Corillion, 1972; Krause, 1986). *Lychnothamnus barbatus* has been also recorded in the Balkans area (Blaženčić *et al.*, 2006), Poland (Sugier *et al.*, 2010) and Ukraine (Borisova and Yakushenko, 2008). This species has been rarely found growing in other areas out of

Europe such as Asia (Gollerbakh and Krasavina, 1983), Australia (Casanova *et al.*, 2003) and North America (Karol *et al.*, 2017).

Species: *Nitellopsis (Tectochara) merianii* (Al. Braun ex Unger, 1852) Grambast &

Soulié-Märsche, 1972

(figs. 74 A-C and 75 A-C)

Material: Hundreds of well-preserved gyrogonites were extracted from samples Z-2, Z-3, Z-12, Z-13 and Z-14. Dozens of well-preserved gyrogonites have been recovered from sample Z-1. Few specimens have been extracted from samples Z-5, Z-6, and Z-17 (Tables 2 and 3). One hundred gyrogonites were measured in this study (fig. 73).

General description: Gyrogonites very large and variable in size, ovoid in general shape 1071-1440 μm high (mean 1265 μm) and 828-1222 μm wide (mean 1035 μm), with isopolarity index ranging between 107% and 147% (mean 123%). Spiral cells concave to convex. Eight to ten (frequently nine) convolutions are visible in lateral view with a mean height value of 154 μm (fig. 73). Apex nitellopsidoid, according to the terminology of Horn af Rantzien (1959) and Feist *et al.* (2005), is flat to slightly convex or sub-rounded, with thinning and narrowing of the spiral cells in the periapical zone. Apical nodules present in the many specimens. The basal pole is rounded or slightly conical with large basal pore, 80 μm across, and located within a characteristic pentagonal funnel.

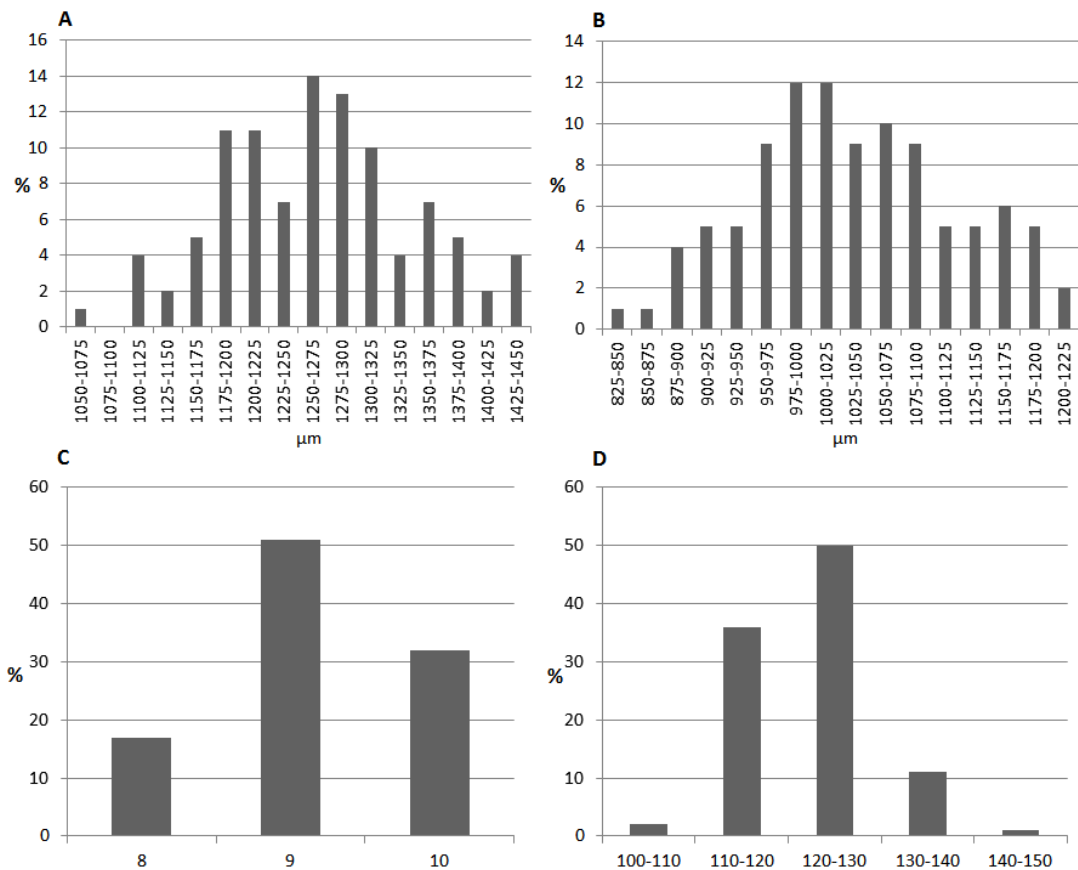


Figure 73: Biometric values of *Nitellopsis (T.) merianii* from sample Zahle 2 (n = 100 gyrogonites). A) Gyrogonite height (µm), B) Gyrogonite width (µm), C) Number of convolutions visible in lateral view and D) Isopolarity index (ISI = $h/w \times 100$).

Ecology/Paleoecology: This fossil species is considered the ancestor of the living species *Nitellopsis obtusa* (Desv. in Loisel.) Groves (Soulié-Märsche *et al.*, 2002; Sanjuan and Martín-Closas, 2015). These authors linked both species to an evolutionary lineage that ranges from the latest Eocene (late Priabonian) to the Quaternary. *N. obtusa* is a boreal species that is exclusively distributed in deep and shallow large, cold lakes of northern Europe, Asia and North America (Corillion, 1972; Soulié-Märsche *et al.*, 2002). In these permanent lacustrine habitats *N. obtusa* forms large and dense meadows of up to 2 m height covering the lake ground. It thrives in oligotrophic/mesotrophic alkaline waters in depths over 4 m (Krause, 1985; Soulié-Märsche *et al.*, 2002).

Biogeography/Paleobiogeography: Fossils of this species have been recovered from many upper Miocene-Pliocene basins in Europe and Asia (Sanjuan and Martin-Closas 2015 and references herein). Gyrogonites of *Nitellopsis obtusa* have been recovered from lacustrine deposits ranging in age from the early Quaternary to the present. Nowadays this species grows from the west coast of Europe to Japan. In recent years, Sleith *et al.* (2015) found *N. obtusa* in North America (USA) but at the moment is considered the product of introduction by humans and not a native taxon.

Species: *Sphaerochara* sp.

(fig. 74 O-Q)

Material: Few gyrogonites have been extracted from sample Z-10 (Table 2). Ten specimens were measured in this study.

General description: Gyrogonites are medium in size, 630 μm high and 533 μm wide (mean values), spheroidal in shape showing nine convolutions in lateral view displaying a characteristic ornamentation formed by large and regularly spaced tubercles arranged along the spiral cells. The apical ends of cells are slightly widening showing well-developed rounded nodules. The basal plate is visible from outside. In cases that basal plate is removed, a large basal pore with pentagonal shape is observed.

Ecology/Paleoecology: No ecological requirements can be deduced for this species since it does not have extant representatives.

Biogeography/Paleobiogeography: Very similar gyrogonites have been recovered from upper Miocene lacustrine deposits in the northeast of Spain (Moneva locality, Aragón). However, no formal taxonomic classification has already been performed (pers. comm. Dr. Sanjuan).

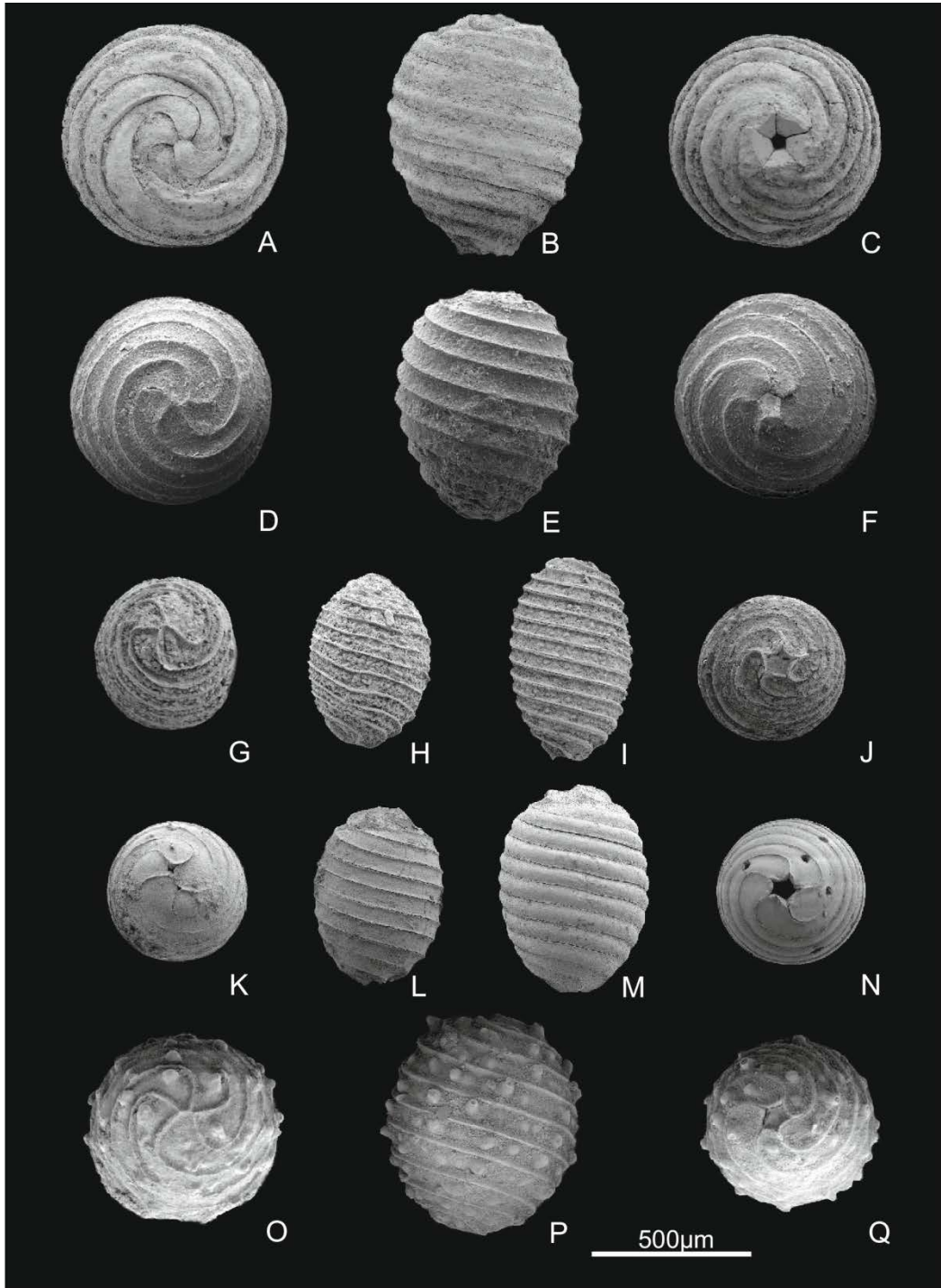


Figure 74: Gyrogonites from lacustrine deposits of sections 1 and 3 near Zahle. A–C) *Nitellopsis* (*T.*) *merianii*, sample Z-2 (A. apical view, B. lateral view, C. basal view). D–F) *Lychnothamnus barbatus* var. *megalicarpus*, sample Z-2 (D. apical view, E. lateral view, F. basal view). G–J) *Chara microcera*, sample Z-1 (G. apical view, H. lateral view, I. lateral view, J. basal view). K–N) *Chara* cf. *globularis*, sample Z-1 (K. apical view, L. lateral view); sample Z-8 (M. lateral view, N. basal view). O–Q) *Sphaerochara* sp., sample Z-10 (O. apical view, P. lateral view, Q. basal view).

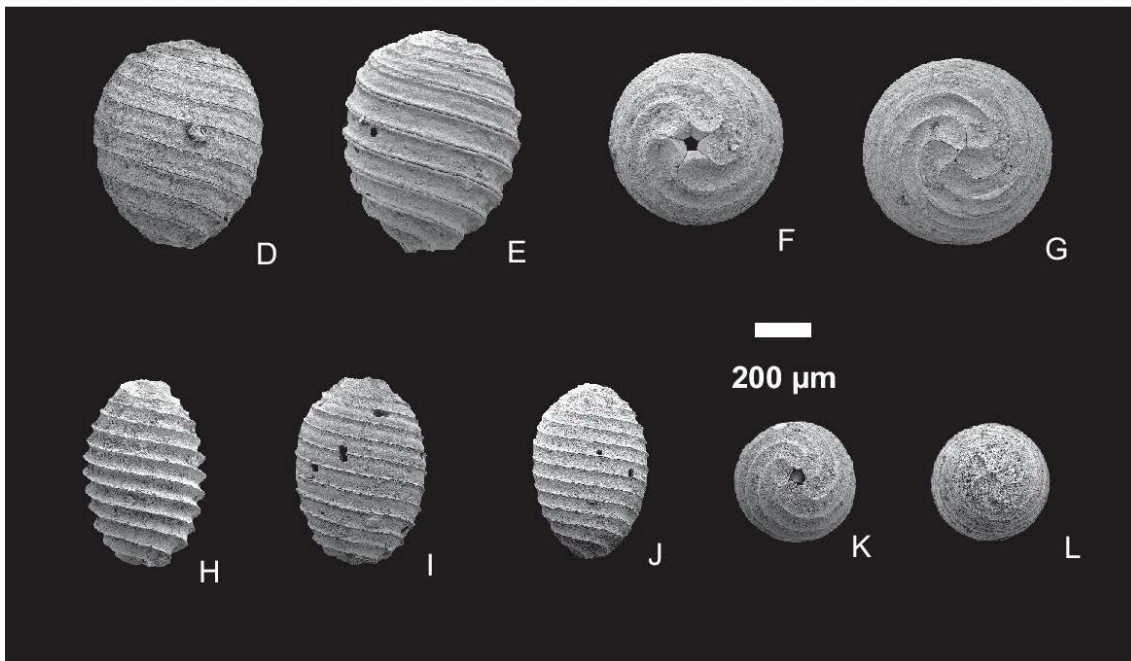
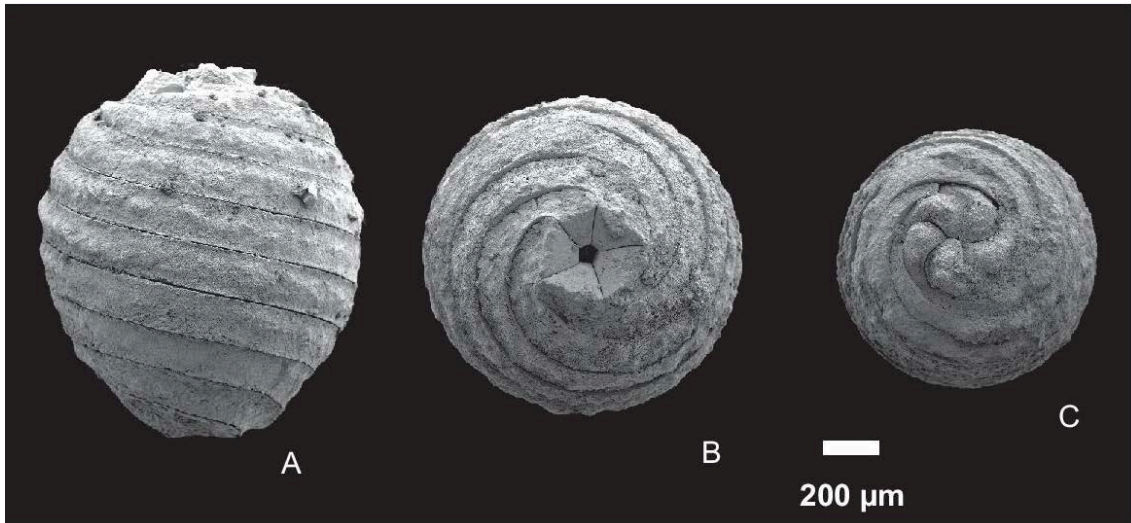


Figure 75: Assemblage of gyrogonites extracted from section 4 near Zahle (sample Z-13). A-C) *Nitellopsis* (*T.*) *merianii* (A. lateral view, B. basal view, C. apical view). D-G) *Lychnothamnus barbatus* var. *megalicarpus* (D-E. lateral view, F. basal view, G. apical view). H-L) *Chara* cf. *globularis* (H-J. lateral view, K. basal view, L. apical view).

5.5 Other Microfossils

Other fossils have been recovered from the sections near Zahle. However, their occurrence within the samples is relatively low. Then, an SEM image and a preliminary broad description are here provided.

5.5.1 MAMMALIA, RODENTIA

Several rodent teeth have been extracted from two samples i.e. Z-8 and Z-16. The assemblage is composed of a variety of remains preliminarily classified by Dr. Raquel López-Antoñanzas who is an authority on Neogene rodents. Sample Z-8 provided one tooth belonging to a lower molar (M2) of the extinct rodent genus *Progonomys* and one indeterminate incisor tooth. A complete assemblage composed of 6 rodent molars have been extracted from sample Z-16. This assemblage (fig. 78) is composed by: a molar tooth (M2) of a *Progonomys* (family Muridae), 3 molar teeth (M1, M2 and M3) of *Byzantinia* (family Cricetidae), 1 molar tooth (M3) of an undetermined Murid (family Muridae) and one molar tooth (M1) of an undefined Cricetid (family Cricetidae). The figure 76 illustrates the location of the molars in a rodent jaw. Moreover, few postcranial mammal bones were recovered from sample Z-16. At least 2 indeterminate phalange bones have been identified (fig. 80 B and C).

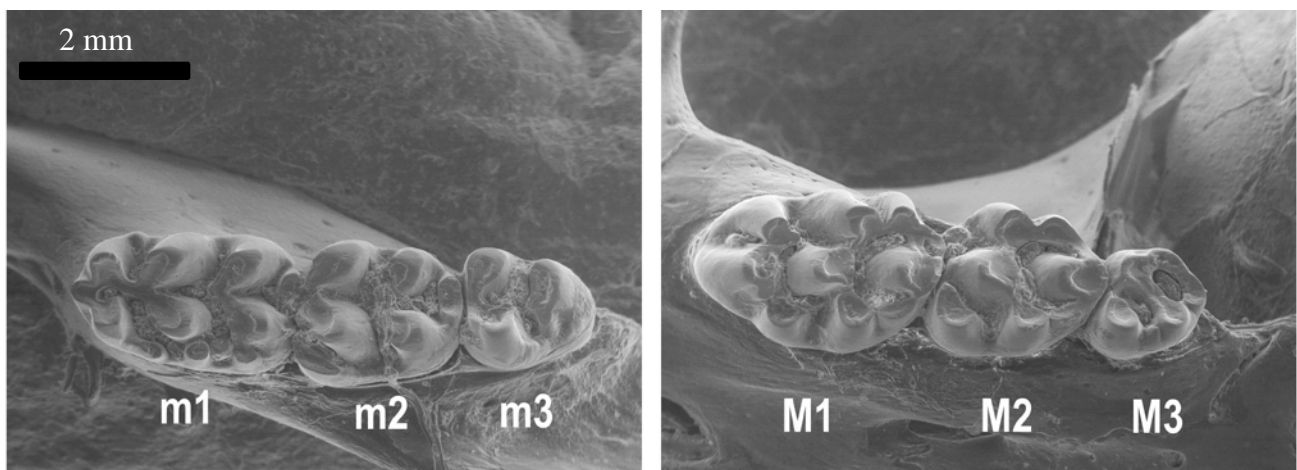


Figure 76: SEM image of a rodent jaw of *Apodemus* sp. showing the location of the three lower and upper molars respectively in plan view. Image provided by Dr. Raquel López-Antoñanzas.

Molar teeth show different sizes and although part of their upper portion has been removed, they still preserve their morphological structures such as the protocone, hypocone, paracone and metacone (fig. 77).

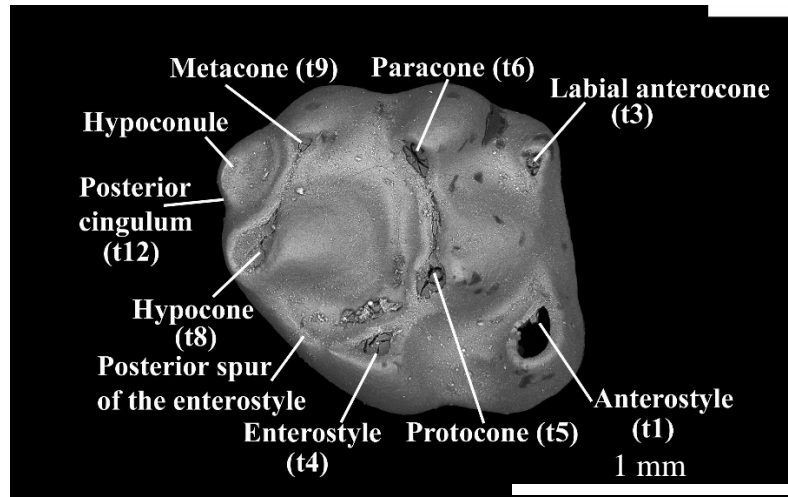


Figure 77: Plan view of a M2 of *Progonomys* showing its major morphological features. (Dr. Raquel López-Antoñanzas personal photo).

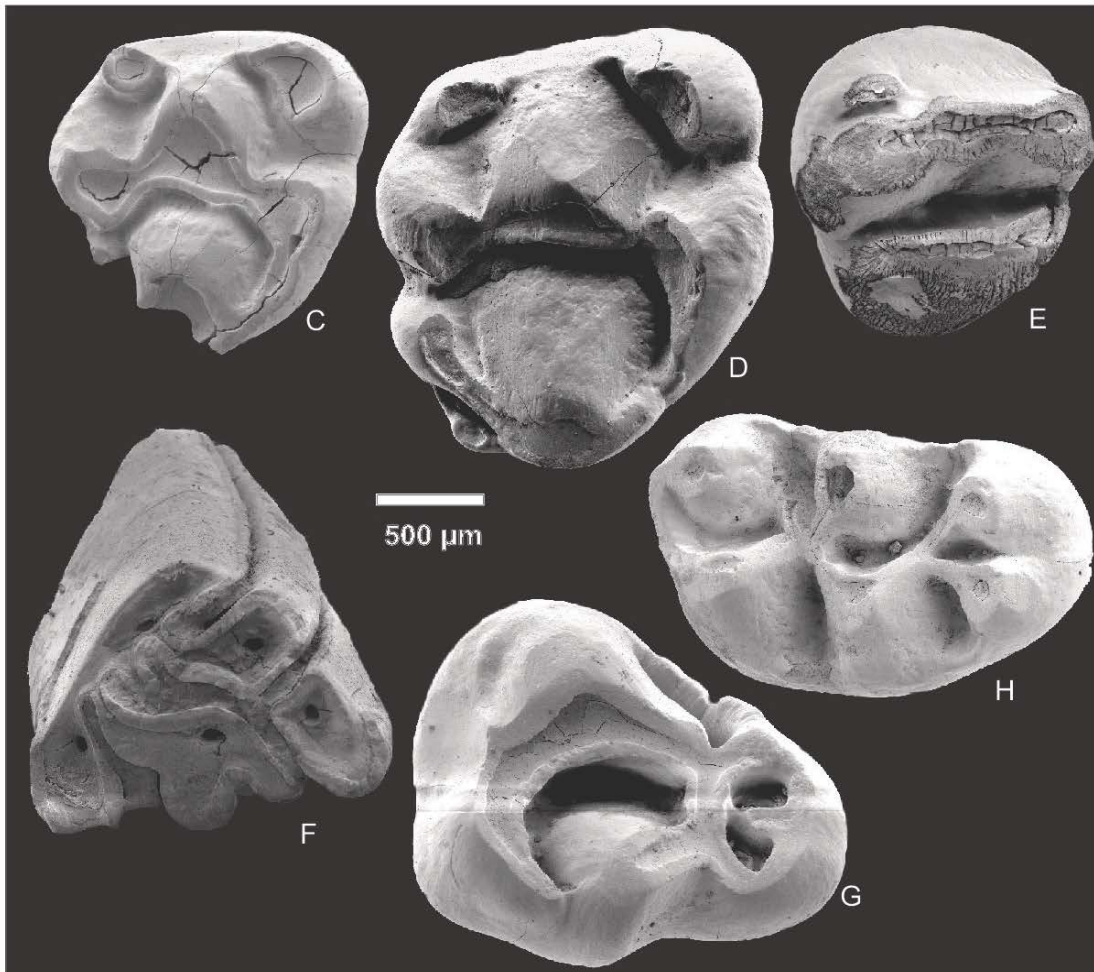
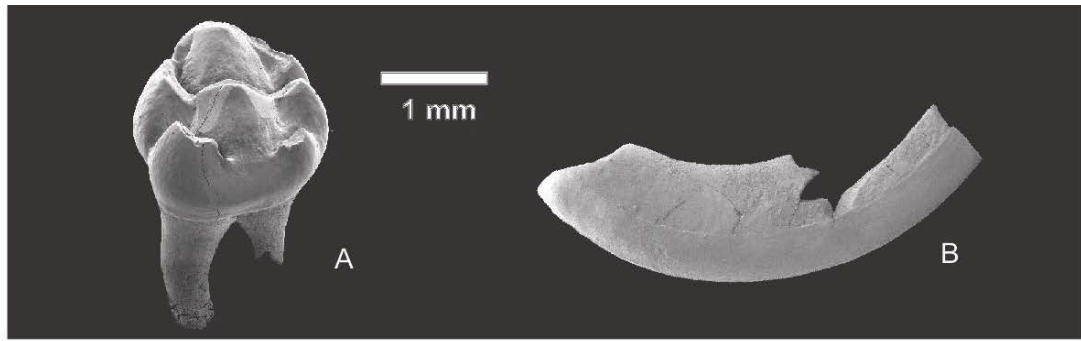


Figure 78: Assemblage of rodent and lagomorph teeth extracted from sections 3 and 5 near Zahle. A and D) Second upper molar (M2) of a *Progonomys* sp., sample Z-16. C) Second upper molar (M2) of a *Progonomys* sp., sample Z-8. B) Incisive tooth of an undetermined Murid, sample Z-8. E) Third molar (M3) of an undetermined Murid, sample Z-16. F) Tooth of *Prolagus* sp., sample Z-16. G) Third molar (M3) of *Byzantinia* sp., sample Z-16. H) First molar (M1) of an undetermined Cricetid, sample Z-16.

5.5.2 MAMALIA, LAGOMORPHA

A fragment of a lagomorph tooth (mammal order for the group of rabbits and pikas) has been extracted from Z-16 (fig. 78 F). The tooth characteristics resemble the extinct genus *Prolagus* which first appeared in the early Miocene in Europe. However, further taxonomic study is required. Few species of *Prolagus* survived until historical times and were restricted in some Mediterranean islands such as Sardinia (south Italy) being hunted by first humans in that area (Vigne, 1996). This finding may represent the easternmost locality of this genus.

5.5.3 MAMALIA, EULIPOTYPHILA

A single tooth of an indeterminate shrew (family Soricidae) has been extracted from the sample Z-16 (fig. 81 A and B). The molar tooth is 3.65 mm in length and 1.08 mm in height showing extremely pointed cuspids. The presence of shrew remains suggests that humid forests existed near the paleolake.

5.5.4 FISH REMAINS (ACTINOPTERYGII)

Fish remains extracted from the sections 3, 5, 6 and 7 mainly comprise otoliths and teeth (Tables 1 and 2). Two types of otoliths belonging to *Cichlidae* and *Gobiidae* families were broadly classified (pers. comm. Dr. Werner Schwarzhans). One type of otolith has been identified by Dr. Bettina Reichenbacher in a specific level belonging to the genus *Aphanius* sp. (fig. 79 D). The teeth assemblage recovered from Zahle belong to the large family of the Cyprinidae. They are elongated in shape (about 3.5 mm length and 2 mm in width) showing a slightly depressed anterior face and a concave posterior face. The crown is oval in section and its top is roughly conical and bent (fig. 79 A, B

and C). More specifically, the teeth assemblage displays close similarities with certain groups of African barbids (pers. comm. Dr. Olga Otero).

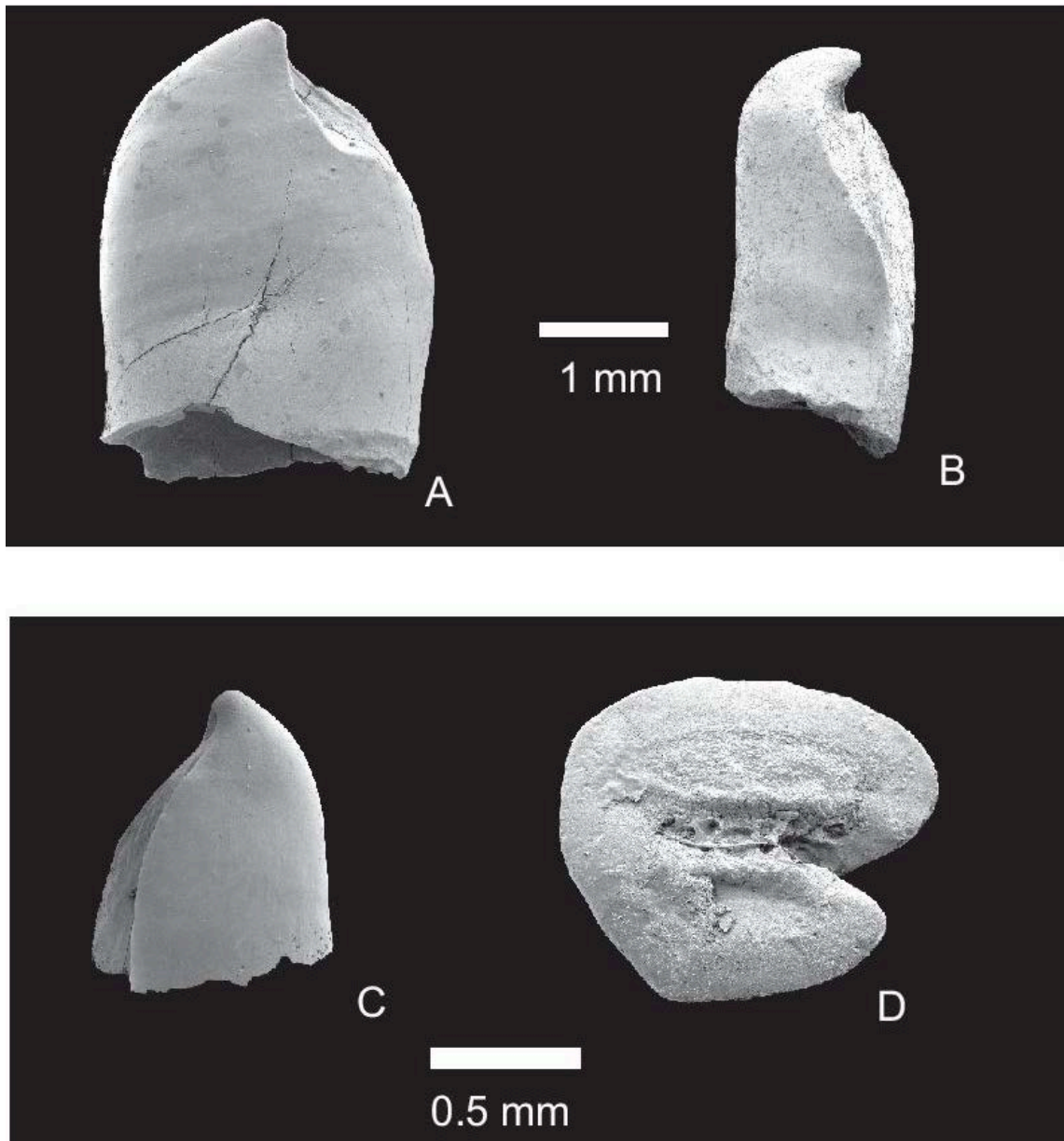


Figure 79: Assemblage of fish remains extracted from Zahle. A-B) Fish teeth of the Cyprinidae family, sample Z-16. C) Small fish tooth of the Cyprinidae family, sample Z-17. D) Otolith of *Aphanius* sp., sample Z-15.

5.5.5 AMPHIBIA

A fragment of a lower jaw (maxilia) of an indeterminate amphibian has been recovered from sample Z-16 (fig. 80 E). The general shape and structures suggests that it may belong to a frog i.e. Anura Order (Pers. comm. Dr. Arnau Bolet).

5.5.6 REPTILIA

One tooth related to an indeterminate crocodile (Crocodylidae family) has been extracted from the sample Z-2 (fig. 81 C). Moreover, a large number of undetermined osteoderms probably related to crocodiles were picked out from the sample Z-16 (fig. 80 A and D).

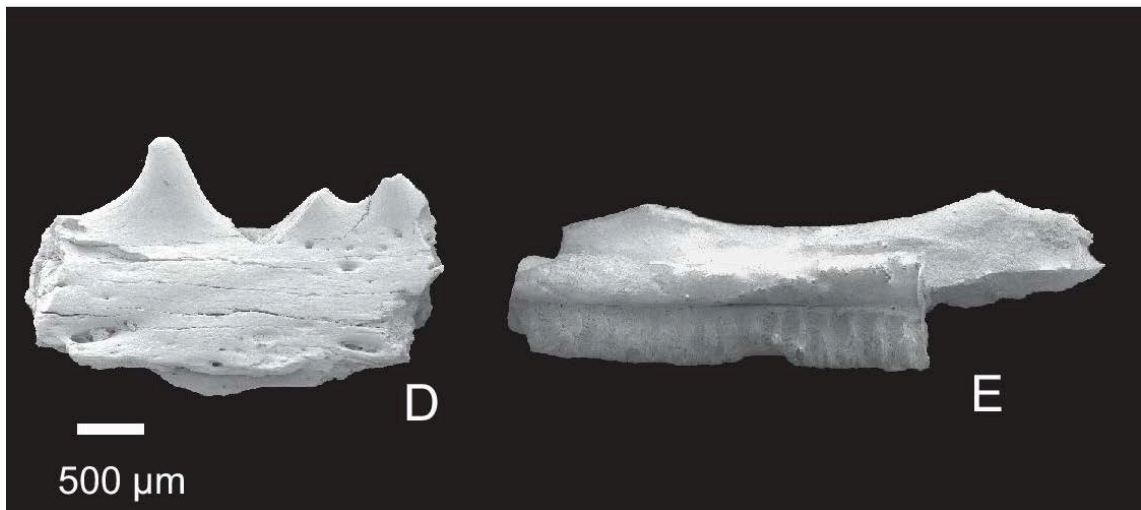
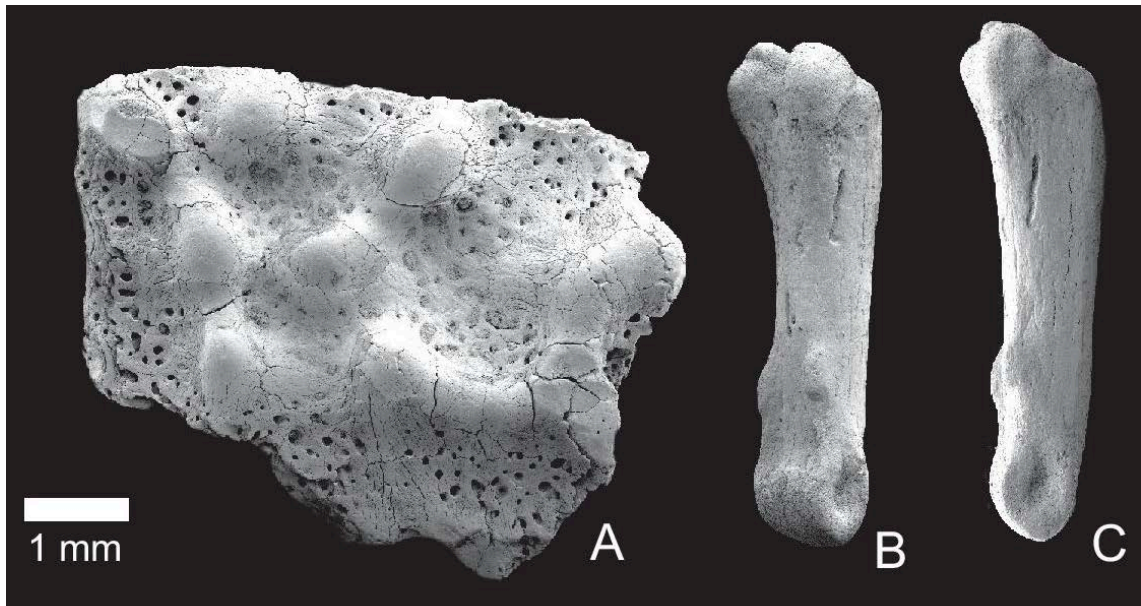


Figure 80: Assemblage of vertebrate fragments extracted from section 5 near Zahle. A) Crocodile osteoderm, sample Z-16. B-C) Micromammal phalange bone, sample Z-16. D) Reptile osteoderm fragment, sample Z-16. E) Fragment of a lower frog jaw, sample Z-16.

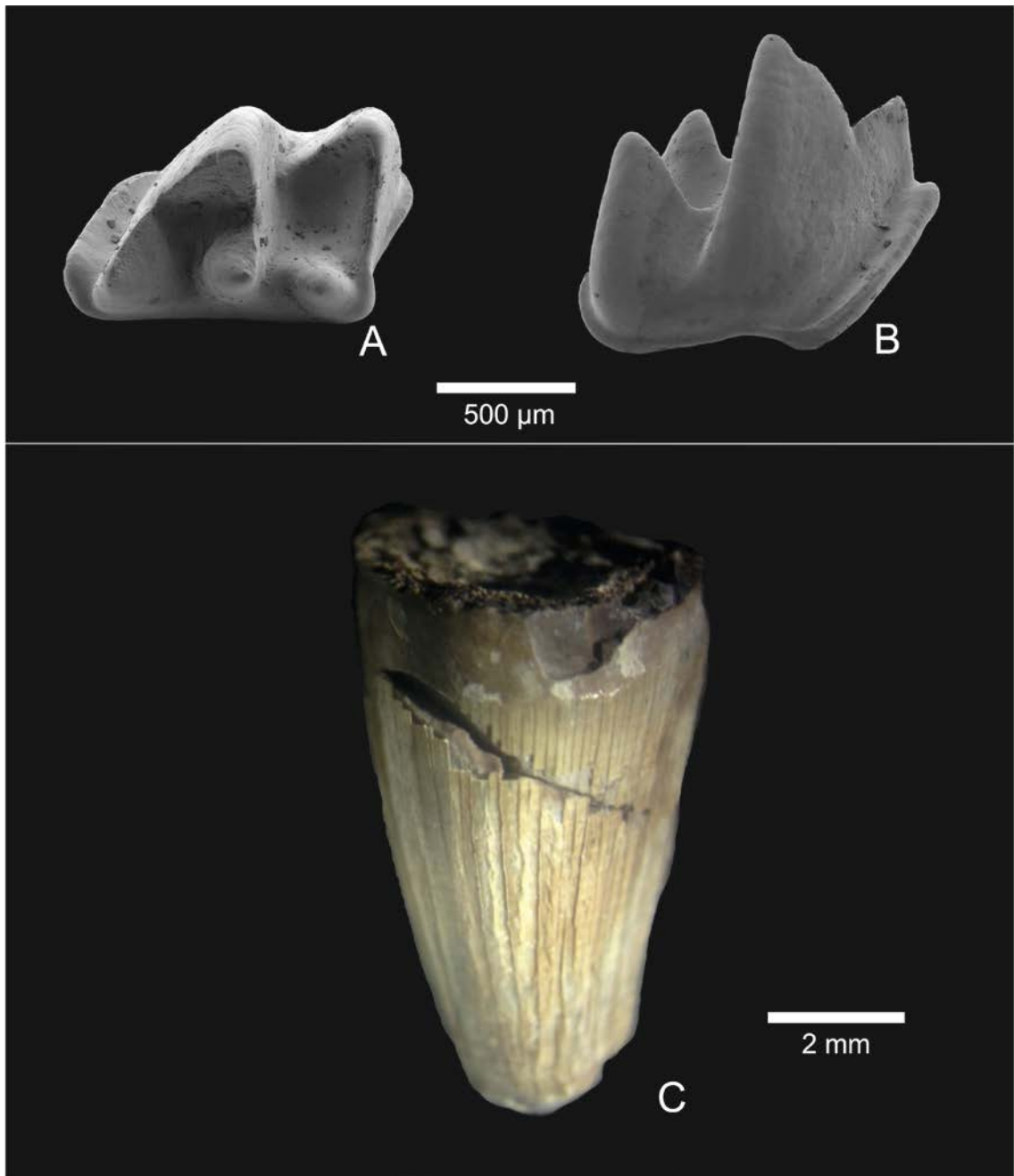


Figure 81: A-B) Undetermined molar tooth of a shrew from sample Z-16 (A. plan view, B. lateral view) and C) Broken tooth of a crocodile from sample Z-2.

CHAPTER 6

DISCUSSION

6.1 Microfossil Taphonomy and Paleoecology

The lacustrine deposits from Zahle yielded a large and diverse number of microfossils (charophytes, mollusks, ostracods and vertebrate remains) that display a vertical succession and facies association which provide valuable information for the understanding of the paleoenvironmental evolution of the paleolake through time. In general, two microfossil assemblages can be distinguished in agreement with the facies succession: 1) one assemblage from lacustrine marls and marly limestones (top of the section 1, base of the section 3 and sections 2, 4, 6, 7 and 8) another assemblage from the palustrine marls (upper part of section 3 and the complete section 5).

1) Ten species of aquatic gastropods have been recognised in marls from these sections. Three hydrobiid species (*Semisalsa* sp., *Islamia* sp., and *Pseudamnicola* sp.) represent the dominant fossils in these deposits, accompanied by, *Melanopsis buccinoidea*, *Gyraulus*, *Valvata saulcyi* and *Bithynia* sp. (Tables 2 and 3). Living representatives of *Semisalsa* and *Pseudamnicola* have broad ecological requirements and live in brackish or freshwater water environments (estuaries, rivers, springs, ponds and lakes). Similarly, species of *Islamia* are found in a wide array of habitats, ranging from subterranean waters and springs to lakes and rivers. The presence of the freshwater bivalve *Pisidium moitessierianum* suggests that well oxygenated, calm and alkaline waters conditions prevailed in the paleolake. The charophyte assemblage in these deposits is dominated by the species *Nitellopsis (T.) merianii* which appears abundantly in samples from the sections 1 and 4 (Tables 2 and 3). Other species appear less

abundantly also in sections 1, 2, base of the 3 and section 6 i.e. *Lychnothamnus barbatus*, *Chara microcera* and *Chara* cf. *globularis* (Tables 2 and 3). The occurrence of the fossil species *Nitellopsis* (*T.*) *merianii* and *Lychnothamnus barbatus* var. *antiquus* is significant from the paleolimnological viewpoint. The two taxa represent the ancestors of the extant boreal species *Nitellopsis obtusa* and *Lychnothamnus barbatus*, respectively (Sanjuan and Martín-Closas, 2015). The predominance of *Nitellopsis* (*T.*) *merianii* suggests permanent and relatively deep (2–8 m deep), oligotrophic lake conditions (Tables 2 and 3). The ostracod assemblage is dominated by *Cyprideis* sp., which is especially abundant in sections 2, 6 and 7. Notwithstanding uncertainties about the identification of this ostracod species, the ostracod assemblage may suggest moderate-depth (<10 m), possibly dysaerobic and oligohaline water with a low alkalinity/Ca ratio. However, these inferences, which are based on living *Cyprideis torosa*, may not apply to the Miocene-age material. The increase of *Cyprideis* cf. *torosa* carapaces in the second section may suggest an increase of the lake salinity reflecting more arid conditions. Alternatively, this increase may reflect a hydrographic change from an open to a closed lake system. Shells of mollusks are well preserved, showing only few signs of abrasion. Charophytes gyrogonites show their original mineralogical constituents (endocalcine and ectocalcine), without any trace of dissolution or corrosion occurring in association with fragments of charophyte stems (thalli). This evidence suggests that the fossil assemblages from sections 1 and 2 were buried *in situ* or after short-distance transport. The sedimentological, micropaleontological and taphonomic analyses suggest that marls and limestones were deposited in a permanent fresh or oligohaline, relatively shallow, oligotrophic and alkaline lake with a soft muddy bottom (fig. 82).

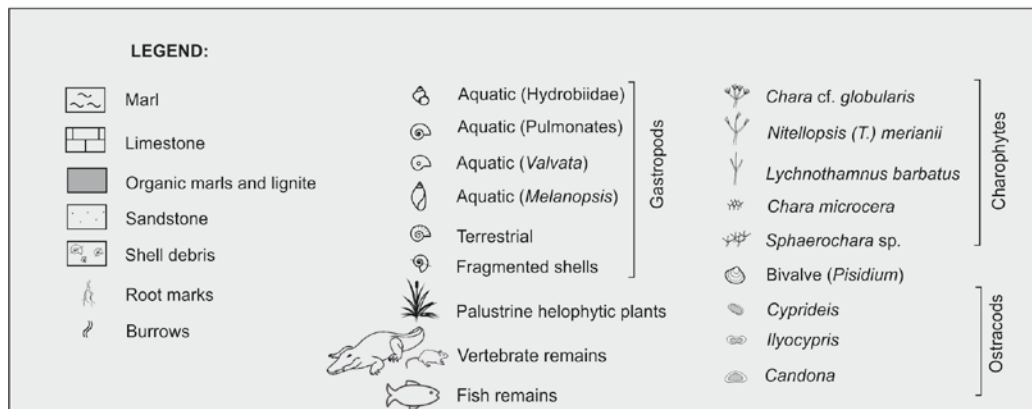
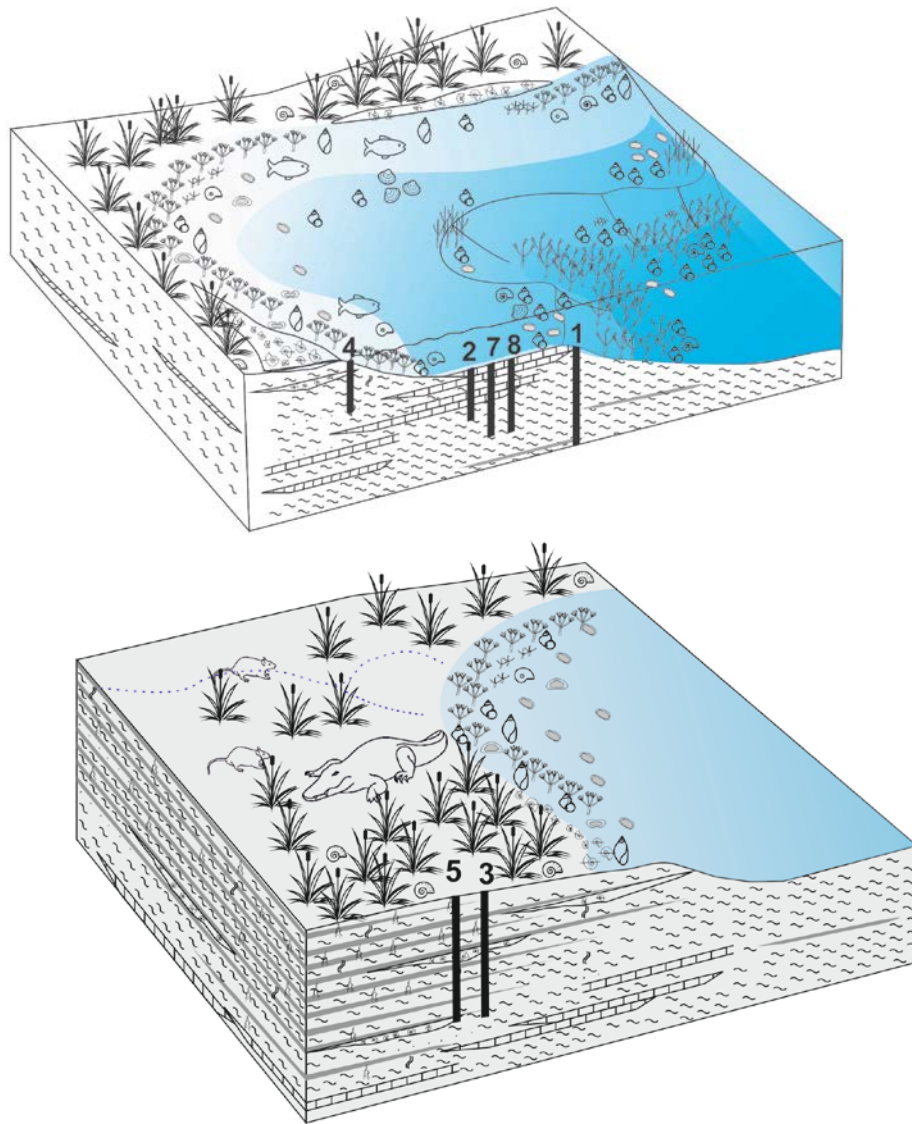


Figure 82: Paleoecological models showing the location of the sections 1 till 8 in Zahle paleolake system, as well as their lithologies and microfossil content. The upper model represents the deep oligotrophic lacustrine conditions in sections 1, 2, 4, 7 and 8 while the lower model represents the extremely shallow and eutrophic palustrine conditions in the upper section 3 and complete section 5.

2) A dramatic change of the microfossil content can be observed in the upper art of section 3 and the complete section 5. Terrestrial microgastropod shells of *Carychium* and *Vertigo* are relatively abundant and the gastropods *Semisalsa* and *Pseudamnicola* generally decrease in relative abundance. Other aquatic groups related to stagnant conditions and vegetated waters (*Valvata*, *Radix* and *Gyraulus*) appear or increase in number at the top of section 3 and in the section 5 (Tables 2 and 3). *Bithynia* sp. opercula and shells of *Melanopsis* are pretty abundant in section 5 along with few shells of *Pisidium*. Similarly, fish and vertebrate remains are common in the section 5. Charophyte species related to perennial-deep and oligotrophic lacustrine conditions such as *N. (T.) merianii* and *L. barbatus* are rare in this palustrine interval. On the other hand, *Chara* cf. *globularis*, which has a wide ecological amplitude, shows a considerable increase at the top of section 3. Shells of large gastropods (*Melanopsis* and *Melanoides*) appear fragmented especially in the uppermost part of the section 3 and in section 5, and some specimens of terrestrial gastropods show signs of abrasion. In contrast, no signs of dissolution or abrasion have been observed in gyrogonites of *Chara*. Hence, while charophytes and some gastropod species (*Islamia*, *Valvata*, *Radix* and *Gyraulus*) thrived *in situ*, larger aquatic and terrestrial gastropods were transported. The sedimentological, micropaleontological and taphonomic analyses indicate that rocks at the top of section 3 and in section 5 were deposited in very shallow, eutrophic conditions at a vegetated lake margin (fig. 82). Terrestrial snails and amphibian remains recovered from these deposits indicate that permanent moist vegetated habitats prevailed around the lake. The presence of broken shells intervals forming coquinas suggests that the lake margin was subjected to current or wave activity or subaerial exposure related to water level fluctuations. Several mammal teeth extracted from these

deposits show evident signals of erosion and abrasion suggesting that they suffered some transport.

6.2 Tectonic Implications

Tectonic activity represents, along with the climate, a key parameter controlling the lake topography, hydrology (open/closed), the mechanisms of water supply and the sources of chemical constituents affecting the water chemistry (Alonso-Zarza and Wright, 2010).

The position of the lake and its morphology were controlled by the location and rates of movement of the Yammouneh fault located about 3 km westward in the same area (north extension of the Dead Sea transform fault). The vertical change of facies described here may respond to tectonic pulses of the fault during the late Miocene and early Pliocene, coinciding with the first and second active tectonic phases in Lebanon respectively. Early Miocene rocks and facies have not been previously described throughout Lebanon. Many authors suggested that the absence of lower Miocene rocks in the Bekaa basin is related to erosional processes or limited sediment input (Dubertret, 1975; Müller *et al.*, 2010; Hawie *et al.*, 2013). According to Walley (1997), conglomerates related to alluvial fans are middle to late Miocene in age and were deposited forming an unconformity at the flanks of the Bekaa basin. Homberg *et al.* (2010) suggested that sedimentary rocks stratigraphically located below this unconformity are middle Miocene in age. These alluvial deposits can be tentatively correlated with the alluvial fans described at the base of section 1 and could clearly indicate a period of erosion and transport due to the very high tectonic activity of the Yammouneh fault during the first tectonic stage. The sedimentological characteristics of

the overlying carbonate deposits, i.e. fossiliferous marls and marly limestone strata related to perennial-lake conditions, suggest that tectonic activity decreased substantially. A fossil charophyte assemblage recovered from the very base of these lacustrine deposits containing biostratigraphically relevant taxa suggested that the establishment of the paleolake probably took place during the early-middle Miocene (Sanjuan and Alqudah, 2018). However, collected vertebrate remains indicate that the paleolake at Zahle was established later during the middle-late Miocene (López-Antoñanzas *et al.*, 2015). Further investigations should be performed to precise the age of the establishment of this paleolake. The presence of palustrine marls and organic-rich clays in sections 3 and 5 may indicate that the fault remained inactive in the region during later stages of the paleolake sequence. According to Nader (2011), early Pliocene fluvial and lacustrine sediments were deposited overlying the Miocene rocks in the Bekaa basin forming an unconformity. This unconformity probably coincides with the red fluvial deposits exposed at the top of the section 6 suggesting that another active phase of the Yammouneh fault took place favoring the displacement of the basin depocenter and the increase of sediment influxes into the valley. This tectonic activity could be related with the second active tectonic phase described by Walley (1998) that took place during the early Pliocene.

6.3 Climatic Implications

6.3.1 *Global Late Miocene Climate Context:*

Microfossils extracted from the lacustrine rocks at Zahle suggest that these sediments are late Miocene in age. However, further studies should be performed to precise the age of these rocks.

Globally, the late Miocene (Tortonian and Messinian ages) witnessed a significant cooling after the mid-Miocene climatic optimum, but it was still considerably warmer than today (Bruch *et al.*, 2006; Micheels *et al.*, 2007). Arid conditions prevailed in the Middle East region during the Tortonian (11.6-7.2 Ma). Evidences of this climatic conditions can be traced by the presence of evaporite sequences and the low amount of clastic deposits in the Gulf of Suez and the Red Sea areas (Griffin, 1999). However, vegetated and humid conditions were prominent across the Sahara region as indicated by vertebrate fossil assemblages recovered from Tortonian sedimentary rocks in Egypt (Pickford *et al.*, 2006). Moreover, remains of aquatic reptiles such as crocodiles have been reported from Tortonian deposits in Tunisia (Pickford, 2000; Agrasar, 2003). The precipitation rates in the area were lower than those of present day and a temperate savanna-type climate prevailed in the Middle East (Eronen *et al.*, 2009; Pound *et al.*, 2011). Reconstructions of global vegetation for the Tortonian suggest warm-temperate mixed forests to temperate deciduous forests for the Levantine region (Pound *et al.*, 2011).

According to Griffin (2002), a wet climatic phase took place in northeast Africa as well as the central Sahara during the early Messinian (7.2-5.3 Ma). On the other hand, low rainfall and more arid conditions existed towards the northwest of Africa and the eastern Mediterranean (Brachert *et al.*, 2006). This climatic pattern suggests that an increase in rainfall would be related to a monsoonal impact derived from the Indian

Ocean. By the mid Messinian time, the climate of the Mediterranean basin became much drier as demonstrated by the abundance of thick halite deposits (e.g. Hsü, 1983). High evaporation and low rainfall rates caused the expansion of deserts and arid conditions throughout the eastern Mediterranean (Mertz-Kraus *et al.*, 2008).

During the late Messinian the Mediterranean Sea dried up due to the drop of global sea level and the tectonic uplift that closed the Rifean sea corridor located between the south of Spain and north of Morocco (Duggen, 2003). During this interval, arid and deserted climatic conditions were displaced towards the north as a result of changing in oceanic-atmospheric circulation causing the desiccation of the Black Sea and other flooded basins (Hsü and Giovanoli, 1979).

At the end of the Miocene and beginning of the Pliocene, the Mediterranean Sea returned to its original level as a result of the reopening of the Rifean corridor resulting in an increase of general humidity (humid climates) in the eastern Mediterranean region (Griffin, 2002; Kovar-Eder, 2003). Simultaneously, dry climates with low precipitation rates existed in central Europe (Morsbruger *et al.*, 2005). This shift towards arid conditions from the eastern Mediterranean to central Europe was probably caused by changes of oceanic and atmospheric circulation patterns (Eronen *et al.*, 2009).

6.3.2 *Microfossil Paleoclimatic Inferences:*

The fossil assemblage recovered from lacustrine deposits at Zahle and neighbouring areas shed light on the paleoclimatic setting of the Bekaa Valley and the eastern Mediterranean region during the late Miocene. Several of the fossil taxa recovered from the Zahle sequence provide information about past temperatures. The two charophyte species recorded in sections 1, 2 and 4, i.e. *Nitellopsis (T.) merianii-*

obtusa and *Lychnothamnus barbatus*, are considered boreal taxa growing mainly in north European cold freshwater lakes (Corillion, 1972). The dominant species *N. merianii-obtusa* grows in permanent lakes with an average summer water temperature of 16 °C (Larkin *et al.*, 2018). This seems surprising, however, given the widespread evidence that the late Miocene, although cooler than the earlier part of the Miocene, was warmer than present. However, *N. (T.) merianii-obtusa* is a fossil species, and its ecology is only inferred from a related extant species. Although *L. barbatus* is living today, it is possible that its ecological preferences have changed since the Miocene. Otherwise, the occurrence of these charophyte species would indicate the existence of cold water sources probably related to a phreatic origin. In contrast, several species of aquatic mollusks suggest a much warmer climate, since they are still living in the Levant region today, and this region is presently characterized by a hot-summer Mediterranean climate. The ostracod taxa found within the Zahle sequence have broad temperature tolerances, although they are not inconsistent with warmer temperatures, and would thus tend to support the climatic inferences drawn from the aquatic mollusks. The prevalence of a hot climate in the Bekaa Valley during the late Miocene is also supported by the presence of reptile remains such crocodiles (teeth and osteoderms) and turtle plates (reported in previous paleontological works performed in the area by Malez and Forsten (1989) and López-Antoñanzas *et al.* (2015).

All of the groups of aquatic fossils (charophytes, mollusks and ostracods) include elements that are tolerant of elevated salinity; this is especially true for the ostracods. Elevated salinity in athalassic lakes is often associated with a more arid climate: although the dissolution of evaporitic rocks within a lake catchment can also

contribute to elevated salinity, the absence of evaporites from the Zahle region suggests that climate was the more likely control.

Based on the complete fossil assemblage recovered in this thesis, the aquatic landscape of the paleolake and its surroundings during the late Miocene can be tentatively inferred. The benthonic lake community was composed by charophyte meadows which were inhabited by a diverse assemblage of aquatic mollusks and ostracods adapted to different bathymetries. This community thrived in the relatively shallow photic zone of the lake. On the other hand, a fish assemblage composed of large African barbs (Cyprinidae) and small pupfishes (*Aphanius*) formed the nektonic community. Moist-dependent animals such as terrestrial snails, frogs, shrews and crocodiles thrived in the lake shore or in humid forests directly surrounding the paleolake. Transported rodents and rabbits' teeth indicate the presence of an open grassland habitat near the lake. This idea is in agreement with previous paleontological studies developed in upper Miocene deposits in the Bekaa Valley (Kefraya and Zahle) by Kansou (1961) as well as Malez and Forsten (1989). Based on fossil herbivore remains i.e. bones and teeth of horses (*Hipparion*), elephants (*Deinotherium*), wild pigs (*Sus*), several antelopes (*Tragocerus*, *Hemistrepsiceros*, *Palaeoreas*, *Palaeoryx*, *Protoryx*, *Gazella* and *Pseudotragus*) and terrestrial turtles (*Testudo*), these authors suggested that the Bekaa Valley landscape was composed by a large and extended grassland, the vegetation of which sustained this herbivore community (fig. 83).

Paleontological studies of the late Miocene Baynunah Formation in Abu Dhabi have yielded a variety of microfossils and macrofossil remains similar to and much more to those of late Miocene Zahle Formation. According to Bibi *et al.* (2013), the assemblage recovered from Baynunah Formation includes terrestrial gastropods

(Mordan, 1999), two families of bivalves (Jeffrey, 1999), a complete assemblage of fish remains (one of which belongs to the genus *Barbus*), four species of crocodiles, aquatic and terrestrial tortoises and turtles (Broin and van Dijk, 1999), ostrich-like eggshell (Bibi *et al.*, 2006), early elephant (Elephantidae) (Tassy, 1999), jumping mice (Dipodidae) and murids (Muridae) (Kraatz *et al.*, 2009), large carnivores, horses of the genus *Hipparion* (Eisenmann and Whybrow, 1999), two species of pigs (Bishop and Hill, 1999), hippopotamuses (Hippopotamidae), two or three species of giraffes, as well as footprints of large elephants such as *Deinotherium* and bovids. According to Bibi *et al.* (2013), a large river existed during the late Miocece in Abu Dhabi. Extended woodlands were located in its direct vicinity as demonstrated by the discovered trunk of a large tree in one site. Away from the river, grasslands extended with arid and desertic conditions. The Bekaa Valley could possibly have a similar landscape during the same period. However, further investigations must be performed in the whole Bekaa Valley to ascertain its most probable landscape.



Figure 83: Photo of the savanna type habitat from NW Nairobi (Kenya, Africa), considered as an analaogous of a possible landscape in the south of the Bekaa Valley during the late Miocene (webpage: <https://www.capitalfm.co.ke/lifestyle/2015/12/31/35833/>).

6.4 Paleobiogeography

This thesis provides significant data regarding the biogeographic distribution of several living groups of aquatic plants (charophytes) and fauna (mollusks and ostracods) during the late Miocene. Because of its geographic position between Europe and Asia, where paleontological studies have been more intensely studied, Lebanon and the whole Middle East region represents an area for biogeographical and paleobiogeographical studies of extant and fossil taxa.

6.4.1 Charophytes:

The fossil charophyte assemblage recovered from upper Miocene deposits at Zahle is composed of two well-known European species i.e. *Nitellopsis (T.) merianii-obtusa* and *Lychnothamnus barbatus* that have been recognized for the first time in Lebanon and in the Middle East. Moreover, the studied sections may represent the southernmost locality where these species have been recovered. The biogeographic distribution of the *N. (T.) merianii-obtusa* has been previously reported by Soulié-Märsche *et al.* (2002) and Sanjuan and Martín-Closas (2015). These authors noted that during the complete Miocene Epoch, this species had a peri-Mediterranean distribution reaching NE China and SE Asia. Fossil populations have been recovered from the entire Eurasian landmass during this time span comprising a wide range of latitudes from 18°N to 50°N (Sanjuan and Martín-Closas, 2015 and references herein). However, during the Quaternary, the biogeographic range of this species dramatically contracted and became restricted in north Europe (fig. 84). A similar pattern can be traced for the species *Lychnothamnus barbatus*. During the Miocene, this species also had a peri-

Mediterranean distribution thriving in well-developed lacustrine systems. However, Quaternary and living populations have been reported in sediments related to cold freshwater lakes from northern Europe (Krause, 1997; Soulié-Märsche and Martín-Closas, 2003). Nowadays, north European living populations of *L. barbatus* are rare and endangered due to lake water pollution and eutrophication.

The paleobiogeographic distribution of these charophyte species during the Miocene suggests that they probably originated in the Mediterranean area and later (Pliocene and Pleistocene) migrated towards north Europe.

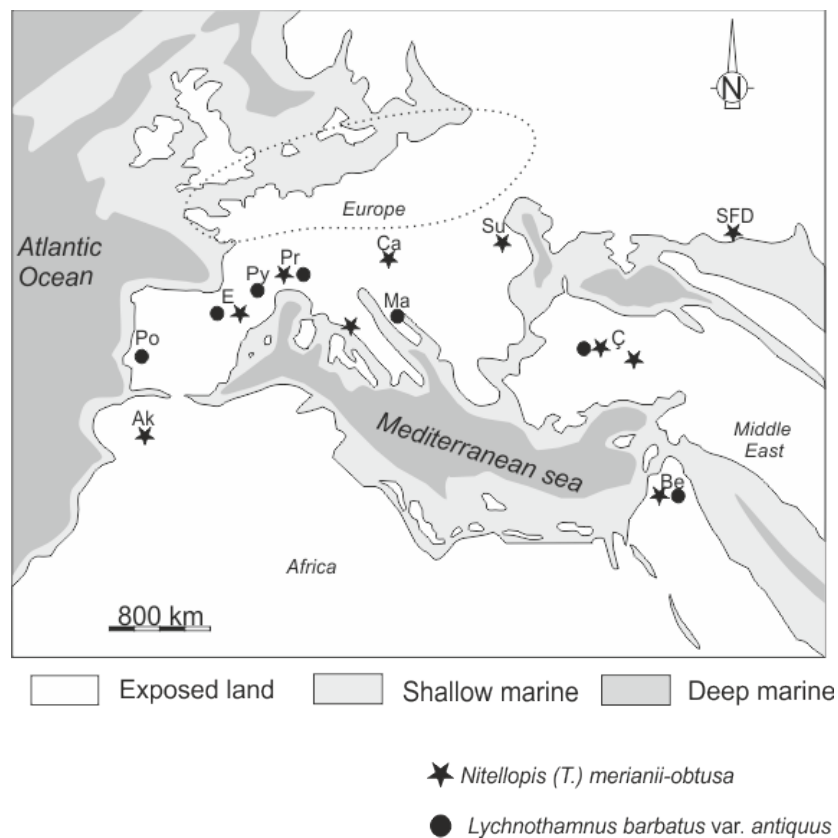


Figure 84: Paleogeographic map of the Mediterranean region during the Late Miocene showing the distribution of the two main charophyte species *Nitellopsis (T.) merianii-obtusa* and *Lychnothamnus barbatus var. antiquus*. Be= Bekaa Valley (Lebanon), Ç= Çankiri Basin (Turkey), Ma= Maoce Basin (Montenegro), Ca= Carpatian Basin (Austria), Su= Suceava area (Romania), SFD= Southern Federal District (Russia), Pr= Provence (France), Py= Pyrenees (Spain), E= Ebro Basin (Spain), Po= Portugal, Ak= Ait Kandoula Basin (Morocco). Dotted line circle represents the present biogeographic distribution of the two considered species. Note position of the new populations in Be= Bekaa Valley (modified from Sanjuan and Martín-Closas, 2015).

6.4.2 Aquatic mollusks:

The freshwater mollusk assemblage extracted from Miocene deposits of Zahle is composed of a variety of living species with different biogeographic distributions. Dominant taxa display a Middle East (Levant) distribution. Populations of *Melanopsis buccionoidea*, *Melanoides tuberculata*, *Gyraulus piscinarum*, *G. hebraicus* and *Valvata saulcy* are currently thriving in freshwater temporary and permanent aquatic environments in the East Mediterranean and southwest European regions along with Turkey, northwest Africa and the Far East (Tchernov, 1979; Van Damme, 1984; Van Damme and Pickford, 2003; Songtham *et al.*, 2005; Amr *et al.*, 2014). Other mollusk species such as the tiny clamshell *Pisidium moitessierianum* and the terrestrial snail *Vertigo antivertigo* display a completely different biogeographic distribution living, as the two aforementioned charophyte species, in cold climates in northern Europe and United States.

In contrast to the substantial amount of knowledge of the biogeographic distribution of aquatic mollusks, little is known about their distribution in the past. According to Heller (2007), aquatic mollusks in the eastern Mediterranean probably originated from southern European regions during the late Miocene (Messinian). Heller (2007) suggested that aquatic mollusks such as *Melanopsis* were originally living in the Paratethys regions and were then widespread by rivers into the Levant regions.

6.4.3 Ostracods:

An assemblage of six ostracod species has been extracted from the lacustrine Miocene deposits of the Bekaa Valley. However, the taxonomy and the historical biogeography of these species is not well understood. The most abundant ostracod

recovered from Zahle is the species *Cyprideis* cf. *torosa* which is considered one of the most geographically widespread species of all *Cyprideis* and is currently thriving in brackish waters of Asia, Europe and Africa (Meisch, 2000; Wouters, 2002, 2016). Time of origin and dispersal of this species is still controversial. Decima (1964) suggested that *C. torosa* originated in the post-evaporitic Messinian crisis from the species *C. tuberculata*. On the other hand, Van Harten (1990) reported that *C. torosa* appeared during the Pliocene, while Gliozzi *et al.* (2017) suggested that the first record of this species is early Pleistocene in age.

6.4.4 Vertebrates:

An interesting assemblage composed of dentary pieces of several groups of micromammals such as rodents, rabbits and shrews is shedding new light about the distribution of Middle East faunas during the late Miocene. Fossils of micromammals are currently known from a small number of Miocene sites within the Arabian Plate (López-Antoñanzas *et al.*, 2015 and references herein). Some of these groups are reported for the first time in Lebanon. However, further taxonomic studies are required to better classify these taxa enhancing the knowledge about their paleobiogeography and dispersion routes.

CHAPTER 7

CONCLUSION

Non-marine Neogene deposits in the western margin of the Bekaa Valley (Lebanon) near the villages of Zahle, Cherara and Niha have been analysed from the sedimentological and micropaleontological viewpoints. The conclusions of this thesis can be divided in 4 main points:

7.1 Stratigraphy and Sedimentology

Eight stratigraphic sections were raised with the aim to ascertain the paleoenvironmental evolution of the area. Four types of facies have been distinguished i.e. alluvial, lacustrine, palustrine and fluvial. Facies analysis of the studied sections indicates that the western margin of the Bekaa Valley was occupied by an alluvial fan system related to the high tectonic activity of the Yammouneh fault. These deposits evolved vertically into a perennial relatively shallow lake grading upwards into palustrine conditions.

7.2 Micropaleontology

Late Miocene lacustrine deposits at Zahle, Cherara and Niha have provided a rich and well-preserved microfossil assemblage which it is here described and illustrated for the first time. The fossil assemblage is composed of 10 species of aquatic gastropods, 4 species of terrestrial gastropods, 1 species of bivalve, 5 species of ostracods, 5 species of charophytes and vertebrate teeth and bone fragments of fishes, amphibians, reptiles (crocodiles) and mammals (rodents, lagomorphs and eulipotyphs).

7.3 Paleocology and Paleoenvironment

This microfossil assemblage shed new light about the limnological characteristics of the paleolake and the reconstruction of the past landscape at Zahle and its surroundings during the late Miocene. During this Epoch, the south of the Bekaa Valley was flooded by a perennial, relatively shallow and oligotrophic freshwater lake that evolved to a very shallow and eutrophic lake with a dense palustrine vegetation belt. Ostracod assemblage suggests that oligohaline conditions may prevailed in some periods. However, the absence of evaporite bedrock in the valley's catchment area suggests that climatic change were the main factor controlling the salinity of the paleolake. The increase of salinity was probably related to higher evaporation rates during dry periods. Later on, this perennial lake changed into very shallow conditions where eutrophic and palustrine vegetated margins prevailed. The subsequent high tectonic activity in the area displaced the basin depocenter towards the south leaving the studied deposits exposed along the SW margin of the valley. Transported terrestrial snails and vertebrate fragments extracted from palustrine deposits indicate that humid forests dominated the lake surroundings and extended grassland plains occupied further areas.

7.4 Paleoclimate and Landscape

The fossil assemblages are somewhat ambiguous indicators of paleotemperature. Some microfossils indicate cooler temperatures (similar to those of present-day boreal environments). However, the majority of the aquatic fossils suggest that paleotemperatures during the late Miocene at Zahle were similar or higher than those of

the present-day Zahle region. These contrasting paleotemperatures would be related to different bathymetries of the lake and to the source of the water. Moreover, the presence of crocodile remains suggests that the climate in the Bekaa Valley was even warmer than present day. Recovered rodent remains suggest that open grassland landscape dominated the area which is in agreement with the previous paleontological works performed in the area.

It is difficult to provide a general overview of the basin and climate evolution based solely on sedimentological/paleontological analyses of one limited area. Additional data from other localities along the Bekaa Valley are required to expand our knowledge regarding basin and climate evolution as well as tectonic activity. Unfortunately, due to the present political situation, field campaigns in the eastern areas of the basin close to the Syrian border is not advisable for safety reasons.

The results of this master's thesis are being disseminated in specific international congresses and published in scientific journals indexed in the Journal of Citation Reports (ISI) focused on micropaleontology, paleoecology and paleoclimatology (Sanjuan *et al.*, 2019). This thesis would successfully initiate a series of future research projects in the Bekaa Valley. For instance, palynological studies of these lacustrine deposits and isotopic analysis of the recovered shells are expected to be performed in the near future with the aim of better understanding and delineating the climate evolution of the region during the late Miocene.

REFERENCES

- Agrasar, E. L. 2003. New fossil crocodylians from the Middle/Upper Miocene of Tunisia. *Annales de Paléontologie* 89, 103-110.
- Alhejoj, I., Bandel, K. 2013. Mollusks of the Pleistocene Al-Qarn Formation of the Jordan Rift-Valley in Jordan. *Paläontologie, Stratigraphie, Fazies* 21, 141-173.
- Alonso-Zarza, A. M. 2003. Palaeoenvironmental significance of palustrine carbonates and calcretes in the geological record. *Earth-Science Reviews* 60, 261-298.
- Alonso-Zarza, A. M., Wright, V. P. 2010. Palustrine carbonates. *In* Alonso-Zarza, A. M., Tanner, L. H. (eds.), *Carbonates in Continental Settings: Facies, Environments, and Processes*. Elsevier, Amsterdam, 103-131.
- Alqudah, M., Monzer, A., Sanjuan, J., Salah, M. K., Alhejoj, I. K. 2019. Calcareous nannofossil, nummulite and ostracod assemblages from Paleocene to Miocene successions in the Bekaa Valley (Lebanon) and its paleogeographic implications. *Journal of African Earth Sciences* 151 82-94.
- Amr, Z., Alnasarat, H., Neubert, E. 2014. Notes on the current and past freshwater snail fauna of Jordan. *Journal of Natural History* 1, 83-115.
- Arconada, B., Ramos, M. A. 2006. Revision of the Genus *Islamia* Radoman, 1973 (Gastropoda, Caenogastropoda, Hydrobiidae) on the Iberian Peninsula and Description of two new Genera and three new species. *Malacologia* 48 (1/2), 77-132.
- Anadón, P., Utrilla, R., Vázquez, A., Martín-Rubio, M., Rodríguez-Lázaro, J., Robles, F. 2008. Palaeoenvironmental evolution of the Pliocene Villarroya Lake, northern Spain, from stable isotopes and trace-element geochemistry of ostracods and molluscs. *Journal of Paleolimnology* 39, 399-419.
- Antunes, M. T., Soulié-Märsche, I., Mein, P., Pais, J. 1992. Le gisement de Asseiceire, Portugal (Miocène Supérieur). Données complémentaires sur Freiria de Rio Maior. *Ciências da Terra (UNL)* 11, 219-253.
- Bailly, G., Schaefer, O. 2010. *Guide illustré des Characées du nord-est de la France*. Besançon, France. Conservatoire Botanique National de Franche-Comté, 96p.
- Balakrishnan, M., Yapp, C. J., Meltzer, D. J., Theler, J. L. 2005. Palaeoenvironment of the Folsom archaeological site, New Mexico, U.S.A., approximately 10,500 14Cyr BP as inferred from the stable isotope composition of fossil land snail shells. *Quaternary Research* 63, 31-44.
- Banarescu, P. 1992. Zoogeography of fresh waters, Distribution and dispersal of freshwater animals in North America and Eurasia. Wiesbaden: Aula Verlag 2, 591-1091.

- Bank, R. A., Butot, L. J. M. 1984. Some more data on *Hydrobia ventrosa* (Montagu, 1803) and "*Hydrobia*" *stagnorum* (Gmelin, 1791) with remarks on the genus *Semisalsa* Radoman, 1974 (Gastropoda, Prosobranchia, Hydrobioidea). *Malakologische Abhandlungen. Staatliches Museum für Tierkunde Dresden* 10 (2), 5-15.
- Bengtsson, S. 1994. The advent of animal skeletons. *In* Bengtsson, S. (ed.), *Early life on earth*, Nobel symposium 84, 412-425.
- Benjamini, Ch. 1995. The stratigraphy of the nummulitic Eocene of Israel. *In* Schaub, H., Benjamini, Ch., Moshkovitz, S. (eds.), *The Biostratigraphy of the Eocene of Israel. Mémoire Suisse de Paléontologie* 117, 7-18.
- Benton, M. J., Harper, D. A. T. 2009. *Introduction to paleobiology and the fossil record*. Chichester, West Sussex, UK: Wiley-Blackwell, 119p.
- Beran, L., Osikowski, A., Hofman, S., Falniowski, A. 2016. *Islamia Zermanica* (Radoman, 1973) (Caenogastropoda: Hydrobiidae): Morphological and molecular distinctness. *Folia Malacologica* 24 (1), 25-30.
- Beydoun, Z. R. 1988. *The Middle East. Regional geology and petroleum resources*. Scientific Press, Beaconfield, 292p.
- Beydoun, Z. R. 1999. Evolution and development of the Levant (Dead Sea Rift) Transform System: a historical –chronological review of structural controversy. *In* Mac Niocaill, C., Ryan, P. D. (eds.), *Continental Tectonics*. Geological Society, London, Special Publication 64, 239-255.
- Bibi, F., Hill, A., Beech, M., Yasin, W. 2013. Late Miocene fossils from the Baynunah Formation, United Arab Emirates: Summary of a decade of new work. *In* Wang, X., Fortelius, M., Flynn, L. J. (eds.), *Neogene Terrestrial Mammalian biostratigraphy and chronology in Asia*. Columbia University. New York, 583-594
- Birks, H. J. B., Birks, H. H. 1980. *Quaternary palaeoecology*. Cambridge, UK: Cambridge University Press, 289p.
- Bishop, L., Hill, A. 1999. Fossil Suidae from the Baynunah Formation, Emirate of Abu Dhabi, United Arab Emirates. *In* Whybrow, P. J., Hill, A. (eds.), *Fossil Vertebrates of Arabia: with Emphasis on the Late Miocene Faunas, Geology, and Palaeoenvironments of the Emirate of Abu Dhabi, United Arab Emirates*. New Haven: Yale University, 254-270.
- Blaženčić, J., Stevanović, B., Blaženčić, Ž., Stevanović, V. 2006. Red Data List of Charophytes in the Balkans. *Biodiversity and Conservation* 15, 3445-3457.
- Bößneck, U. 2011. New records of freshwater and land molluscs from Lebanon

- (Mollusca: Gastropoda & Bivalvia). *Zoology in the Middle East* 54, 35-52.
- Bodon, M., Manganelli, G., Giusti, F. 2001. A survey of the European valvatiform hydrobiid genera, with special reference to *Hauffenia* Pollonera, 1898 (Gastropoda: Hydrobiidae). *Malacologia* 43, 103-215.
- Boggs, S. J. 2011. *Principles of Sedimentology and Stratigraphy*. Boston, Prentice Hall, 688p.
- Boggs, S. J. 2014. *Principles of Sedimentology and Stratigraphy (Fifth Edition)*. Great Britain: Pearson Education Limited, 564p.
- Boomer, I., Frenzel, P., Feike, M. 2017. Salinity-driven size variability in *Cyprideis torosa* (Ostracoda, Crustacea). *Journal of Micropaleontology* 36, 63-69.
- Borisova, O. V., Yakushenko, D. M. 2008. Communities of Charophytes in the south-western part of Lake Svityaz (Valyn Polissia). *Ukrainian Botanical Journal* 2, 226-233.
- Brachert, T., Reuter, M., Felis, T., Kroeger, K., Lohmann, G., Micheels, A., Fassoulas, C. 2006. Porites corals from Crete (Greece) open a window into Late Miocene (10 Ma) seasonal and interannual climate variability. *Earth Planetary Science Letters* 245, 81-94.
- Brew, G., Barazangi, M., Al-Maleh, A. K., Sawaf, T. 2001. Tectonic and geologic evolution of Syria. *GeoArabia* 6, 573-615.
- Broin, F., van Dijk, P. P. 1999. Chelonia from the late Miocene Baynunah Formation, Emirate of Abu Dhabi, United Arab Emirates: paleogeographic implications. *In* Whybrow, P. J., Hill, A. (eds.), *Fossil Vertebrates of Arabia: with Emphasis on the Late Miocene Faunas, Geology, and Palaeoenvironments of the Emirate of Abu Dhabi, United Arab Emirates*. New Haven: Yale University, 136-162.
- Brown, D. 1994. *Freshwater snails of Africa and their medical importance*. London: Taylor & Francis, 609p.
- Bruch, A. A., Utescher, T., Mosbrugger, V., Gabrielyan, I., Ivanov, D. A. 2006. Late Miocene climate in the circum-Alpine realm - a quantitative analysis of terrestrial palaeofloras. *Palaeogeography, Palaeoclimatology, Palaeoecology* 238, 270-280.
- CapitalFm. 2019. Retrieved from:
<https://www.capitalfm.co.ke/lifestyle/2015/12/31/35833/> [Accessed March 2019].
- Carlton, E. B. 2008. "Paleoecology", *In* AccessScience, McGraw-Hill Companies, Retrieved from: <http://www.accessscience.com> [Accessed March 2019].
- Casanova, M. T., Garcia, A., Porter, J. L. 2003. Charophyte rediscoveries in Australia;

- What and why? *Acta Micropalaeontologica Sinica* 20 (2), 129-138.
- Central Administration of Statistics. 2010. Environment and Agriculture. Retrieved from: www.cas.gov.lb/ [Accessed March 2019].
- Cesari, P., Pellizzato, M. 1990. Biology of Tapes Philippinarum. *In* Tapes Philippinarum. *Biologia e Sperimentazione*. Regione Veneto, Ente di Sviluppo Agricolo, Venice, 21-46.
- Cita, M. B., Ryan, W. B .F. 1978. Messinian erosional surfaces in the Mediterranean. *Marine Geology* 27, 193-366.
- Coan, E., Valentich-Scott, P. 2006. Chapter 27 Marine Bivalves. *In* Sturm, C. F., Pearce, T. A., Veldes, A. (eds.), Sturm, Pearce, and Valdés, The mollusks. American Malacological Society, 339-347.
- Cohen, Z. 1976. Early Cretaceous buried canyon: influence on accumulation of hydrocarbons in the Helez oil field, Israel. *AAPG Bulletin* 60, 108-114.
- Colonese A. C., Zanchetta, G., Fallick, A. E., Martini, F., Manganelli, G., Domenico, L. V. 2007. Stable isotope composition of late glacial land snail shells from Grotta del Romito (Southern Italy): Paleoclimatic implications. *Palaeogeography, Palaeoclimatology, Palaeoecology* 254, 550-560.
- Corillion, R. 1972. Les Charophycées de France et d'Europe Occidentale. *Travaux du Laboratoire de Botanique de la Faculté des Sciences d'Angers, Angers*, 11-12.
- Cummings, K. S., Graf, D. L. 2010. Mollusca: Bivalvia. *In* James H. Thorp, Covich, A. P. (eds.), *Ecology and Classification of North American Freshwater Invertebrates* (Third Edition). Elsevier, 309-384.
- Daeron, M., Benedetti, L., Tapponier P., Sursock, A., Finkel, R. C. 2004. Constraint on the post-25ka slip rate of the Yammouneh fault (Lebanon) using *in situ* cosmogenic ³⁶Cl dating of offset limestone-clay fans. *Earth and Planetary Science Letters* 227, 105-119.
- Decima, A. 1964. Ostracodi del genere *Cyprideis* Jones del Neogene e del Quaternario italiani. *Palaeontographia Italica* 57, 81-133.
- De Deckker, P., Lord, A. R. 2017. *Cyprideis torosa*: a model organism for the Ostracoda? *Journal of Micropalaeontology* 36 (1), 3-6.
- Delicado, D., Machordom, A., Ramos, M. A. 2015. Effects of habitat transition on the evolutionary patterns of the microgastropod genus *Pseudamnicola* (Mollusca, Hydrobiidae). *Zoologica Scripta* 44 (4), 403-417.
- Do Carmo, D. A., Whatley, R. C., Timberlake, S. 1999. Variable nodding and

paleoecology of the Middle Jurassic limnocytherid ostracod: implications for modern brackish water taxa. *Paleogeography, Paleoclimatology, Paleoecology* 148, 23-35.

Druckman, Y. 1974. The stratigraphy of the Triassic sequence in southern Israel. *Israel Geological Survey Bulletin* 64, 1-92.

Druckman, Y. 1977. Differential subsidence during the deposition of the Lower Jurassic Ardon Formation in western Jordan, southern Israel and northern Sinai. *Israel Journal of Earth Sciences* 26, 45-54.

Druckman, Y., Gill, D., Fleischer, L., Gelbermann, E., Wolff, O. 1995. Subsurface geology and structural evolution of the northwestern Negev, south Israel. *Israel Journal of Earth Sciences* 44, 115-136.

Dubertret, L. 1945. Géologie du site de Zahle avec carte géologique au 1/50000.

Dubertret, L. 1955. Carte géologique du Liban Au 200000. République Libanaise, Ministère des Travaux Publics.

Dubertret, L. 1975. Introduction à la carte géologique au 1/50000 du Liban. *Notes et Mémoires sur le Moyen-Orient* 23, 345-403.

Duggen, S., Hoernie, K., van den Bogaard, P., Rüpke, L., Phipps Morgan, J. 2003. Deep roots of the Messinian salinity crisis, *Nature* 422, 602-606.

Eerkens, J. W., Byrd, B. F., Spero, H. J., Fritschi, A. K. 2013. Stable isotope reconstructions of shellfish harvesting seasonality in an estuarine environment: Implications for Late Holocene San Francisco Bay settlement patterns. *Journal Archaeological Science* 40, 2014-2024.

Einsele, E. 2000. *Sedimentary Basins: Evolution, Facies, and Sedimentary Budget*. (Second Edition). Springer-Verlag Berlin Heidelberg, 792p.

Eisenmann, V., Whybrow, P. J. 1999. *Hipparions* from the late Miocene Baynunah Formation, Emirate of Abu Dhabi, United Arab Emirates. In Whybrow, P. J., Hill, A., (eds.), *Fossil Vertebrates of Arabia: with Emphasis on the Late Miocene Faunas, Geology, and Palaeoenvironments of the Emirate of Abu Dhabi, United Arab Emirates*. New Haven: Yale University, 234-253.

Eronen, J. T., Ataabadia, M. M., Micheelsb, A., Karme, A., Bernor, R. L., Fortelius, M. 2009. Distribution history and climatic controls of the late Miocene Pikermian chronofauna, *Proceedings of the National Academy of Sciences of the USA* 106, 11867-11871.

Esteban, M., Braga, J. C., Martín, J., de Santisteban, C. 1996. In Franseen, E. K.,

- Esteban, M., Ward, W. C., Rouchy, J. M. (eds.), Models for Carbonate Stratigraphy from Miocene Reef Complexes of Mediterranean Regions, Society for Sedimentary Geology, Tulsa, 55-72.
- Esu, D. 1984. La malacofauna continentale pliocenica di Mandriola (Sardegna occidentale): sistematica e paleobiogeografia. *Geologica Romana* 23, 23-50.
- Esu, D., Girotti, O. 2015. A contribution to the knowledge of Late Miocene freshwater hydrobiids from Tuscany (Central Italy) (Gastropoda Prosobranchia: Rissosoidea). *Archiv für Molluskenkunde* 144 (2), 139-147.
- Feist, M., Grambast-Fessard, N., Guerlesquin, M., Karol, K., Lu, H., McCourt, R. M., Wang, Q., Zang, S. 2005. Treatise on Invertebrate Paleontology, Part B., Protozoista 1, Volume 1: Charophyta. Geological Society of America and the University of Kansas Press, Lawrence, KS, 175p.
- Flügel, E. 2004. Microfacies of Carbonate Rocks Analysis Interpretation and Application. (Second Edition). Springer-Verlag Berlin Heidelberg, 984 p.
- Forsyth, R. G., Oldham, M. J. 2014. Distribution of *Strobilops aeneus* Pilsbry, 1926, in Canada, with two new Ontario records (Mollusca: Gastropoda: Strobilopsidae) *Checklist* 10 (2), 397-401.
- Fossilworks.org. 2019. Fossilworks: Gateway to the Paleobiology Database. Retrieved from: <http://fossilworks.org> [Accessed February 2019].
- Frenzel, P., Ewald, J., Pint, A. 2017. Salinity-dependent sieve pore variability in *Cyprideis torosa*: an experiment. *Journal of Micropalaeontology* 36, 57-62.
- Frenzel, P., Schulze, I., Pint, A. 2012. Noding of *Cyprideis torosa* valves (Ostracoda)- a proxy for salinity? New data from field observations and a long-term microcosm experiment. *International Review of Hydrobiology* 97, 314-329.
- Freytet, P. 1973. Petrography and paleo-environment of continental carbonate deposits with particular reference to the Upper Cretaceous and Lower Eocene of Languedoc (Southern France). *Sedimentary Geology* 10, 25-60.
- Freytet, P., Verrecchia, E. P. 2002. Lacustrine and palustrine carbonate petrography: an overview. *Journal of Paleolimnology* 27, 221-237.
- Frisch, D., Green, A., Figuerola, J. 2007. High dispersal capacity of a broad spectrum of aquatic invertebrates via waterbirds. *Aquatic Sciences, Research Across Boundaries* 69 (4), 568-574.
- Garcés, M., Krijgsman, W., Agustí, J. 1998. Chronology of the late Turolian deposits of the Fortuna basin (SE Spain): implications for the Messinian evolution of the eastern Betics. *Earth and Planetary Science Letters* 163, 69-81.

- García, A. 1994. Charophyta: their use in paleolimnology. *Journal of Paleolimnology* 10, 43-52.
- García, A., Chivas, A. R. 2006. Diversity and ecology of extant and Quaternary Australia charophytes (Charales). *Cryptogramie, Algologie* 27, 323-340.
- Gardosh, M. 2002. The sequence Stratigraphy and Petroleum Systems of the Mesozoic, Southeastern Mediterranean Continental Margin. PhD thesis. Tel Aviv University, 159 p.
- Gardosh, M., Druckman, Y., Buchbinder, B., Rybakov, M. 2006. The Levant Basin Offshore Israel: Stratigraphy, Structure, Tectonic Evolution and Implications for Hydrocarbon Exploration. Geophysical Institute of Israel, 1-119.
- Gardosh, M. A., Garfunkel, Z., Druckman, Y., Buchbinder, B. 2010. Tethyan rifting in the Levant region and its role in the Early Mesozoic crustal evolution. *In* Homberg, C., Bachmann, M., (eds.), *Evolution of the Levant Margin and Western Arabia Platform since the Mesozoic*. Geological Society, London, Special Publications 341, 9-36.
- Garfunkel, Z., Ben-Avraham, Z. 1996. The structure of the Dead Sea basin. *Tectonophysics* 266, 155-176.
- Gierlowski-Kordesch, E. H., 2010. Lacustrine carbonates. *In* Alonso-Zarza, A. M., Tanner, L. H. (eds.), *Continental Carbonates*. Developments in Sedimentology 61, 1-102.
- Girdler, R. W., Southern, T. C. 1987. Structure and evolution of the northern Red Sea. *Nature* 330, 716-721.
- Giusti, F., Manganelli, G., Schembri, P. 1995. The non-marine molluscs of the Maltese Islands. *Monographie Museo Regionale di Scienze Naturali (Torino)* 15, 1-607.
- Glibert, M. 1973. Revision des Gastropoda du Danien et du Montien de la Belgique. I. Les Gastropoda du Calcaire de Mons. Institut Royal des Sciences naturelles de Belgique, Mémoires 173, 1-305.
- Gliozzi, E., Rodriguez-Lazaro, J., Pipik, R. 2017. The Neogene Mediterranean origin of *Cyprideis torosa* (Jones, 1850). *Journal of Micropalaeontology* 36, 80-93.
- Glöer, P. 2002. Die Süßwassergastropoden Nord- und Mitteleuropas. Bestimmungsschlüssel, Lebensweise, Verbreitung. ConchBooks, Hackenheim, 327p.
- Glöer, P., Bouzid, S., Boeters, H. D. 2010. Revision of the genera *Pseudamnicola* PAULUCCI 1878 and *Mercuria* BOETERS 1971 from Algeria with particular emphasis on museum collections (Gastropoda: Prosobranchia: Hydrobiidae). *Archiv für Molluskenkunde* 139 (1), 1-22.

- Glöer, P., Girod, A. 2013. A new Pleistocene *Valvata* species from lake Beyehir and two new *Gyraulus* species from lake Eđirdir (Mollusca: Gastropoda: Valvatidae, Planorbidae) in Turkey. *Folia Malacologica* 21(1), 25-31.
- Gobert, S. 2012. Freshwater Ostracods as Palaeoenvironmental Proxies in the Moervaart Depression, a Palaeolake in Sandy Flanders (NW Belgium). UGhent Unpublished Masters Thesis, Ghent.
- Gollerbakh, M., Krasavina, L. 1983. Determination Key for Freshwater Algae of USSR. Charophyta. *Nauka, Leningrad* 14, 190 (in Russian).
- Gomez, F., Khawlie, M., Tabet, C., Darkal, A. N., Khair, K. & Barazangi, M. 2006. Late Cenozoic uplift along the northern Dead Sea transform in Lebanon and Syria. *Earth and Planetary Science Letters* 241, 913-931.
- González-Pardos, M. 2012. Carófitos del Mioceno Inferior de la Formación Tudela (Cuenca del Ebro, Navarra). Master's Thesis, Universitat de València, 68p.
- Griffin, D. L. 1999. The late Miocene climate of northeastern Africa: unravelling the signals in the sedimentary succession. *Journal of the Geological Society* 156, 817-826.
- Griffin, D. L. 2002. Aridity and humidity: two aspects of late Miocene climate of North Africa and the Mediterranean. *Palaeogeography, Palaeoclimatology, Palaeoecology* 182, 65-91.
- Grigorovich, I. A., Korniushev, A.V., MacIsaac, H. J. 2000. Moitessier's pea clam *Pisidium moitessierianum* (Bivalvia, Sphaeriidae): a cryptogenic mollusk in the Great Lakes. *Hydrobiologia* 435, 153-165.
- Guernet, C., Keraudren, B., Sauvage, J. 1976. La série Levantine du Cap Phocas (Ile de Kos, Dodecanese, Grece): Stratigraphie, palinologie et paleoécologie. *Revue de Micropaléontologie* 19, 61-73.
- Gülen, D., Özüluğ, O. A., Bilgin, F. H. 1996. Ostracoda (Crustacea) fauna of Kabaklı Spring (Diyarbakır). *Ulusal Biyoloji Kongresi, Istanbul* 8, 162-172.
- Hajj Chahine, T. 1973. Etude sédimentologique des formations lacustres Néogènes de la région de Zahlé, Liban. PhD thesis. Lebanese University. 172p.
- Håkanson, L. 2007. Lake environments. *In* Perry, C., Taylor, K. (eds.), *Environmental sedimentology*. Blackwell Publishing, Oxford, 109-143.
- Hancock, P. L., Atiya, M. S. 1979. Tectonic significance of mesofracture systems associated with the Lebanese segment of the Dead Sea transform fault, *Journal of Structural Geology* 1(2), 143-153.

- Harzhauser, M., Neubauer, T. A., Georgopoulou, E., Harl, J. 2014. The Early Miocene (Burdigalian) mollusc fauna of the North Bohemian Lake (Most Basin). *Bulletin of Geosciences* 89 (4), 819-908.
- Harzhauser, M., Neubauer, T. A. 2018. Opole (Poland) -a historical key locality for middle Miocene terrestrial mollusc faunas. *Bulletin of Geosciences* 93 (1), 71-146.
- Hawie, N. 2014. Architecture, geodynamic evolution and sedimentary filling of the Levant Basin: a 3D quantitative approach based on seismic data. PhD thesis, Universite Pierre et Marie Curie, 250p.
- Hawie, N., Gorini, C., Deschamps, R., Nader, F. H., Montadert, L., Granjeon, D., Baudin, F. 2013b. Tectono-stratigraphic evolution of the northern Levant Basin (offshore Lebanon), *Marine and Petroleum Geology* 48, 392-410.
- Heller, J. 2007. A historic biogeography of the aquatic fauna of the Levant. *Biological Journal of the Linnean Society* 92, 625-639.
- Heller, J. 2009. Land snails of the land of Israel. Natural History and a field guide. Pensoft Publishers, Sofia, 360p.
- Heller, J., Mordan, P., Ben-Ami, F., Sivan, N. 2005. Conchometrics, systematics and distribution of *Melanopsis* (Mollusca: Gastropoda) in the Levant. *Zoological Journal of the Linnean Society* 144(2), 229-60.
- Hempton, M. R. 1987. Constraints on Arabian plate motion and extensional history of the Red Sea. *Tectonics* 6, 687-705.
- Hirsch, F., Bassoullet, J. P., Cariou, E., Conway, B., Feldman, H. R., Grossowitch, L., Honigstein, A., Owen, E. F., Rosenfeld, A. 1998. The Jurassic of the southern Levant: biostratigraphy, paleogeography and cyclic event. *In* Crasquin-Soleau, S., Barrier, E. (eds.), Peri-tethys Memoir 4: Epicratonic Basin of Peri-tethyan Platforms 179. *Memoires du Museum National d'Histoire Naturelle, Paris*, 213-235.
- Hodell, D. A., Elmsstrom, K. M., Kennett, J. P. 1986. Latest Miocene benthic $\delta^{18}O$ changes, global ice volume, sea level and the 'Messinian salinity crisis'. *Nature* 320, 411-414.
- Homberg, C., Bachmann, M. 2010. Evolution of the Levant Margin and Western Arabia Platform since the Mesozoic. *In* Geological Society, London, Special Publication 341, 9-36.
- Horn, G. W., Zorilla-Rios, J., Akin, D. E. 1989. Influence of stage of forage maturity and ammoniation of wheat straw on ruminal degradation of wheat forage tissues. *Animal Feed Science and Technology* 24, 201-218.

- Horn af Rantzien, H. 1959. Morphological types and organ-genera of Tertiary Charophyte fructifications. *Stockholm Contributions in Geology* 4, 45-197.
- Horne, D. J., Lord, A. R., Robinson, J. E., Whittaker, J. E. 1990. Ostracods as climatic indicators in interglacial deposits or, On some new and little known British Quaternary Ostracoda. *Courier Forschungsinstitut Senckenberg* 123, 129-140.
- Hsü, K. J. 1983. *The Mediterranean was a Desert. A Voyage of the Glomar Challenger*. Princeton University Press, Princeton, NJ, 216p.
- Hsü, K. J., Ryan, W. B. F., Cita, M. B. 1973. Late Miocene dessication of the Mediterranean. *Nature* 242, 240-244.
- Hsü, K. J., Giovanoli, F. 1979. Messinian event in the Black Sea. *Palaeogeography, Palaeoclimatology, Palaeoecology* 29, 75-93.
- IUCNRedlist.org. 2019. Retrieved from: <http://www.iucnredlist.org> [Accessed March 2019].
- Jeffrey, P. A. 1999. Late Miocene swan mussels from the Baynunah Formation, Emirate of Abu Dhabi, United Arab Emirates. *In* Whybrow, P. J., Hill, A. (eds.), *Fossil Vertebrates of Arabia: with Emphasis on the Late Miocene Faunas, Geology, and Palaeoenvironments of the Emirate of Abu Dhabi, United Arab Emirates*. New Haven: Yale University, 111-115.
- Jochum, A., Weigand, A. M., Bochud, E., Inäbnit, T., Dörge, D. D., Ruthensteiner, B., Favre, A., Martels, G., Kampschulte, M. 2017. Three new species of *Carychium* O.F. Müller, 1773 from the Southeastern USA, Belize and Panama are described using computer tomography (CT) (Eupulmonata, Ellobioidea, Carychiidae). *ZooKeys* 675, 97-127.
- Johnson, A. L. A., Hickson, J. A., Bird, A., Schone, B. R., Balson, P. S., Heaton, T. H. E., Williams, M. 2009. Bivalve sclerochronology and the mid-Pliocene (c. 3.5 Ma) climate of the Southern North Sea Basin. *Palaeogeography, Palaeoclimatology, Palaeoecology* 284, 164-179.
- Kadolsky, D. 2008. Mollusks from the Late Oligocene of Oberleichtersbach (Rhön Mountains, Germany). Part 2: Gastropoda. Neritimorpha and Caenogastropoda. *Courier Forschungsinstitut Senckenberg* 260, 103-137.
- Kalbe, J., Mischke, S., Dulski, P., Sharon, G. 2015. The Middle Palaeolithic Nahal Mahanayem Outlet site, Israel: reconstructing the environment of Late Pleistocene wetlands in the eastern Mediterranean from ostracods, *Journal of Archaeological Sciences* 54, 385-395.
- Kansou, M. 1961. Découverte de vertébrés pontiens au Liban dans la plaine de la Békaa. *Bulletin of Science and Construction Academy RPF Yougoslavie* 6 (3), 65.

- Karanovic, I. 2005a. On the genus *Strandesia Stuhlmann*, 1888 (Crustacea, Ostracoda, Cyprididae) with description of *Strandesia kimberleyi* n. sp. and a key to the extant species of the genus. *Contribution to Zoology* 74, 77-95.
- Karanovic, I. 2012. *Recent Freshwater Ostracods of the World: Crustacea, Ostracoda, Podocopida*: Springer, 610p.
- Karanovic, I., Lee, W. 2013. On the ostracod genus *Ilyocypris*, with description of one new species from Korea and the first report of males of *I. bradyi* (Crustacea: Ostracoda: Podocopida). *Proceedings of the Biological Society of Washington* 126, 39-71.
- Karczmarz, K. 1967. Variabilité et distribution géographique de *Lychnothamnus barbatus* (Meyen) Leonh. *Acta Societatis Botanicorum Poloniae* 35 (3), 431-439.
- Karol, K. G., Skawinski, P. M., McCourt, R. M., Nault, M. E., Evans, R., Barton, M. E., Berg, M. S., Perleberg, D. J., Hall, J. 2017. First discovery of the charophycean green alga *Lychnothamnus barbatus* (Charophyceae) extant in the New World. *American Journal of Botany* 104 (7), 1106-1116.
- Kerney, M. P., Cameron, R. A. D., Jungbluth, J. H. 1983. *Die Landschnecken Nord- und Mitteleuropas*. Paul Parey, Hamburg und Berlin, 384p.
- Keyser, D. 1978. Ecology and zoogeography of recent brackish-water Ostracoda (Crustacea) from south-west Florida. In Löffler, H., Danielopol, D. L. (eds.), *Aspects of ecology and zoogeography of recent and fossil ostracoda*. Junk, The Hague, 207-222.
- Khair, K., Tsokas, G. N., Sawaf, T. 1997. Crustal structure of the northern Levant region: Multiple source Werner deconvolution estimates for Bouguer gravity anomalies, *Geophysical Journal International* 128 (3), 605-616.
- Kovar-Eder, J. 2003. In Reumer, J. W. F., Wessels, W. (eds.), *Distribution and migration of Tertiary mammals in Eurasia. A volume in honour of Hans de Bruijn*, (Deinsea 10, Utrecht, The Netherlands) 373-392.
- Kraatz, B., Bibi, F., Hill, A. 2009. New rodents from the Late Miocene of the United Arab Emirates. *Journal of Vertebrate Paleontology* 29 (3), 129A.
- Krause, W. 1985. Über die Standortsansprüche und das Ausbreitungsverhalten der Stern- Armleuchteralge *Nitellopsis obtusa* (Desvaux) J. Groves. *Carolina* 42, 31-42.
- Krause, W. 1986. Die Bart-Armleuchteralge *Lychnothamnus barbatus* im Klopeiner See. *Carinthia* 176, 337-354.

- Krause, W. 1997. Charales (Charophyceae). Süßwasserflora von Mitteleuropa. Band 18. Gustav Fischer Verlag, Jena, 1-202.
- Krenkel, E. 1924a. Der Syrische Bogen. Zentralblatt Mineralogie 9, 274-281.
- Krenkel, E. 1924b. Der Syrische Bogen. Zentralblatt Mineralogie 10, 301-313.
- Krolopp, E., Sümegi, P. 1993: Pleistocene Vertigo species from Hungary. Scripta Geologica, special issue 2, 263-268.
- Krstić, N., Soulié-Märsche, I., Žic, J., Đorđević-Milutinović, D., Savić, L. 2010. Miocene Charophyta of Maoče, Pljevlja (Northern Montenegro). In Proceedings of the XIX CBGA Congress, Aristotle University of Thessaloniki. Scientific Annals of the School of Geology 99, 85-90.
- Kuiper, J. G. J., Økland, K. A., Knudsen, J., Koli, L., von Proschwitz, T., Valovirta, I. 1989. Geographical distribution of the small mussels (Sphaeriidae) in North Europe (Denmark, Faroes, Finland, Iceland, Norway and Sweden). Annales Zoologici Fennici 26, 73-101.
- Larkin, D. L., Monfils, A. K., Boissezon, A., Sleith, R. S., Skawinski, P. M., Welling, C. H., Cahill, B. C., Karol, K. G. 2018. Biology, ecology, and management of starry stonewort (*Nitellopsis obtusa*; Characeae): A Red-listed Eurasian green alga invasive in North America. Aquatic Botany 148, 15-24.
- Lateef, A. S. A. 2003. Quaternary terrestrial stratigraphic correlations between the Levant and the circum-North Atlantic region: Current knowledge and constraints. Studia Quaternaria 20, 61-72.
- Lateef, A. S. A. 2004b. The Bekaa Valley-Lebanon: some paleoenvironmental, paleoclimatic and sedimentological features and their tectonical implications. In Chatzipetros, A. A., Pavlides, S. B. (eds.), Proceedings of the 5th International Symposium on Eastern Mediterranean Geology, Thessaloniki, Greece, 478-481.
- Lateef, A. S. A. 2006b. Lithostratigraphical framework for the Continental Deposits of the Bekaa Valley of-Lebanon. Bulletin of the Tethys Geological Society 1, 103-115.
- Lateef, A. S. A. 2007. Geological History of the Bekaa Valley-Lebanon. Second International Conference on the Geology of the Tethys, Cairo University, 391-402.
- Ligios, S., Gliozzi, E. 2012. The genus Cyprideis Jones, 1857 (Crustacea, Ostracoda) in the Neogene of Italy: a geometric morphometric approach. Revue de Micropaleontologie 55, 171-207.
- Li, X., Liu, W., Zhang, L., Sun, Z. 2010. Distribution of recent ostracod species in the

Lake Qinghai area in northwestern China and its ecological significance.
Ecological Indicators 10, 880-890.

- Litak, R. K., Barazangi, M., Brew, G., Sawaf, T., Al-Imam, A., Al-Youssef, W. 1997. Structure and evolution of the petroliferous Euphrates graben system, southeast Syria. AAPG Bulletin 82 6, 1173-1190.
- López-Antoñanzas, R., Sen, S., Saraç, G. 2004. A new large Ctenodactylid species from the Lower Miocene of Turkey. Journal of Vertebrate Paleontology 24, 676-688.
- López-Antoñanzas, R., Knoll, F., Maksoud, S., Azar, D. 2015. First Miocene rodent from Lebanon provides the 'missing link' between Asian and African gundis (Rodentia: Ctenodactylidae). Scientific Reports 5, 12871.
- Ložek, V. 1964. Quartärmollusken der Tschechoslowakei. Rozprawy Ústředního Ústavu Geologického 31, 374p.
- Lyman, R. L. 2010. What taphonomy is, what it isn't, and why taphonomist should care about the difference. Journal of Taphonomy 8 (1), 1-16.
- Madsen, H. 1992. Food selection by freshwater snails in the Gezira irrigation canals, Sudan. Hydrobiologia 228, 203-217.
- Malez, M., Forsten, A. 1989. *Hipparion* from the Bekaa valley of Lebanon. Geobios 22, 665-670.
- Malz, H., Triebel, E. 1970. Ostracoden aus dem Sannois und jüngeren Schichten des Mainzer Beckens. 2: *Hemicyprideis* n.g. *Senkenbergiana Lethaea* 51, 1-47.
- Marin, F., Le Roy, N., Marie, B. 2012. The formation and mineralization of mollusk shell. Frontiers in Bioscience 4, 1099-1125.
- Martens, K., Horne, D. J. 2000. Preface: Ostracoda and the four pillars of evolutionary Wisdom. Hydrobiologia 419, 7-11.
- Mazzini, I., Hudáčková, N., Joniak, P., Kováčová, M., Mikes, T., Mulch, A., Rojay, B., Luci-Fora, S., Esu, D., Soulié-Märsche, I. 2013. Palaeoenvironmental and chronological constraints on the Tuğlu Formation (Çankırı Basin, Central Anatolia, Turkey). Turkish Journal of Earth Sciences 22, 1-31.
- Meier-Brook, C. 1983. Taxonomic studies on Gyraulus (Gastropoda: Planorbidae).- Malacologia 24(1-2), 1-113.
- Meisch, C. 2000. Freshwater Ostracoda of western and central Europe. Süßwasserfauna von Mitteleuropa 8/3. Spektrum, Gustav Fischer, Heidelberg, 1-522.
- Meisch, C., Fuhrmann, R. and Wouters, K. 1996. *Ilyocypris getica* Masi, 1906

(Crustacea, Ostracoda): taxonomy, ecology, life history, distribution, fossil occurrence and first record for Germany. *Travaux Scientifiques du Musée National d'Histoire Naturelle de Luxembourg* 23, 3-28.

Mertz-Kraus, R., Brachert, T. C., Reuter, M. 2008. *Tarbellastraea* (Scleractinia): A new stable isotope archive for Late Miocene paleoenvironments in the Mediterranean. *Palaeogeography, Palaeoclimatology, Palaeoecology* 257, 294-307.

Micheels, A., Bruch, A. A., Uhl, D., Utescher, T., Mosbrugger, V. 2007. A Late Miocene climate model simulation with ECHAM4/ML and its quantitative validation with terrestrial proxy data. *Palaeogeography, Palaeoclimatology, Palaeoecology* 253, 251-270.

Mienis, H. K. 1987. A note concerning a small collection of freshwater molluscs from Lake Karaoun, Southern Lebanon. *De Kreukel* 23, 09-110.

Mienis, H. K. 1993. Notities betreffende *Lauria cylindracea*, 5-8. -Correspondentieblad van de Nederlandse Malacologische Vereniging 274, 119-120.

Migula, W. 1897. Die Characeen. In Rabenhorst L. (eds.), *Kryptogamen-Flora von Deutschland, Oesterreich und der Schweiz*. E. Kummer, Leipzig, 772p.

MolluscaBase.org. 2019. Retrieved from: www.molluscabase.org/ [Accessed September 2018].

Moore, T. C., Echols, R. J. 1979. Micropaleontology. In *Paleontology. Encyclopedia of Earth Science*. Springer, Berlin, Heidelberg, 470-475.

Mordan, P. B. 1999. A terrestrial pulmonate gastropod from the late Miocene Baynunah Formation, Emirate of Abu Dhabi, United Arab Emirates. In Whybrow, P. J., Hill, A. (eds.), *Fossil Vertebrates of Arabia: with Emphasis on the Late Miocene Faunas, Geology, and Palaeoenvironments of the Emirate of Abu Dhabi, United Arab Emirates*. New Haven: Yale University, 116-119.

Mosbrugger, V., Utescher, T., Dilcher, D. 2005. Cenozoic continental climatic evolution of Central Europe. *Proceedings of the National Academy of Sciences at the USA* 102, 14964-14969.

Mtlakebook.org. 2019. Retrieved from: <http://mtlakebook.org/how-lakes-function/> [Accessed January 2019].

Müller, C., Higazi, F., Hamdan, W., Mroueh, M. 2010. Revised stratigraphy of the Upper Cretaceous and Cenozoic series of Lebanon based on nannofossils. In Homberg, C., Bachmann, M. (eds.), *Evolution of the Levant Margin and Western Arabia Platform since the Mesozoic*. Geological Society, London, Special Publication 341, 287-303.

Nader, F. H. 2014. *The geology of Lebanon*. Scientific Press Ltd, United Kingdom,

108p.

- Namietko, T., Danielopol, D. L., Baltanás, A. 2011b. Soft body morphology, dissection and slide-preparation of Ostracoda: a primer. *Joannea Geologie und Paläontologie* 11, 151-153.
- Nazik, A., Türkmen, I., Koç, C., Aksoy, E., Avşar, N., Yayık, H. 2008. Fresh and Brackish Water Ostracods of Upper Miocene Deposits, Arguvan/Malatya (Eastern Anatolia). *Turkish Journal of Earth Sciences* 17, 81-495.
- Neubauer, T., Harzhauser, M., Mandic, O., Georgopoulou, E., Kroh, A. 2016. Paleobiogeography and historical biogeography of the non-marine caenogastropod family Melanopsidae. *Palaeogeography, Palaeoclimatology, Palaeoecology* 444, 124-143.
- Neubert, E. 1998. Annotated checklist of the terrestrial and freshwater mollusks of the Arabian Peninsula with descriptions of new species. *Fauna of Arabia* 17, 333-461.
- Newell, N. D. 1969. Classification of the Bivalvia. *In* Moore, R. (ed.), *Treatise on Invertebrate Paleontology, Part N, Mollusca 6, Bivalvia*. Geological Society of America and University of Kansas, Boulder Lawrence 1, 205-244.
- Ozawa, H. 2013. Chapter 4. The history of sexual dimorphism in Ostracoda (Arthropoda, Crustacea) since the Palaeozoic. *In* Moriyama, H. (ed.), *Biochemistry, Genetics and Molecular Biology. Sexual Dimorphism*, 80p.
- Palmer, R. 1979. Fish predation and the evolution of gastropod shell sculpture: experimental and geographic evidence. *Evolution* 33, 697-713.
- Panha, S., Burch, J. 2004. Mollusca. *In* Yule, C. M., Yong, H. S. (eds.), *Freshwater Invertebrates of the Malaysian Region*, Academy of Sciences Malaysia, Kuala Lumpur, 207-224.
- Parkhaev, P. Y. 2007a, The Cambrian 'basement' of Gastropod evolution: Geological Society, London, Special Publications 286, 415-421.
- Pelechaty, M., Brozowski, M., Karol, P. 2017. Overwintering and gyrogonite formation by the rare and endangered indicative macroalga *Lychnothamnus barbatus* (Meyen) Leonh. in eutrophic conditions. *Aquatic Botany* 139, 19-24.
- Pfenninger, M., Cordellier, M., Streit, B. 2006. Comparing the efficacy of morphologic and DNA-based taxonomy in the freshwater gastropod genus *Radix* (Basommatophora, Pulmonata). *BMC Evolutionary Biology*, 14p.
- Pickford, M. 2000. Crocodiles from the Beglia Formation, Middle/Late Miocene boundary, Tunisia, and their significance for Saharan palaeoclimatology. *Annales de Paleontologie* 86, 59-67.

- Pickford, M., Wanas, H., Soliman, H. 2006. Indications for a humid climate in the Western Desert of Egypt 11-10 Myr ago: evidence from Galagidae (Primates, Mammalia). *Comptes Rendus Palevol* 5, 935-943.
- Pilsbry, H. A. 1927-1935. *Manual of Conchology, Second Series: Pulmonata*, 28. Geographic Distribution of Pupillidae; Strobilopsidae, Valloniidae and Pleurodiscidae. Academy of Natural Sciences of Philadelphia, Philadelphia, 226p.
- Pint, A., Frenzel, P. 2016. Ostracod fauna associated with *Cyprideis torosa* –an overview. *Journal of Micropalaeontology* 36, 113-119.
- Pint, A., Frenzel, P., Fuhrmann, R., Scharf, B., Wennrich, V. 2012. Distribution of *Cyprideis torosa* (Ostracoda) in Quaternary athalassic sediments in Germany and its application for palaeoecological reconstructions. *International Review of Hydrobiology* 97, 330-55.
- Pokryszko, B. M. 1990. The Vertiginidae of Poland (Gastropoda: Pulmonata: Pupilloidea) -a systematic monograph. *Annales Zoologici* 43, 133-257.
- Pokryszko, B. M., Auffenberg, K., Hlaváč, J., Naggs, F. 2009. Pupilloidea of Pakistan (Gastropoda: Pulmonata): Truncatellinae, Vertigininae, Gastrocoptinae, Pupillinae (In Part). *Annales Zoologici* 59, 423-458.
- Ponikarov, V. P., and many others. 1967. The geology of Syria: explanatory notes on the geologic map of Syria, scale 1:500000. Part 1, Stratigraphy, igneous rocks and tectonics. Ministry of Industry, Damascus, 230p.
- Pound, M. J., Haywood, A. M., Salzmann, U., Riding, J. B., Lunt, D. J., Hunter, S. A. 2011. A Tortonian (Late Miocene, 11.61-7.25 Ma) global vegetation reconstruction. *Paleogeography, Paleoclimatology, Paleoecology* 300, 29-45.
- Quennell, A. M. 1958. The structural and geomorphic evolution of the Dead Sea rift, *Quarterly Journal of the Geological Society* 114, 1-4.
- Quennell, A. M. 1984. The Western Arabia rift system, Geological Society of London Special Publication 17(1), 775-788.
- Radea, C., Parmakelis, A., Vardinoyannis, S., Vardinoyannis, K. 2017. A new *Islamia* species (Gastropoda: Hydrobiidae) from Cyprus. *Folia Malacologica* 25, 231-236.
- Raj, P. 2017. Morphology of ostracods [web presentation]. Retrieved from: <https://www.slideshare.net/pramodgpramod/morphology-of-ostracods> [Accessed March 2019].
- Rodriguez-Lazaro, J., Ruiz-Muñoz, F. 2012. A General Introduction to Ostracods:

- Morphology, Distribution, Fossil Record and Applications. *In* Horne, D. J., Holmes, J. A., Rodríguez-Lazaro, J., Viehberg, F. (eds.), *Ostracoda as Proxies for Quaternary Climate Change, Developments in Quaternary Science*. Elsevier 17, 1-14.
- Roberts, G., Peace, D. 2007. Hydrocarbon plays and prospectivity of the Levantine Basin, offshore Lebanon and Syria from modern seismic data. *GeoArabia* 12, 99-124.
- Ruiz, F., Abad, M., Bodergat, A. M., Carbonel, P., Rodríguez-Lázaro, J., González Regalado, M. L., Toscano, A., García, E. X., Prenda, J. 2013. Freshwater ostracods as environmental tracers. *International Journal of Environmental Science and Technology* 10, 1115-1128.
- Ruppert, E. E., Fox, R. S., Barnes, R. D. 2004. *Invertebrate zoology: a functional evolutionary approach*: Thomson-Brooks/Cole, 1008 p.
- Sälgeback, J. 2006. Functional morphology of gastropods and bivalves. *Acta Universitatis Upsaliensis Uppsala*, 31p.
- Salvador, R. B., Höltke, O., Rasser, M. W., Kadolsky, D. 2016. Annotated type catalogue of the continental fossil gastropods in the Staatliches Museum für Naturkunde Stuttgart, Germany. *Palaeodiversity* 9, 15-70.
- Salvador, R. B., Höltke, O., Rasser, M. W. 2017. Fossil land and freshwater gastropods from the Miocene of Hohenmemmingen, Germany. *Palaeodiversity* 10, 41-48.
- Sandberg, P. A. 1964. The ostracod genus *Cyprideis* in the Americas. *Stockholm Contributions in Geology* 12, 1-178.
- Sanjuan, J., Martín-Closas, C. 2014. Taxonomy and palaeobiogeography of charophytes from the Upper Eocene-Lower Oligocene of the eastern Ebro Basin (Catalonia, NE Spain). *Geodiversitas* 36(3), 385-420.
- Sanjuan, J., Martín-Closas, C. 2015. Biogeographic history of two Eurasian Cenozoic charophyte lineages. *Aquatic Botany* 120 (A), 18-30.
- Sanjuan, J., Alqudah, M. 2018. Charophyte flora from the Miocene of Zahle (Beeka Valley, Lebanon). *Biostratigraphic, palaeoenvironmental and palaeobiogeographical implications*. *Geodiversitas* 40, 195-209.
- Sanjuan, J., Martín-Closas, C., Costa E., Barberà, X., Garcés, M. 2014. Calibration of Eocene- Oligocene charophyte biozones in the Eastern Ebro Basin (Catalonia, Spain). *Stratigraphy* 11(1), 61-81.
- Savazzi, E., Sasaki, T. 2004. Function and construction of synchronized sculpture in gastropods. *American Malacological Bulletin* 18, 87-114.

- Schäfer, H. W. 1952. Über Süswasser-Ostracoden aus der Türkei. Istanbul Üniversitesi Fen Fakültesi Aras, tırma Enstitüsü Yayınları, Hidrobiologi, Seri B 1(1), 7-32.
- Schneider, S., Garcia, A., Martín-Closas, C., Chivas, A. R. 2015. The role of charophytes (Charales) in past and present environments: an overview. *Aquatic Botany* 120, 2-6.
- Searle, M. P., Chung, S., Lo, C. 2010. Geological offsets and age constraints along the northern Dead Sea fault, Syria. *Journal of the Geological Society, London* 167, 1001-1008.
- Seddon, M. B. 2014. *Gyraulus hebraicus*. The IUCN Red List of Threatened Species 2014: e.T164820A1075506. <http://dx.doi.org/10.2305/IUCN.UK.2014-1.RLTS.T164820A1075506.en>. [Accessed March 2019].
- Şereflişan, H., Yıldırım, M. Z., Şereflişan, M. 2009. The gastropod fauna and their abundance, and some physicochemical parameters of Lake Gölbaşı (Hatay, Turkey). *Turkish Journal of Zoology* 33, 287-296.
- Shileyko, A. A. 1984. Terrestrial mollusks of the suborder Pupillina of the USSR fauna. (Gastropoda, Pulmonata, Geophila). Leningrad, Nauka: Fauna SSSR. *Mollusca* 3 (3), 399p.
- Sleith, R., Havens, A. J., Stewart, R. A., Karol, K. G. 2015. Distribution of *Nitellopsis obtusa* (Characeae) in New York, U.S.A. *Brittonia* 67 (2), 166-172.
- Sigwart, J. D, Sutton, M. D. 2007. Deep molluscan phylogeny: synthesis of palaeontological and neontological data. *Proceedings of the Royal Society B* 274, 2413-2419.
- Smith, O. J. 2005. Shell Shapes. Museum of National History. Retrieved from: <http://www.stitchingnature.com/snails/mollusca/gastropoda/GastropodaMorp009.htm> [Accessed March 2019].
- Sommer, M. 2001. The Bekaa Valley in Antiquity. A regional-historic survey. *Bulletin d'Archéologie et d'Architecture Libanaises* 5, 71-91.
- Songtham, W., Ugai, H., Imsamut, S., Maranate, S., Tansathien, W., Meesook, A., Saengrichan, W. 2005. Middle Miocene molluscan assemblages in Mae Moh Basin, Lampang Province, Northern Thailand. *Science Asia* 31, 183-191.
- Soulié-Märsche, I. 1989. Étude comparée de gyrogonites de charophytes actuelles et fossiles et phylogénie des genres actuels. Millau, Imprimerie des Tilleuls, 37p.
- Soulié-Märsche, I., Benammi, M., Gemayel, P. 2002. Biogeography of living and fossil *Nitellopsis* (Charophyta) in relationship to new finds from Morocco. *Journal of Biogeography* 29, 1703-1711.

- Soulié-Märsche, I., Martín-Closas, C. 2003. *Lychnothamnus barbatus* (charophytes) from the upper Miocene of la Cerdanya (Catalonia, Spain): Taxonomic and palaeoecological implications. *Acta Micropalaeontologica Sinica* 20 (2), 156-165.
- Stancheva, M. 1963. Ostracoda from the Neogene in North-Western Bulgaria. *Travaux de la Geologie de Bulgarie, Serie Paleontologie* 5, 5-71.
- Stancheva, M. 1990. Upper Miocene ostracods from Northern Bulgaria. *Geologica Balcanica, serie operum singularum* 5, 1-111.
- Suárez-Hernando, O., Martínez-García, B., González- Pardos, M., Pascual, A., Larraz, M., Ruíz-Sánchez, F. J., Cruz-Larrasoña, J., Murelaga, X. 2013. Preliminary palaeontological data from the Loma Negra section (Bardenas Reales de Navarra, Lower-Middle Miocene). *Geogaceta* 54, 63-66.
- Sugier, P., Pelechaty, M., Gabka, M., Owsiany, P., Pukacz, A., Ciecierska, H., Kolada, A. 2010. *Lychnothamnus barbatus*: global history and distribution in Poland. *Charophytes* 2, 19-24.
- Szarowska, M. 2006. Molecular phylogeny, systematics and morphological character evolution in the Balkan Rissooidea (Caenogastropoda). *Folia Malacologica* 14 (3), 99-168.
- Tassy, P. 1999. Miocene Elephantids (Mammalia) from the Emirate of Abu Dhabi, United Arab Emirates: palaeobiological implications. *In* Whybrow, P. J., Hill, A. (eds.), *Fossil Vertebrates of Arabia: with Emphasis on the Late Miocene Faunas, Geology, and Palaeoenvironments of the Emirate of Abu Dhabi, United Arab Emirates*. New Haven: Yale University, 209-233.
- Tchernov, E. 1979. Quaternary fauna. *In* Horowitz, A. (ed.), *The Quaternary of Israel*. New York: Academic Press, 92-260.
- Tibert, N. E., Colin, J. P., Leckie, M. R., Babinot, J. F. 2003. Revision of the ostracode genus *Fossocytheridea* Swain and Brown, 1964: Mesozoic ancestral root for the modern eurytopic *Cyprideis* Jones. *Micropaleontology* 49, 205-230.
- Tsukagoshi A., Ikeya, N., 1987. The ostracod genus *Cythere* O. F. Müller, 1785 and its species. *Transactions and Proceedings of the Palaeontological Society of Japan, New Series*, 1987 148, 197-222.
- Udomkan, B., Ratanasthien, B., Takayasu, K., Fyfe, W. S., Sato, S., Kandharosa, W., Wongpornchai, P., Kusakabe, M. 2003. Fluctuation of depositional environment in the Ban Mark Coal deposit, Krabi Mine, southern Thailand: stable isotope implication. *Science Asia* 29, 307-317.
- Van Damme, D. 1984. *The freshwater mollusca of Northern Africa*. Dordrecht: Dr Junk, 164p.

- Van Damme, D. 2014. *Melanopsis buccinoidea*. The IUCN Red List of Threatened Species 2014: e.T156110A42422389. <http://dx.doi.org/10.2305/IUCN.UK.2014-1.RLTS.T156110A42422389.en>. [Accessed April 2019].
- Van Damme, D., Pickford, M. 2003. The late Cenozoic Thiaridae (Mollusca, Gastropoda, Cerithioidea) of the Albertine Rift Valley (Uganda-Congo) and their bearing on the origin and evolution of the Tanganyikan thalassoid malacofauna. *Hydrobiologia* 498, 1-83.
- Van Damme, M. B., Kebapçı, U. 2014. *Valvata saulcyi*. The IUCN Red List of Threatened Species 2014: e.T155862A42422803. <http://dx.doi.org/10.2305/IUCN.UK.2014-1.RLTS.T155862A42422803.en>. [Accessed May 2018].
- Van Harten, D. 1975. Size and environmental salinity in the modern euryhaline ostracod *Cyprideis torosa* (Jones, 1850), a biometrical study. *Palaeogeography, Palaeoclimatology, Palaeoecology* 17(1), 35-48.
- Van Harten, D. 1990. The Neogene evolutionary radiation in *Cyprideis* Jones (Ostracoda: Cytheracea) in the Mediterranean Area and the Paratethys. *Courier Forschungsinstitut Senckenberg* 123, 191-198.
- Van Harten, D. 2000. Variable nodding in *Cyprideis torosa* (Ostracoda, Crustacea): an overview, experimental results and a model from Catastrophe Theory. *Hydrobiologia* 419, 131-139.
- Vermeij, G. J. 1977. The Mesozoic marine revolution: evidence from snails, predators and grazers. *Paleobiology* 3, 245-258.
- Vermeij, G. J. 1993. *A natural history of shells*: Princeton University Press 207. Princeton, N.J, 207p.
- Vigne, J. D. 1996. Did Man Provoke Extinctions of Endemic Large Mammals on the Mediterranean Islands? The View from Corsica. *Journal of Mediterranean Archaeology* 9 (1), 117-120.
- Walley, C. D. 1997. The lithostratigraphy of Lebanon: a Review. *Lebanese Scientific Bulletin* 10, 81-108.
- Walley, C. D. 1998. Some outstanding issues in the geology of Lebanon and their importance in the tectonic evolution of the Levantine region. *Tectonophysics* 145, 63-72.
- Walley, C. D. 2001. The Lebanon passive margin and the evolution of the Levantine Neotethys. In Ziegler, P. A., Cavazza, W., Robertson, A. H. F., Crasquin-Soleau, S. (eds.), *Peri-tethys Memoir 6: Peri-Tethyan Rift/Wrench Basins and Passive Margins*. *Mémoire du Muséum national d'Histoire naturelle Paris* 86, 407-439.

- Weigand, A. M., Jochum, A., Slapnik, R., Schnitzler, J., Zarza, E., Klusmann-Kolb, A. 2013. Evolution of microgastropods (Ellobioidea, Carychiidae): integrating taxonomic, phylogenetic and evolutionary hypotheses BMC Evolutionary Biology 13 (18), 1-23.
- Welter-Schultes, F. W. 2012. European non-marine molluscs, a guide for species identification. Planet Poster Editions, Göttingen, 757p.
- Wenz, W. 1923-1930. Fossilium Catalogus I: Animalia. Gastropoda extramarina tertiaria. W. Junk, Berlin, 3387p.
- Wood, B. G. M. 2001. Intraplate primary and subsidiary basin formation and deformation: an example from central Cyria, Ph.D Thesis, University of Oxford, United Kingdom.
- Wouters, K. 2002. On the distribution of *Cyprideis torosa* (Jones) (Crustacea, Ostracoda) in Africa, with the discussion of a new record from the Seychelles. Bulletin de l'Institut royal des sciences naturelles de Belgique, Biologie 72, 131-140.
- Wouters, K. 2016. On the modern distribution of the euryhaline species *Cyprideis torosa* (Jones, 1850) (Crustacea, Ostracoda). Journal of Micropaleontology. Retrieved from: <http://doi.org/10.1144/jmpaleo2015-021>. [Accessed April 2019].
- Yang, F., Sun, Z., Zhang, Y., Qiao, Z. 2002. Taxonomic significance of nodal ornamentation of Quaternary genus "*Ilyocypris*" (Ostracoda) from Qaidam Basin, Qinghai Province. Acta Micropalaeontologica Sinica 19, 15-32.
- Youssef, M., Moustafa, A. R., Shann, M. 2010. Structural setting and tectonic evolution of offshore north Sinai, Egypt. In Homberg, C., Bachmann, M. (eds.), Evolution of the Levant Margin and Western Arabia Platform since the Mesozoic. Geological Society, London, Special Publications 341, 65-84.
- Zak, I. 1963. Remarks on the stratigraphy and tectonics of the Triassic of Makhtesh Ramon. Israel Journal of Earth Sciences 12, 87-89.
- Zak, I. 1968. Geological map of Israel: Makhtesh Ramon, HarGevanim 1:20,000. Israel Geological Survey.
- Ziegler, M. A. 2001. Late Permian to Holocene paleofacies evolution of the Arabian plate and its Hydrocarbon occurrences. GeoArabia 6, 445-504.

